

**BIODEGRADATION OF DIESEL CONTAMINATED WASTEWATER USING A
THREE-PHASE FLUIDIZED BED REACTOR**

BY

GISSELY ANANIA MUÑOZ

Bachelor of Science in Chemical Engineering

Jose Antonio Echeverria Polytechnic University

Havana, Cuba, July 1997

A thesis presented to Ryerson University

in partial fulfillment of the requirements for the degree of

Master of Applied Science

In

Chemical Engineering

Toronto, Ontario, Canada, 2004

©Gisselly Anania Muñoz, 2004

**- PROPERTY OF
RYERSON UNIVERSITY LIBRARY**

UMI Number: EC53414

INFORMATION TO USERS

The quality of this reproduction is dependent upon the quality of the copy submitted. Broken or indistinct print, colored or poor quality illustrations and photographs, print bleed-through, substandard margins, and improper alignment can adversely affect reproduction.

In the unlikely event that the author did not send a complete manuscript and there are missing pages, these will be noted. Also, if unauthorized copyright material had to be removed, a note will indicate the deletion.



UMI Microform EC53414
Copyright 2009 by ProQuest LLC
All rights reserved. This microform edition is protected against
unauthorized copying under Title 17, United States Code.

ProQuest LLC
789 East Eisenhower Parkway
P.O. Box 1346
Ann Arbor, MI 48106-1346

I hereby declare that I am the sole author of this thesis.

I authorize Ryerson University to lend this thesis to other institutions or individuals for the purpose of scholarly research.

Gisselly Anania Muñoz

I further authorize Ryerson University to reproduce this thesis by photocopying or by other means, in total or in part, at the request of other institutions or individuals for the purpose of scholarly research.

Gisselly Anania Muñoz

Ryerson University requires the signatures of all persons using or photocopying this thesis.

Please sign below, and give address and date.

1.

2.

3.

4.

5.

6.

7.

8.

9.

10.

11.

12.

13.

14.

15.

ABSTRACT

BIODEGRADATION OF DIESEL CONTAMINATED WASTEWATER USING A THREE-PHASE FLUIDIZED BED REACTOR

Master of Applied Science in Chemical Engineering (2004)

Gisselly Anania Muñoz

Chemical Engineering Department

Ryerson University

The use of petroleum-derived products has given rise to environmental concerns regarding hydrocarbon pollution. Therefore, the development of innovative technologies for the clean up of contaminated sites is a challenge. This thesis is an investigation of a three-phase fluidized bed biofilm reactor, as an effective technology for biological treatment of diesel-contaminated wastewater.

The three-phase fluidized bed utilized in this research consists of support media (diameter of 600 μm) with biofilm, and gas phase (air at 1.0 cm/s) in up flowing liquid (feedwater at 0.02 cm/s). The reactor influent is synthetic wastewater varying in COD concentrations in the range of 550-1300 mg/l and diesel concentrations between 70 and 200 mg/L. The results indicate that diesel fuel can be removed in the reactor with efficiencies up to 100 % at a hydraulic detention time of 4 hours. Good quality effluent means a good reactor performance, where 55 % of the diesel fuel was removed due to biological process.

ACKNOWLEDGMENTS

I would like to offer special thanks to Dr. Alvarez Cuenca, for many helpful discussions on wastewater engineering and especially for supervising this thesis. His guidance in this research was crucial for the success of this investigation. Thank you for allowing me to present this research at two international congresses: "2nd International Environmental Congress of the Caribbean" held in Colombia and "Water and Wastewater Europe 2004" held in Spain where I personally presented this research. I would also like to acknowledge Dr. Ali Lohi, for his support in this research and for providing guidance at "Water and Wastewater Europe 2004". I also wish to thank the following people at Ryerson University who supported the investigation and gave me helpful comments and suggestions: Dr. Mario Estable, Mr. Dennis Walmsley, Mr. Ali Hemmati and Mr. Peter Scharping.

I also wish to thank Sean Black, my partner in life, thanks for so much advice... thanks for supporting me with your love, patience and unconditional help. I would like to offer my special gratitude to Randall for so many wonderful nights alone just you and me rubbing your belly, you brought me much needed support while in front of the computer.

I also wish to thank to Peter Weeks (President of "Nuco Products"), Robin Sluce (General Manager) and Marjorie Blumfeld (Manager) for the support and help during two years. Thanks for trusting in me and teaching me all I know about the jewelry business. I will always have beautiful memories from such a beautiful workplace.

Me gustaria ofrecer mis mas sinceras gracias para mi familia en Cuba, por confiar en mi en todos estos años, en especial para mi mama Graciela, mi hermana Greisy y mi papa Jose ... tanta dedicacion y amor seria imposible plasmar en estas cortas lineas.

TABLE OF CONTENTS

	Page
Author's Declaration	ii
Borrower's Page	iii
Abstract	iv
Acknowledgements	v
Table of Contents	vi
List of Tables	ix
List of Figures	xi
List of Appendices	xiii
Nomenclature	xiv
Chapter 1: Introduction	1
Chapter 2: Literature Review	5
2.1 Aerobic Biofilm Processes Applied to Wastewater Engineering	5
2.1.1 Substrate Utilization in Biofilm Reactors	7
2.2 Three-Phase Fluidized Bed Biofilm Technology	10
2.2.1 Process Description	13
2.2.2 Industrial and Municipal Applications	16
2.2.3 Bioreactor Performance	21
2.2.4 Models of Three-Phase Fluidized Bed Biofilm Reactor	22
2.2.5 Validation and Use of the Larachi's Model	24

2.3 Diesel Fuel Biodegradability	27
Chapter 3: Experimental	32
3.1 Experimental Program	32
3.2 Experimental Facilities	33
3.2.1 Three-Phase Fluidized Bed Bioreactor	36
3.2.2 Biofilm Support	41
3.2.3 Instrumentation	42
3.3 Analytical Methods	44
3.3.1 Chemical Oxygen Demand Determination	44
3.3.2 Liquid-Liquid Extraction and Gas Chromatography Technique	46
3.3.3 Microscopy	46
3.3.4 Total Suspended Solids Determination	47
3.4 Experimental Procedure and Data Collection	47
3.4.1 Phase I: Preparation of Microorganisms Inoculum and Reactor Start-Up Procedure	48
3.4.2 Phase II: Reactor Operation in Intermittent Mode	50
3.4.3 Phase III: Reactor Operation at Steady-State	52
3.4.4 Phase IV: Validation of Diesel Biodegradation	53
Chapter 4: Interpretation and Discussion of Experimental Data	55
4.1 Interpretation of the Experimental Results Obtained in Phase II: Reactor Operation in Intermittent Mode	56
4.2 Interpretation of the Experimental Results Obtained Phase III:	63

Reactor Operation at Steady-State	
4.2.1 Estimation of the Attached Biomass Concentration using Larachi's Model	73
4.3 Interpretation of the Experimental Results Obtained in Phase IV: Validation of Diesel Biodegradation	77
4.4 Sources of Errors	80
Chapter 5: Conclusions and Recommendations	81
5.1 Conclusions	81
5.2 Recommendations and Future Work	83
Bibliography	84
Appendices	95

LIST OF TABLES

	Page
Table 1.1 Composition of diesel fuels by hydrocarbon type	2
Table 1.2 Hydrocarbons standards guideline for soil and groundwater clean-up criteria	3
Table 2.1 Different support particles employed for various investigators	14
Table 2.2 Commercial applications of the TPFBR reactor: Municipal Wastewater Treatment	17
Table 2.3 Commercial applications of the TPFBR reactor: Industrial Wastewater Treatment	18
Table 2.4 Selected application of three-phase fluidized bed bioreactor	19
Table 2.5 Summaries of operating conditions of fluidized bed bioreactors for aerobic wastewater treatment employed by various investigators	20
Table 2.6 Correlation used in the three-phase fluidized bed biofilm reactor	23
Table 2.7 Composition of diesel fuel # 2 used in this research	28
Table 3.1 Description of the equipments used in this research	34
Table 3.2 Lava rock characteristics	41
Table 3.3 Essential nutrients added into the reactor for bacterial growth of diesel degrading organisms	49
Table 4.1 Operational conditions during intermittent mode	57
Table 4.2 Biofilm properties and hydrodynamic parameters at steady state operation	67

Table 4.3	Characteristics of the regions formed in the reactor	71
Table 4.4	Parameter used in simflui3p and for prediction of the biomass concentration	73
Table 4.5	Hydrodynamic parameters	74
Table 4.6	Estimated and experimental solids hold-up	75
Table 4.7	Biomass concentration determined by other investigators	76
Table 4.8	Summaries of selected parameters of steady state operation	79

LIST OF FIGURES

	Page
Figure 2.1 Biofilm reactor types used in wastewater treatment engineering	6
Figure 2.2 An idealized biofilm	8
Figure 2.3 Schematic diagram of a three-phase fluidized-bed bioreactor	16
Figure 2.4 Flow chart to predict the biomass concentration in the three-phase fluidized bed bioreactor	26
Figure 2.5 Ring structures of representative polycyclic aromatic compounds in diesel fuel	27
Figure 2.6 Pathway of diterminal alkane oxidation under aerobic conditions	30
Figure 2.7 Pathway of benzene oxidation under aerobic conditions	31
Figure 3.1 Schematic of the three-phase fluidized bed reactor set-up	35
Figure 3.2 Air and liquid distribution in the reactor	37
Figure 3.3 The full-scale equipment used for the experimental research	39
Figure 3.4 Three-phase fluidized bed dimensions	40
Figure 3.5 Lava rock photograph	42
Figure 3.6 Dissolved oxygen meter and probe used in this research	43
Figure 3.7 pH meter and turbidity meter used in this research	43
Figure 3.8 Colorimeter and heater block set up for the measurements of COD	45
Figure 3.9 Microorganisms inoculums	50
Figure 3.10 Diesel concentrations during intermittent mode	52
Figure 4.1 Diesel loading rates during the 12 days of intermittent mode	56

Figure 4.2	Percent of diesel removed and diesel loading rate during intermittent mode	58
Figure 4.3	Percent of COD removed and COD concentrations during intermittent mode	59
Figure 4.4	Dissolved oxygen during intermittent mode	61
Figure 4.5	pH during intermittent mode	62
Figure 4.6	Percent diesel removed and diesel loading rate during steady state	63
Figure 4.7	Percent COD removed and COD concentrations during steady state	64
Figure 4.8	Dissolved oxygen versus height of the reactor	64
Figure 4.9	Total suspended solids at steady state	65
Figure 4.10	Turbidity values during steady state	66
Figure 4.11	Microscopy photograph of active biofilm developed in the lower part of the reactor	68
Figure 4.12	Microscopy photograph of active biofilm developed in the upper part of the reactor	69
Figure 4.13	Reactor operation at steady state	72
Figure 4.14	Diesel volatilization in the reactor	77

LIST OF APPENDICES

		Page
APPENDIX A	CALIBRATION CURVE GAS CHROMATOGRAMS	96
APPENDIX B	RAW DATA AND GAS CHROMATOGRAMS FOR PHASE II: REACTOR OPERATION IN INTERMITTENT MODE	101
APPENDIX C	RAW DATA AND GAS CHROMATOGRAMS FOR PHASE III REACTOR OPERATION AT STEADY STATE	115
APPENDIX D	RAW DATA AND GAS CHROMATOGRAMS FOR PHASE IV VALIDATION OF DIESEL BIODEGRADATION	122
APPENDIX E	Simflui3p SOFTWARE: DESCRIPTION AND RESULTS	128

NOMENCLATURE

A	Column Cross Sectional Area	m^2
D_f	Diffusion Coefficient of Substrate in Water	m^2/d
DO	Dissolved Oxygen	mg/L
d_p	Clean Particle Diameter	m
g	Gravitational Acceleration Coefficient	9.8 m/s^2
H	Fluidized Height of Bioparticles	m
K_s	Substrate Concentration at One-Half the Maximum	g/m^3
	Substrate Utilization Rate	
k	Maximum Substrate Utilization Rate	$g_{ss}/g_{microorg} \cdot d$
NTU	Nephelometric Turbidity Units	(-)
r_{diff}	Rate of Substrate Flux	$g/m^2 d$
r_{sub}	Rate of Substrate Utilization in Biofilm	$g/m^2 d$
S_f	Substrate Concentration	g/m^3
TPFBR	Three-Phase Fluidized Bed Biofilm Reactor	(-)
U_g	Superficial Gas Velocity	m/s
U_L	Superficial Liquid Velocity	m/s
V	Reactor Volume	m^3
W_{pt}	Weight of Clean Particles	g
X	Biomass Concentration	Kg/m^3

Greek Letters

δ	Biofilm Thickness	μm
ε	Bed Porosity	(-)
ε_g	Gas Hold-up	(-)
ε_s	Solids Hold-up	(-)
ε_L	Liquid Hold-up	(-)
μ_g	Gas Viscosity	Kg/m.s
μ_l	Liquid Viscosity	Kg/m.s
π	Sphericity Factor of Bioparticles	(-)
ρ_{wb}	Biofilm Wet density	Kg/m^3
ρ_{db}	Biofilm Dry Density	Kg/m^3
ρ_l	Liquid Density	Kg/m^3
ρ_g	Gas Density	Kg/m^3
ρ_p	Clean Particle Density	Kg/m^3
γ	Recycle Ratio	(-)
σ_L	Liquid Surface Tension	Kg/s^2
τ	Hydraulic Detention Time	Time



CHAPTER ONE

INTRODUCTION

As two billion tons of petroleum are refined each year worldwide, accidental releases of petroleum and its products into the environment is a widespread problem. Therefore, the development of effective technologies to treat industrial wastewater is a challenge. Since diesel fuels are commonly used, large quantities are accidentally released into groundwater environment e.g. accidental spills, leaking of storage tanks, or through inadvertent releases during use, transportation or disposal. Dowd (1994) has estimated that up to 400,000 leaking underground storage tanks in the United States have promoted soil and groundwater remediation.

Diesel fuel toxicity is due to the presence of aromatic hydrocarbons such as benzene, alkylbenzenes and naphthalene. A typical diesel fuel composition based on type of hydrocarbon is shown in Table 1.1. Paul and Edward (1992) have indicated that the carcinogenic potential of diesel fuel is because of the presence of co-carcinogens such as C₁₀ and C₂₀ alkenes and alkylated benzenes. Humans and animals can be exposed to diesel-

contaminated sites by inhalation, dermal and ingestion; thereby diesel fuels also represent a health hazard for aquatic and terrestrial ecosystems.

HYDROCARBON TYPE	MASS %
Paraffins	39.7
Cycloparaffins	50.8
Alkylbenzenes	3.2
Indans + Tetralins	0.8
Indenes	0.1
Naphthalene	0.2
Alkyl Naphthalenes	1.6
Acenaphthenes/Biphenyls	2.2
Acenaphthenes/Fluorenes	1.7

Adapted from Song et al. 2000

TABLE 1.1 COMPOSITIONS OF DIESEL FUELS BY HYDROCARBON TYPE

Environmental regulations have become more and more strict regarding hydrocarbon pollution and green house gas emissions. Standards applicable to pollution by hydrocarbons are well developed in countries such as Germany and Canada. The clean up reference levels for aquifer protection is shown in Table 1.2.

Several methods for remediation of petroleum-contaminated sites such as mechanical (oil-water separators), chemical (chemicals dispersants such as surfactants) and biological treatment (bioremediation) already exist. Yang et al. (2000) have indicated that the removal of spilled oils by mechanical means is usually incomplete and chemical dispersants tend to increase the dissolution of oil in the water. Sepic et al. (1996), Margesin and Schnner (1998) and Erickson et al. (1998) have suggested that aerobic biodegradation by natural population of microorganisms is a favorable possibility by which diesel fuel can be eliminated from a

contaminated environment. Yang et al. (2000) have also indicated the potential of biological degradation of diesel fuel in water using a trickling filter.

COUNTRY	CLEAN UP VALUES					
	Soil (mg/Kg DS)			Groundwater (µg/L)		
	Benzene	Toluene	Xylene	Benzene	Toluene	Xylene
Germany ^a	0.5	5	5	5	20	20
Canada ^b	0.05-0.5	3	5	5	24	30

^a Data were adapted from Lecomte and Mariotti, 1997

^b Abstracted from Environment Canada, 2002

Note: DS, dry substance

**TABLE 1.2 HYDROCARBONS STANDARDS GUIDELINE FOR SOIL AND
GROUNDWATER CLEAN-UP CRITERIA**

Over the last few years, considerable attention has been devoted to biological three-phase fluidized-bed as an effective technology for treating organic pollutants. This technology seems to be more effective than both dispersed biomass processes and fixed bed systems such as trickling filters and activated sludge. The main advantage of this technology is that it retains a higher biomass concentration when compared with suspended biomass growth, allowing higher loading rates at lower hydraulic detention times as well as smaller area requirements. There are a number of advantages of fluidized beds compared to other processes. Rittmann (1982) has reported biomass concentrations up to 50 g/L, this value is higher than that found with activated sludge. Tavares et al. (1995) have reported COD removal efficiencies of 82 percent at a hydraulic detention time of 30 minutes. This is a very

low detention time when compared to 1 to 3 days in activated sludge systems (Alvarez-Cuenca, 2003).

Three-phase fluidized bed has been investigated for BOD removal, nitrification, denitrification, and industrial effluents (Boaventura and Rodrigues 1988, Harada et al. 1987, Hermanowicz and Cheng 1983, Mulcahy and Shieh 1987 and Trinet et al. 1991). In addition, Alvarez-Cuenca (2004) has indicated the potential of rotating biological contactors and three-phase fluidized beds as effective technologies for treating wastewater contaminated with organic pollutants.

This thesis describes a laboratory investigation that took place at the “Water and Wastewater Treatment Technologies” laboratory at Ryerson University.

The main objectives of this research are:

- To determine experimentally the feasibility and performance of a three-phase fluidized bed bioreactor for treatment of feedwater contaminated with diesel fuel.
- To determine the optimal operational conditions for the three-phase fluidized bed bioreactor treating feedwater contaminated with diesel fuel.
- To assess biofilm characterization and hydrodynamic properties at the optimal operating conditions to enable process scale-up.

The secondary objective of this thesis is:

- To set-up an appropriate technique for biomass immobilization and start-up procedures in a three-phase fluidized bed bioreactor.



CHAPTER TWO

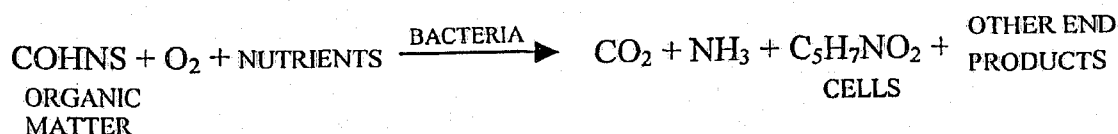
LITERATURE REVIEW

2.1 AEROBIC BIOFILM PROCESSES APPLIED TO WASTEWATER ENGINEERING

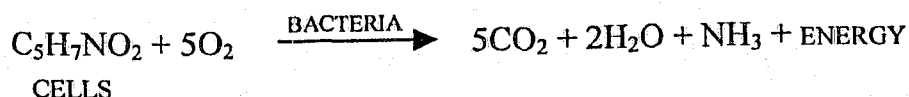
In aerobic biofilm processes, a film consisting of natural aggregations of microorganisms and their extra cellular substances are attached and cover a solid surface. The solid surface can be plastic, rock, activated carbon or other materials attractive for bacterial growth. The attached microbial growth is responsible for the removal, through microbial metabolism, of the biodegradable components in the wastewater.

Complete oxidation of organic matter in aerobic biofilm processes is carried out inside the biofilm in presence of oxygen and nutrients. During aerobic oxidation, part of the organic matter is oxidized to maintain bacteria cells essential processes and part of it is used for synthesis of new cells tissue. Furthermore, if there is no organic matter available, the new cell tissue will begin to consume their own cell tissue as a source of energy. The processes of oxidation of the substrate are presented as follows:

Oxidation and Synthesis:



Endogenous respiration:



In this oxidation–reduction reactions, the electron acceptor (oxygen) is consumed in proportion to the electron donor (substrate) utilization.

Trickling filters, rotating biological contactors, fixed-beds and fluidized-beds are examples of biofilm processes that can achieve aerobic biological oxidation of the organic matter and organic pollutants. Attached biofilm processes have many advantages over suspended growth processes such as activated sludge. The advantages, due to the accumulation of a large amount of biomass, include high volumetric removal rates, short liquid detention times, and good performance stability. Figure 2.1 shows three types of biofilm reactors applied to wastewater treatment.

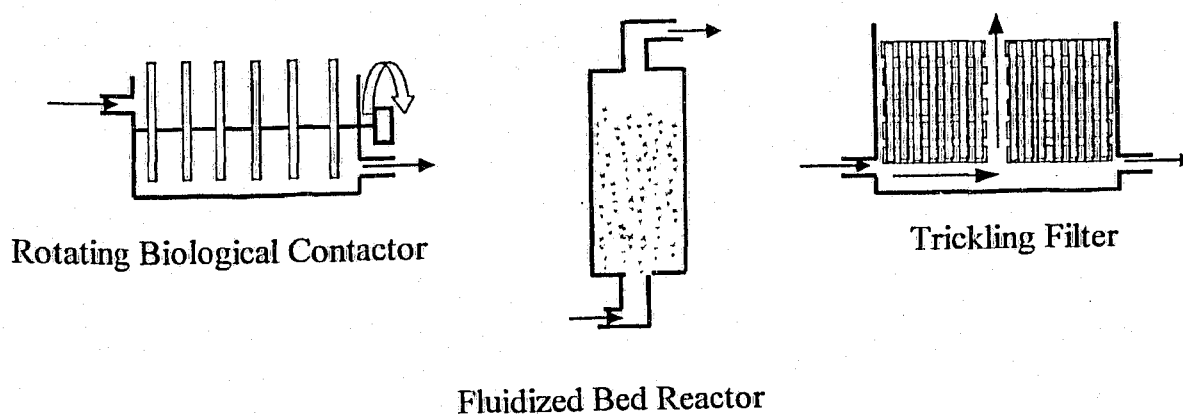


FIGURE 2.1 BIOFILM REACTOR TYPES USED IN WASTEWATER TREATMENT ENGINEERING

In the tricking filter the media is fixed and the wastewater flows passing the film while exposed to air for aerobic purposes. In the rotating biological contactor the media rotates and the wastewater to be treated passes through the stages. In the fluidized bed the media consisted of solid particles covered with a biofilm, forming a bioparticle while the wastewater to be treated is passed upward through the fluidized bed of particles.

2.1.1 Substrate Utilization in Biofilm Reactors

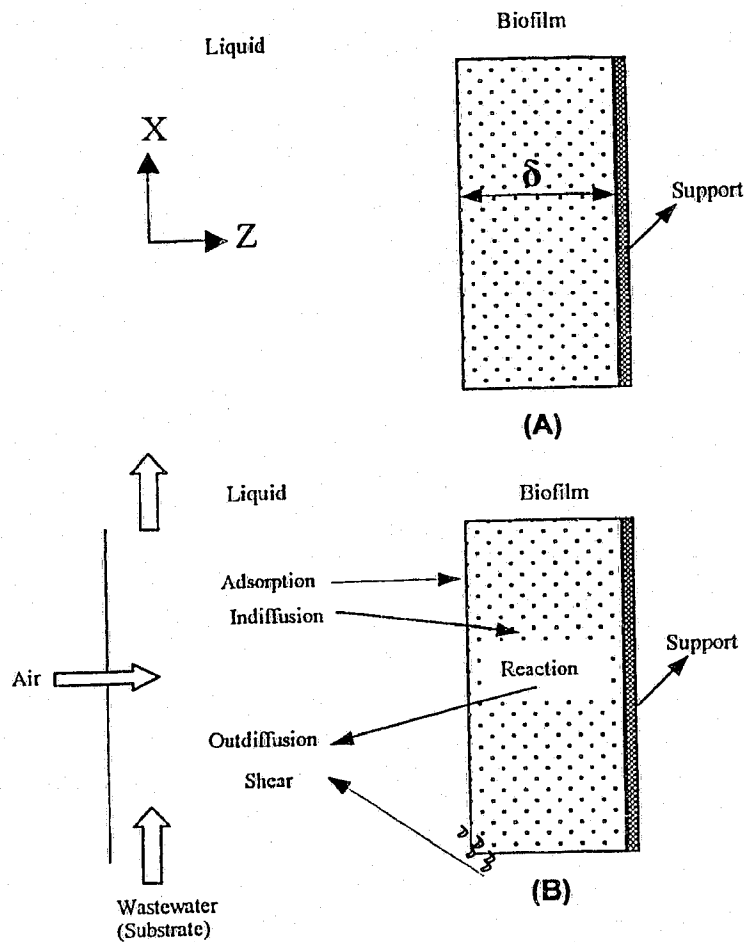
Various models have been developed by a number of investigators to describe the phenomena inside a biofilm (Rittmann and McCarty 1980; 1981; 1982 and Ngian and Martin 1980). It is generally accepted that biofilm kinetics of substrate utilization is due to molecular diffusion, mass transfer of substrate and subsequent oxidation of the substrate inside the biofilm.

Substrate, nutrients and oxygen diffuse into the biofilm and products of biodegradation from the biofilm are released into the liquid. Substrate, either carbonaceous material or organic pollutant, is consumed within a biofilm. Arvin and Harremoes (1990) suggested that the degradation of the substrate takes place by hydrolysis through the action of extracellular enzyme releasing soluble products into the liquid medium.

Rittmann and McCarty (1981) have shown that a substrate utilization reaction and molecular diffusion are two primary phenomena that describe the accumulation of substrate in a control volume of the biofilm. This phenomenon is depicted in Figure 2.2. Mass transfer of the substrate within a biofilm, is given by Fick's second law:

$$r_{diff} = D_f \frac{d^2 S_f}{dz^2} \quad (1)$$

Where, r_{diff} is the rate of substrate flux into the biofilm, D_f is the molecular diffusivity of the substrate into the biofilm, and $\frac{d^2 S_f}{dz^2}$ is the gradient of the substrate concentration.



^a Developed in part from Rittmann and McCarty, 1981.

FIGURE 2.2 AN IDEALIZED BIOFILM

(A) PHYSICAL PROPERTIES (B) PHENOMENA IN THE BIOFILM^a

The substrate utilization rate at any point in the biofilm is assumed to follow the Monod kinetic model for the specific growth rate of bacteria. This model for substrate removal has been referred to as the Michaelis-Menten equation (Metcalf and Eddy, 2003) and it is given by:

$$r_{sub} = - \frac{k S_f X}{K_s + S_f} \quad (2)$$

In which, r_{sub} is the rate of substrate utilization in biofilm, S_f is the substrate concentration at a point in the biofilm, k is the maximum specific substrate utilization rate, X is the biomass concentration, K_s is the substrate concentration at one-half the maximum specific substrate utilization rate.

Since diffusion and utilization of the substrate occur simultaneously, by combining equation (1) and (2), the overall mass balance on substrate for a steady-state concentration profile in the biofilm that the substrate utilization is according to Michaelis-Menten relationship can be obtained as:

$$D_f \frac{d^2 S_f}{dz^2} = \frac{k S_f X}{K_s + S_f} \quad (3)$$

Although Monod kinetics have been widely used to describe wastewater treatment process, other kinetics models have also been suggested depending on the substrate and the microbial species used. Tsuneda et al. (2002) suggested that Haldane Model and Edwards Model might also be applicable to describe biodegradation kinetics for phenol and other aromatic substrates.

The assumptions for the model presented in equation (3) are:

1. Steady-state conditions.
2. Spherical support particles.
3. Homogenous biofilm of uniform thickness.
4. Values of biokinetics and diffusivity parameters are constant within the biofilm.

Solutions for equation (3) require knowledge of all kinetic and mass transfer parameters as well as biofilm properties. Rittmann and McCarty (1981) and Suidan et al. (1987) demonstrated that the solution of the equation (3) varies depending on conditions of biofilm: (a) deep biofilm (b) shallow biofilm or, (c) fully penetrated biofilm. Detailed information for the solution of these three cases can be found in the above-mentioned reference and at Lewandoski et al. (1994) and Bignami et al. (1991). Due to the complexity of the kinetics and the inability to define accurately the parameters for each substrate, empirical correlations are used for the design of bioreactors.

2.2 THREE-PHASE FLUIDIZED BED BIOFILM TECHNOLOGY

Three-phase fluidized bed biofilm reactor (TPFBR) is an effective wastewater treatment technology based on biofilm processes. Three-phase fluidization involves a solid-liquid-gas bed, where the solid particles are called bioparticles, and air is supplied for aerobic processes. Sutton and Mishra (1993) have indicated the potential of this technology as a high-rate unit for both industrial and domestic wastewater treatment. Lazarova and Manem (1994) have also indicated that this technology combines the best features of activated sludge and trickling filtration into one process.

The first patent was conceded to Manhattan College researchers, assigned to Ecolotrol, Inc., in 1974 for the application of TPFBR for denitrification processes. The first commercial-scale plant for municipal wastewater treatment was installed in Florida around 1975 and it was used for denitrification processes. The first commercial-scale plant for industrial application occurred around 1980 in Alabama, USA for the anaerobic treatment of wastewater from a soft drink bottling plant (Mishra and Sutton, 1990).

Since the implementation of the first commercial fluidized-bed for municipal wastewater treatment, other design have been developed such as:

- OXITRON activated Carbon system by Dorr Oliver.
- The GAC-Fluid Bed developed and supplied by Envirex Ltd.
- The BIOLIFT Fluidized-Bed system developed by OTV (Badot et al. 1994)

Detailed information about these innovative biofilm technologies for water and wastewater treatment can be found at Bryers (2000).

Other investigators such as Wu and Huang (1996), and Diez-Blanco et al. (1995) have reported the use of fluidized bed bioreactor for anaerobic treatments. Anaerobic fluidized bed reactors are capable of treating low strength municipal sewage. Polanco et al., (1994) and Wilson et al., (1998) have found that anaerobic fluidized bed is more efficient when used as a pretreatment step followed by conventional aerobic treatment.

The following points summaries the major advantages and disadvantages associated with the use of TPFBR for industrial and municipal wastewater treatment:

ADVANTAGES

1. TPFBR retain higher biomass concentration when compared to suspended biomass growth such as activated sludge processes. Mishra and Sutton (1990) have indicated that the biomass concentration in fluidized bed is approximately 5-10 times greater than that normally achieved in activated sludge reactors.
2. Three-phase fluidized bed biofilm reactors operate at a significantly reduced hydraulic detention time with high removal efficiencies. Typical hydraulic detention time for the BOD removal in a fluidized bed ranges from 30-100 minutes, compare

to activated sludge that takes 1 to 3 days for aerobic processes (Alvarez-Cuenca, 2003).

3. Reduction in reactor size due to the development of a high biomass concentration.
4. Three-phase fluidized beds solve the problems of oxygen demand by using simultaneous injections of air and liquid. This also induces high shear stress that controls biofilm thickness and sludge production.
5. Fluidization overcome problems such as bed clogging, poor mixing, sludge recycle and low transfer of substrate between the liquid and the biomass.
6. Absence of mechanical moving parts.

DISADVANTAGES

1. Complex interrelation between kinetic processes and fluidization makes it difficult to model mathematically the fluidized-bed biofilm process.
2. It is difficult to maintain homogenous biofilm formation otherwise particle elutriation and bed stratification, two unwanted phenomena, will arise in the reactor.
3. There is a limit on operating velocities and support particle size.

Substrate removal in fluidized bed biofilm processes can be performed either in aerobic or anaerobic reactors. The power economy is one of the most important factors in evaluating the feasibility of aerobic versus anaerobic operation. The power economy of organic removal is expressed as the amount of pollutant (BOD or COD) removed per unit power consumption.

In three-phase fluidized bed aerobic reactor, the energy is mainly consumed by supplying oxygen to the reactor and by the liquid pump for fluidization of bioparticles. Fan (1989) has indicated that under optimum operating conditions, the power consumption by the liquid pump for fluidization of bioparticles amounts to one-third of the total power consumption. According to Lazarova et al. (1994), the energy consumption in these reactors is around 1 KWh/ Kg COD removed, similar to that in activated sludge processes and lower than that in two-phase fluidized bed reactors with pre-oxygenation (Bryers, 2000; MetCalf and Eddy, 2003).

Anaerobic reactors have been considered as energy producers instead energy users, as is the case of aerobic processes. This statement is due to the production of methane as a product of biodegradation. Metcalf and Eddy (2003) have indicated that a net energy production on the order of 10.4×10^6 kJ/d can be achieved with anaerobic treatment. This value is about 5 times the energy required for aerobic treatment. Anaerobic conditions require constant checking of temperature and alkalinity because of it is very sensitive to the effect of low temperature and low pH in reaction rate. Metcalf and Eddy (2003) recommend alkalinity concentration of 2000 to 3000 mg/l as CaCO_3 to maintain an acceptable pH. A significant cost may be incurred to purchase CaCO_3 , which can affect the overall economics of the process. The effluent from anaerobic reactors may require further treatment in an aerobic reactor to meet discharge requirement

2.2.1 Process Description

A three-phase fluidized bed biofilm reactor consists of a fluidized bed of support particles favorable to microbial growth. Organisms grow on the support particles in the form of biofilm and inside the pores of the particles to form a bioparticle. Bioparticles remain

suspended while the contaminated water or wastewater passes continuously throughout the reactor. Fan (1989) has suggested that the density of optimal support for biological growth and fluidization purposes ranges from 1015 to 1600 Kg/m³. Table 2.1 shows various support particles with higher density that has been used for cell immobilization.

REFERENCE	SUPPORT PARTICLE	DIAMETER (mm)	DENSITY (kg/m ³)	U _L (cm/s)
Coelhoso et al. (1992)	Activated carbon	1.69	1180	1.4
Eggers and Terlouw (1979)	Sand	1.0	2650	1.34
Boaventura and Rodrigues (1988)	Sand	0.4	2150	1.4
Briens et al. (1997)	Polypropylene with mineral inclusions	3	2471	2.3
Karapinar and Kargi (1996)	Sponge surrounded by stainless steel wires	4	1350	4.5

TABLE 2.1 DIFFERENT SUPPORT PARTICLES EMPLOYED BY VARIOUS INVESTIGATORS

When the wastewater to be treated passes upward at a sufficient velocity to bring particles in the bed from rest to motion, it is said to be at the point of incipient fluidization at a minimum liquid velocity. At this point, the bed media particles provide a large surface area for microbial growth. The attached microbial growth is responsible for the removal, through microbial metabolism, of the biodegradable components. Fan (1989) also reported that the

classic equations used to calculate the minimum liquid velocity and terminal velocity of rigid particles could be used for bioparticles. Larachi et al. (2000) have also reported dimensional and dimensionless correlations describing minimum liquid velocity, terminal velocity and phase hold ups for TPFBR. The authors claim that these correlations can be used with bioparticles.

The upper and lower limit of operation can be set at the minimum fluidization velocity and at the terminal velocity of the particles. The lower level is the minimum fluidization velocity since velocity below this value will not produce fluidization. The upper level is set at the terminal velocity since velocity higher than this value will cause particle elutriation.

A schematic diagram of a three-phase fluidized bed bioreactor is shown in Figure 2.3.

The most important mechanical components of the reactor are:

1. Liquid distributor.
2. Air distributor.
3. The device used to control bed expansion due to biomass growth.

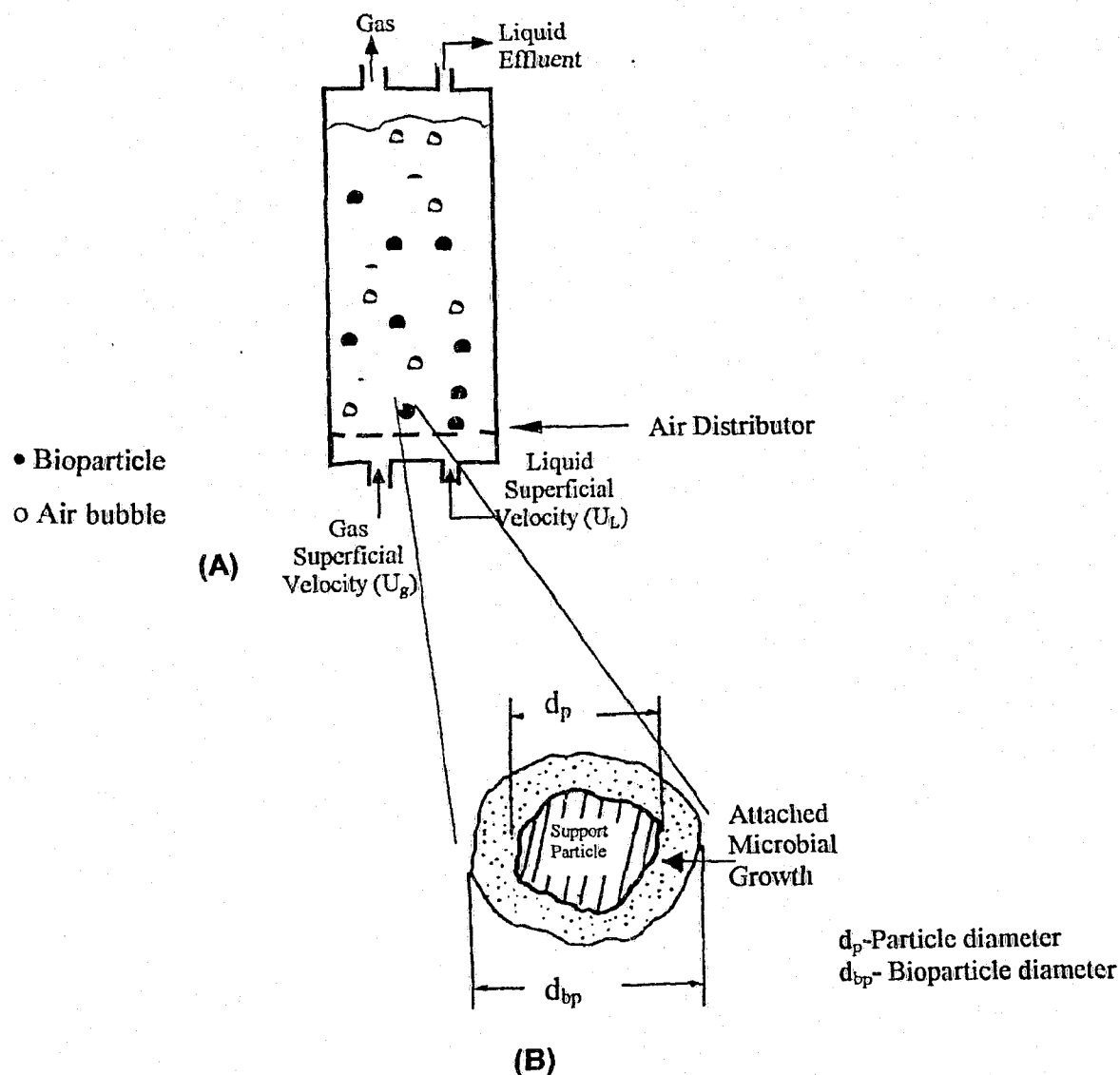


FIGURE 2.3 SCHEMATIC DIAGRAM OF A THREE-PHASE FLUIDIZED-BED BIOREACTOR

(A) THREE-PHASE FLUIDIZED BIOREACTOR

(B) SOLID PARTICLE WITH A LAYER OF ATTACHED MICROBIAL GROWTH

2.2.2 Industrial and Municipal Applications

Fluidized bed bioreactors have shown to be an effective technology in carbonaceous oxidation, nitrification and denitrification of a wide variety of wastewaters. Detailed descriptions of these applications can be found elsewhere (Mulcahy and Shieh 1987, Harada

et al. 1987, Trinet et al. 1991, Boaventura and Rodriguez 1988, Hermanowicz and Cheng, 1983). A number of full-scale fluidized beds are currently in operation for treating industrial effluents as well as municipal wastewaters. These applications are shown in Table 2.2 and 2.3, respectively.

FACILITY AND LOCATION	APPLICATION	SYSTEM INFORMATION
Bay Park Wastewater Treatment Plant, East Rockaway, NY, USA ^a	Aerobic carbonaceous oxidation of sanitary wastewater	Five reactors, each 37.2 m ² by 9 m high
Hayward Wastewater Treatment Plant, Hayward, CA, USA ^a	Aerobic carbonaceous oxidation of sanitary wastewater	Two reactors, each 47.6 m ² by 7 m high
Pensacola Wastewater Treatment Plant, Pensacola, FL, USA ^b	Denitrification of nitrified sanitary wastewater	Two reactors, each 33.5 m ² by 5.8 m high
Lansing Wastewater Treatment Plant, Lansing, MI, USA ^b	Anaerobic treatment of liquor from solids heat treatment process	Four reactors, each 35.3 m ² by 11.3 m high

^a Adapted from Mishra and Sutton (1990), ^b Adapted from Sutton and Mishra (1993)

**TABLE 2.2 COMMERCIAL APPLICATIONS OF THE TPFBR REACTOR:
MUNICIPAL WASTEWATER TREATMENT**

Some other applications for fluidized bed reactors have been explored at the laboratory and pilot-scale levels for complex organic pollutants in recent years. These applications are summarized in Table 2.4.

FACILITY AND LOCATION	APPLICATION	SYSTEM INFORMATION
Algoma Steel Plant, Sault Ste. Marie, Ontario, Canada ^a	Aerobic carbonaceous oxidation of wastewater from coke-making operations	Two reactors, each 65.6 m ² by 8.5 m high
General Motors Plant, Lansing, MI, USA ^a	Aerobic carbonaceous oxidation of wastewater from automotive manufacturing operation	One reactor, 18.7 m ² by 6.7 m high
Grindsted Products Plant, Grindsted, Denmark ^a	Aerobic carbonaceous oxidation of wastewater from chemical operations.	Two reactors, each 59.8 m ² by 6.1 m high
Hoogovens Plant, IJnuiden, Holland ^a	Aerobic carbonaceous oxidation of wastewater from coke-making operations	Two reactors, each 84.3 m ² by 8.7 m high
Formosa, Point Comfort, TX, USA ^b	Aerobic treatment of chemical plant wastewater for organics removal	Two reactors, each 23.6 m ² by 7.3 m high

^aAdapted from Mishra and Sutton (1990) , ^b Adapted from Sutton and Mishra (1993)

TABLE 2.3 COMMERCIAL APPLICATIONS OF THE TPFBR REACTOR:
INDUSTRIAL WASTEWATER TREATMENT

Badot et al. (1994) reported the results of the three-phase fluidized bed process applied to tertiary treatment in a municipal wastewater treatment plant filled with sand (0.2-0.6 mm diameter). Polanco et al. (1994) reported a use of 6.5 m³ anaerobic/aerobic fluidized bed for carbonaceous removal in a municipal wastewater treatment plant. Over 80 % of COD were removed at organic loading of around 0.2 and 1.2 Kg/m³d. Other applications and a summary of the operating conditions of fluidized bed bioreactors employed in aerobic treatment are shown in Table 2.5.

SYSTEMS	REFERENCE
Bench scale aerobic fluidized bed reactor used to treat simulated acetic acid wastewaters	Safferman and Bishop (1997)
Lab-scale fluidized bed for quinoline degradation	Buchtmann et al. (1997)
Lab-scale aerobic fluidized bed for reduction of chlorophenol in groundwater	Melin et al. (1998)
Lab-scale anaerobic/aerobic fluidized bed system for degradation of pentachlorophenol	Wilson et al. (1998)
Pilot-scale fluidized bed for the treatment of aqueous-phase dichloromethane	Flanagan (1998)
Lab-scale fluidized bed for treatment of metalworking wastewater	Schreyer and Coughlin (1999)
Lab-scale fluidized bed for biodegradation of phenolic Industrial wastewater	Gonzales et al. (2001)
Pilot-scale fluidized bed for COD reduction of a brewery wastewater	Ochieng et al. (2002)

TABLE 2.4 SELECTED APPLICATION OF THREE-PHASE FLUIDIZED BED BIOREACTOR

In general, the main applications of this technology when used in industrial wastewater treatment are:

1. To remove large quantities of substrate generated in industrial processes.
2. To treat wastewater that is not continuously discharged into the reactor (Intermittent loading).

AUTHOR	DIMENSION OF THE BIOREACTOR	SOLID SUPPORT	WASTEWATER (SUBSTRATE)	OPERATIONAL CONDITIONS	LOADING AND REMOVAL RATE	COMMENTS
Gonzales et al. (2001)	Lab scale $H_R = 42$ cm $V = 3$ L	Calcium-alginate gel beads. $d_p = 1-2$ mm	Phenolic industrial wastewater $S = 250-2500$ ppm	$Q = 85$ L/h	$W_o = 62.5 - 625.0$ mg/L d Phenol Removed 100%	$\tau = 4$ h $DO = 2-4.5$ mg/L $pH = 4.5$
Wilson et al. (1998)	Lab scale $H_R = 96.5$ cm $V = 10$ L	Granular activated carbon 16x20 mesh	Pentachlorophenol artificial wastewater (PCP) $S = 200$ ppm	$Q = 3-24$ L/d	$W_o = 0.6-4.8$ g/Ld PCP Removed 95%	Anaerobic/ Aerobic System $\tau = 2.3$ h
Flanagan (1998)	Lab Scale $H_R = 244$ cm $V = 12.7$ L	Granular activated carbon 10x30 mesh	Dichloromethane artificial wastewater (DCM) $S = 2018-2596$ ppm	$Q = 65.4$ L/d $U_L = 4$ cm/s $\gamma = 23.6$	$W_o = 28.3-48.7$ KgDCM/m ³ day DCM Removed 100 %	$\tau = 1.72$ h $\gamma = 23.6$ $pH = 7.0 \pm 0.5$
Buchtmann et al. (1997)	Lab Scale $H_R = 58$ cm $V = 5$ L	Bayvitec® Aquacel® $d_p = 100-700$ μ m	Artificial quinoline wastewater $S = 390-980$ ppm	$U_g = 1.5$ cm/s	$W_o = 0.31-0.35$ g/L h	$pH = 7.2$ τ vary upon support
Hosaka et al. (1985) and Fan (1989)	Lab Scale $H_R = 240$ cm $V = 8.1$ L	Activated carbon particle $d_p = 272$ μ m	Artificial phenol wastewater $S = 100-120$ ppm	$Q = 14.4-17.3$ L/h $U_L = 7.3-8.8$ m/h $U_g = 9$ m/h $\gamma = 0$	$W_o = 4-6$ Kg/m ³ day Phenol removed 100 %	$DO = 2-4$ ppm $\delta = 50-100$ μ m $\tau = 4$ h

Note: S, substrate concentration in ppm; H_R , Height of the reactor

TABLE 2.5 SUMMARY OF OPERATING CONDITIONS OF FLUIDIZED BED BIOREACTORS FOR AEROBIC WASTEWATER TREATMENT EMPLOYED BY VARIOUS INVESTIGATORS

2.2.3 Bioreactor Performance

The performance of fluidized bed biofilm reactors depends in general on the biomass concentration, the overall biodegradation rates and the reactor configuration (Fan, 1989).

The biomass concentration within the reactor depends on:

1. Biofilm thickness
2. Biofilm detachment
3. Support particle characteristics
4. Dissolved oxygen and pH

Ruggiere et al. (1994) have shown how with an increase of biofilm thickness, anaerobic activities in deeper biofilm layers occur due to the mass diffusion limitation of essential nutrients, the substrate or oxygen. This phenomenon reduces the reaction rate or the formation of other by products due to anaerobic reactions.

Nicolella et al. (1996) have pointed out that biofilm detachment in fluidized beds increase with increasing the shear stress produced due to high liquid and gas velocities. Therefore, particle interaction and liquid turbulence make the biofilm denser and thinner. Information about biofilm detachment models in fluidized bed biofilm reactors can be found elsewhere (Nicolella et al., 1996; 1997; Picioreanu et al., 1999; 2000, Chang et al. 1991).

One of the most important aspects of the fluidized bed biofilm reactor is the fact that the biomass growth around the support particle decreases the overall density of the particle. This phenomenon leads to different segregation of the bioparticles in which the bigger particles arise to the top of the reactor and the smaller remain at the bottom of the reactor. This problem arises when the support particles are not uniform in size.

The pH, dissolved oxygen and the presence of inhibitors can increase or decrease the substrate flux into the biofilm. Metcalf and Eddy (2003) have shown that the optimal pH for microorganism growth is around neutral values of 6-8. The text also recommends a dissolved oxygen concentration around 2-4 mg/L to achieve aerobic processes. Ngian and Martin (1980) have reported change in the biodegradation pathway of the substrate due to the lack of dissolved oxygen.

The overall biodegradation rates depend on the type of substrate and the microbial species used. Several kinetic models for substrate biodegradation and their corresponding rate constant for aromatic hydrocarbons have been given by Arcangeli and Arvin, 1995 and Zhang et al. 1995. These kinetic models include rate expressions with respect to the substrate of zero order, first order, Monod type and Haldane type.

With respect to reactor configuration, one of the most important engineering features of fluidized beds is liquid and airflow distribution. Poor flow distribution allows short-circuiting and uneven bed expansion.

2.2.4 Models of Three-Phase Fluidized Bed Biofilm Reactor

In general, the model discussed in section 2.1.1 applies to three-phase fluidized bed bioreactors. However, due to the inability to define accurately the physical and biokinetic parameters and model coefficients, empirical correlations based on experimental works are used for design and modeling purposes.

Several models have been developed to calculate the bed height, phase holdups and overall biomass concentration in a three-phase fluidized bed bioreactor. Ngian and Martin (1980), Shieh et al. (1981) and Hermanowicz and Ganczarczyk (1990) found that the same

expression that is applied to a liquid fluidized bed of rigid particles is applicable to bioparticle as well.

Different models can be applied depending of the nature of the process. Mulcahy and Shieh (1987) have proposed a model for denitrify biofilm in fluidized beds. Ozturk et al. (1994) have proposed a model for anaerobic biofilm in fluidized beds, using the well-known Richardson-Zaki correlations for rigid particles. Nicolella et al. (1995 and 1998), Abdul-Aziz and Asolekar (2000) and Andrews and Trapasso (1985) have developed empirical correlations for the calculations of density and terminal velocity of bioparticles for aerobic biofilm. Some of the correlations used for biofilm-covered particles in fluidized systems are shown in Table 2.6.

CORRELATION	EQUATION	UNITS	REMARKS
$H = (W_{pl} / \epsilon_s \rho_p A) (1 + 2\delta/d_p)^3$	(4)	m	Fluidized Bed Height Yu and Rittmann (1997)
$X = \rho_{db} (1 - \epsilon) [1 - (d_p/d_{bp})]^3$	(5)	Kg/m ³	Biomass Concentration Chang and Rittmann (1994)
$\rho_{bp} = \rho_p (1 + 2\delta/d_p)^3 + \rho_{wb} [1 - (1 + 2\delta/d_p)^3]$	(6)	Kg/m ³	Bioparticle Density Trinet et al. 1991
$d_{bp} = d_p + 2\delta$	(7)	m	Bioparticle Diameter

TABLE 2.6 CORRELATIONS USED IN THE THREE-PHASE FLUIDIZED BED BIOFILM REACTOR

2.2.5 Validation and Use of the Larachi's Model

The software used in this research predicts the hydrodynamics of the three-phase fluidized bed reactor based on Larachi's Model.

Larachi et al. (2000) have developed the most recent model for predictions of phase's hold-ups for a three-phase fluidized bed reactor. Using the basis of multilayer perceptron artificial neural network, modeling technique and dimensional analysis, the authors established simflui3p software for prediction of the hydrodynamics of the three-phase fluidized bed. This software is appropriate for a number of applications where three-phase fluidized bed technology is used (fermentation, wastewater treatment and coal liquefaction). The authors elaborated the simflui3p software based on data published since 1970. Description of this software as well as the results obtained in this study can be found in Appendix E.

The mentioned software offered by Laval University, Quebec, Canada is used in this research to predict fluidization parameters mainly bed porosity and phase's hold-ups. The model assumption are:

- The individual bioparticle is assumed to have smooth surface and a spherical shape.
- The wastewater properties were taken as clean water properties.
- Type of system: Foaming
- The biofilm dry density and wet density were adopted from Zhang and Bishop, 1993 and 1994, and its value is shown as follows:

$$\rho_{wb} = 1020.0 \text{ Kg/m}^3$$

$$\rho_{db} = 1170.0 \text{ Kg/m}^3$$

- The support particle is assumed to be uniform in size with 600 μm of diameter.

Once ϵ , ϵ_g , ϵ_L , ϵ_s are known, the prediction of the attached biomass concentration is estimated from correlations used for biofilms in fluidized reactors showed in Table 2.6.

A step-by-step procedure to compute the attached biomass concentration is presented in the flowchart in Figure 2.4. Once hydrodynamics and biofilm parameters are known, the calculation of the bioparticles properties is performed in step 2. The calculation of fluidization parameters (bed porosity and phase's hold-ups) is performed using `simflui3p` in step 3. Validation of Larachi's Model (`simflui3p`) is performed in step 4, comparing the experimental and estimated values of solids hold-up (ϵ_s) with an acceptance of 10 % relative error. Once fluidization parameters are known the attached biomass concentration is predicted using Equation 5.

It is important to point out that the procedure to estimate attached biomass concentration was selected over other procedures based on the following considerations:

1. Fluidization and biomass correlation have been developed for denitrification data, anaerobic systems, two-phase fluidized beds and carbonaceous removal. Mulcahy and Shieh (1987) have recommended further refinement of these correlations with other types of substrate.
2. The inability to accurately estimate the bubble rising velocity and gas hold-up.
3. The inability of experimentally determining the attached biomass concentration using biological analytical methods such as confocal scanning electron microscopy.

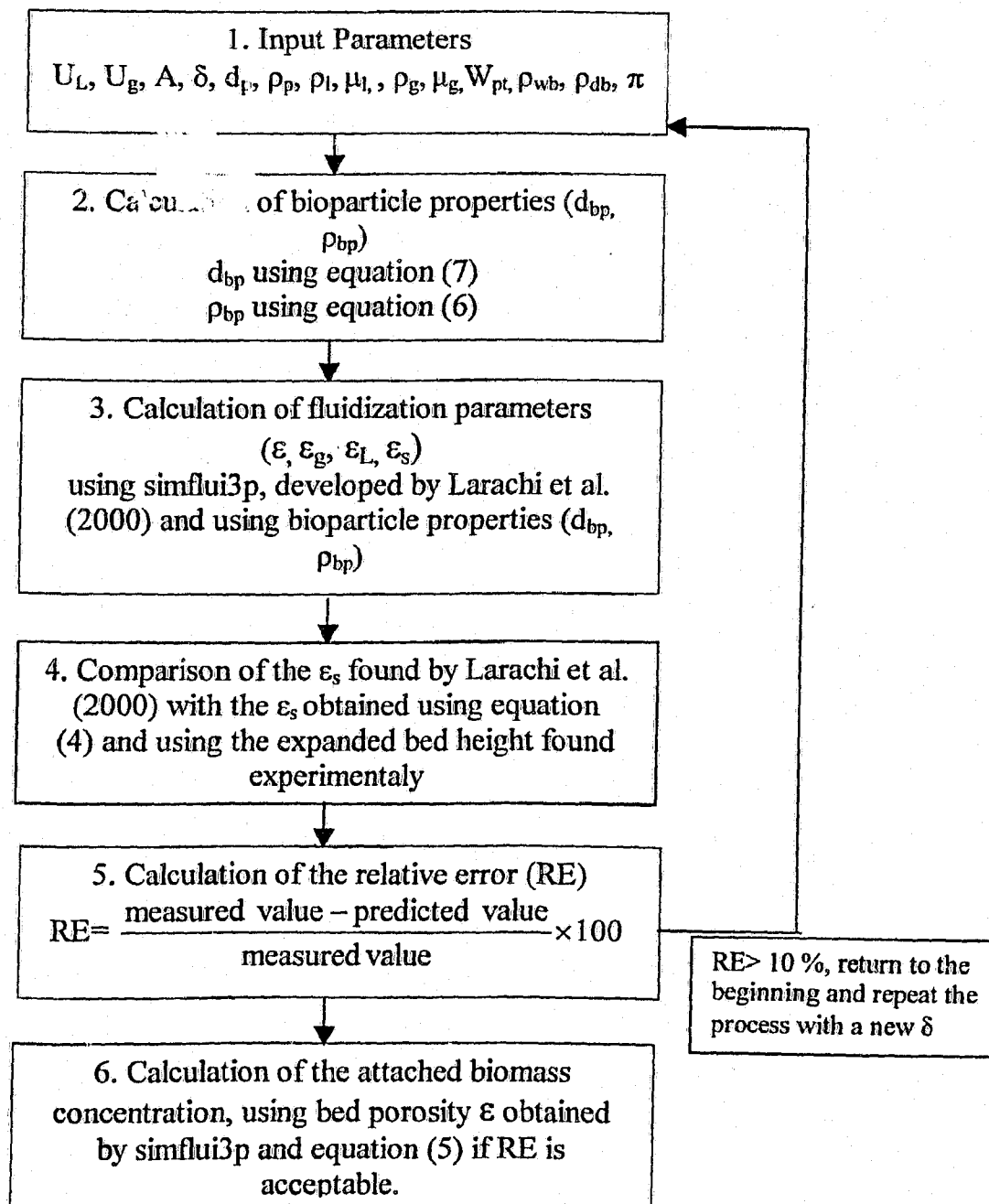
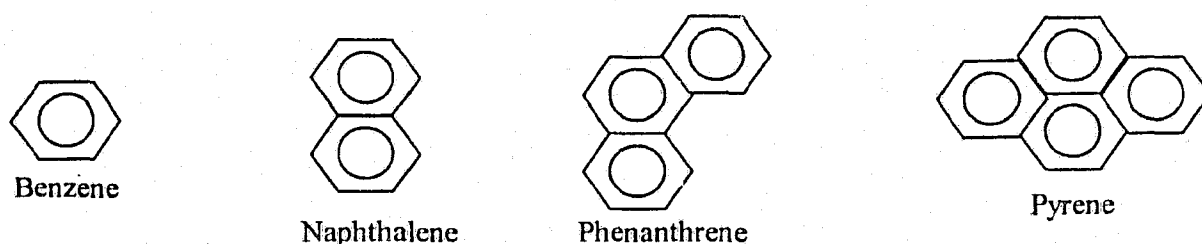


FIGURE 2.4 FLOW CHART TO PREDICT THE BIOMASS CONCENTRATION IN THE THREE-PHASE FLUIDIZED BED BIOREACTOR

2.3 DIESEL FUEL BIODEGRADABILITY

Diesel fuels are a complex mixture of hundreds of different hydrocarbons, mainly n-paraffin, branched paraffin, cyclo-paraffin and aromatic hydrocarbons. Generally long chain alkanes with carbon numbers in the range of C_{10} to C_{20} are the major paraffinic components. The aromatic and polynuclear aromatic compounds in diesel fuels include alkylated benzenes, indanes, naphthalenes, biphenyls, acenaphthenes, phenanthrenes, and pyrenes (Song et al. 2000). Diaromatic hydrocarbons with naphthalene-type structure are the more abundant aromatic components in diesel fuels. Figure 2.5 shows the ring structures of representative polycyclic aromatic compounds in diesel fuels. Most sulfur compounds in diesel fuel are alkylated benzothiophene-type and dibenzothiophene-type (Sepic et al. 1996). Trace amounts of nitrogen compounds in diesel fuels include indoles, carbazoles, quinolines, acridines, and phenanthridines. The oxygen compounds are alkylated phenols and dibenzofuran. Formulated diesel fuel also contains trace amounts of additives. Table 2.7 shows the composition of diesel fuel # 2 used in this research.



Adapted from Song et al. 2000.

FIGURE 2.5 RING STRUCTURES OF REPRESENTATIVE POLYCYCLIC AROMATIC COMPOUNDS IN DIESEL FUEL

COMPONENT	CONCENTRATION (% VOLUME)	COMPONENT	CONCENTRATION (% VOLUME)
C ₁₀ Paraffins	0.9	C ₁₅ Paraffins	7.4
C ₁₀ Cycloparaffins	0.6	C ₁₅ Cycloparaffins	5.5
C ₁₀ Aromatics	0.4	C ₁₅ Aromatics	3.2
C ₁₁ Paraffins	2.3	C ₁₆ Paraffins	5.8
C ₁₁ Cycloparaffins	1.7	C ₁₆ Cycloparaffins	4.4
C ₁₁ Aromatics	1.0	C ₁₆ Aromatics	2.5
C ₁₂ Paraffins	3.8	C ₁₇ Paraffins	5.5
C ₁₂ Cycloparaffins	2.8	C ₁₇ Cycloparaffins	4.1
C ₁₂ Aromatics	1.6	C ₁₇ Aromatics	2.4
C ₁₃ Paraffins	6.4	C ₁₈ Paraffins	4.3
C ₁₃ Cycloparaffins	4.8	C ₁₈ Cycloparaffins	3.2
C ₁₃ Aromatics	2.8	C ₁₈ Aromatics	1.8
C ₁₄ Paraffins	8.8	C ₁₉ Paraffins	0.7
C ₁₄ Cycloparaffins	6.6	C ₁₉ Cycloparaffins	0.6
C ₁₄ Aromatics	3.8	C ₁₉ Aromatics	0.3

Adapted from Perryman, 2003.

TABLE 2.7 COMPOSITION OF DIESEL FUEL # 2 USED IN THIS RESEARCH

Diesel fuels have been previously degraded in soils, water, and groundwater using microorganisms under aerobic and anaerobic conditions (Marquez-Rocha et al. 2001, Cassidy and Irvine 1997, Gao et al. 1999). It has been reported that microorganisms such as *Pseudomonas aeruginosa*, *Pseudomona putida*, *Azolla*-derived bacterial consortium can successfully degrade diesel fuel under aerobic conditions (Cohen et al. 2002, Rahman and Rahman 2002, Richard and Vogel 1999 and Sepic et al. 1996). Bioremediation of contaminated environments can take place on the affected area or in a bioreactor and can be performed under aerobic or anaerobic conditions. Zhang et al. (1995) have indicated that

transformation of petroleum hydrocarbons in general under aerobic conditions takes place faster than under anaerobic conditions.

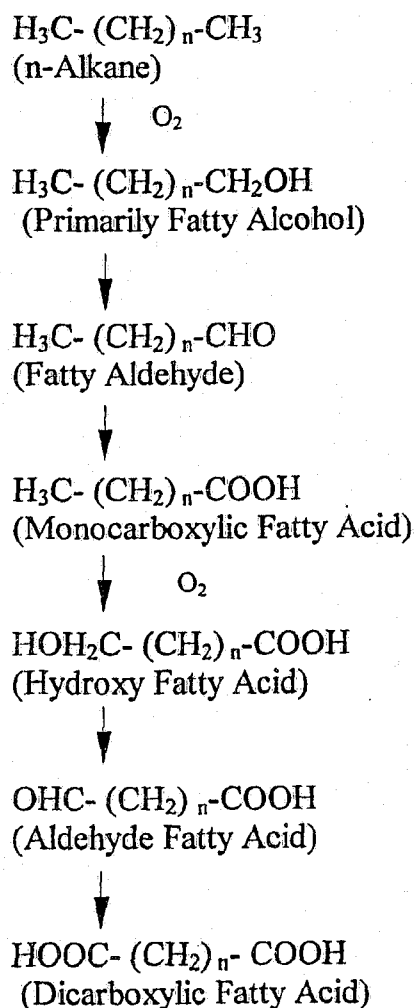
In addition to the electron acceptor (oxygen), and the substrate (the carbon in diesel fuels), another factor that can control the success of biodegradation is an adequate supply of nutrients (nitrogen, phosphorus and sulfur). Microbial populations in diesel-contaminated environments are likely to be under deficit of nitrogen due to the fact that diesel only contains trace amounts of nitrogen containing compounds.

Another factor that control the success of biodegradation is the structure of the substrate. It has been demonstrated that alkanes in the range of C_{10} to C_{26} show the most rapid biodegradation, and complex structures (branches and ring structures) are more resistant to biodegradation processes (Sepic et al. 1996). Rittmann and McCarty (2001) have indicated that the greater the complexity of the hydrocarbon's structure, the slower the rates of degradation and the greater the possibility of intermediary metabolites products.

Although diesel fuels are an essentially water-insoluble compound, microorganisms posses a mechanism for the uptake of hydrophobic, water-insoluble compounds across the cell. The processes of hydrocarbon utilization, transport and uptake by microbial cells have been widely reviewed by Atlas (1984).

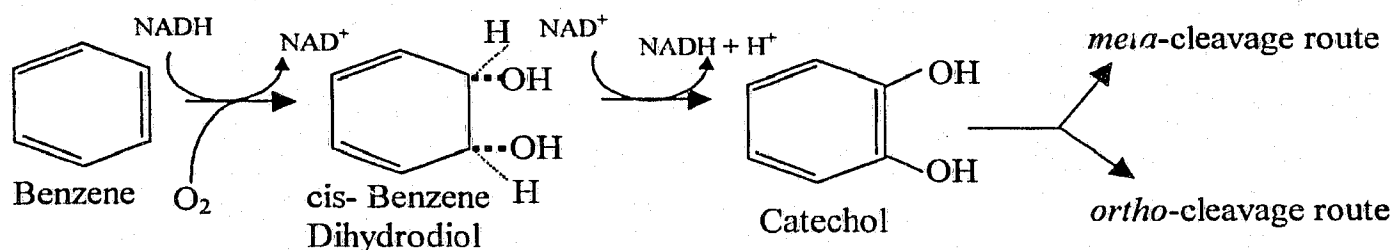
The major metabolic pathway for hydrocarbons has been elucidated in recent years. It is generally accepted that either short or long chains alkane are oxidized to the corresponding alcohol, aldehyde and fatty acid via β -oxidation using oxygenases enzyme for which molecular oxygen is required (Atlas 1984 and 1985, Rittmann and McCarty, 2001). The major metabolic pathway for aromatic hydrocarbons involves the formation of catechol (Smith, 1990). Figures 2.6 and 2.7 show the major metabolic pathway for a diterminal

alkane and part of the biodegradation routes of benzene. It is important to point out that little information is available related to the kinetic of biodegradation of aromatic hydrocarbons in biofilm system. Arcangeli and Arvin (1995) have reviewed some kinetics of biodegradation of aromatics compounds such as benzene, toluene, phenol and ethylbenzene.



Adapted from Atlas, 1984.

FIGURE 2.6 PATHWAY OF DITERMINAL ALKANE OXIDATION UNDER AEROBIC CONDITIONS



Adapted from Smith, 1990.

FIGURE 2.7 PATHWAY OF BENZENE OXIDATION UNDER AEROBIC CONDITIONS

A common characteristic of the biodegradation of hydrocarbons under aerobic conditions is the introduction of oxygen into the hydrocarbon molecule, which requires an energy investment in the form of NADH (Nicotinamide Adenine Dinucleotide). Oxygenation reactions introduce one or two -OH groups into the hydrocarbon structure. Figure 2.7 shows the two divergent pathways during benzene biodegradation. Both share the same initial steps resulting in the formation of catechol. The *ortho*-cleavage route and the *meta*-cleavage route involve the formation of the derivatives of the catechol. Figure 2.6 shows the major metabolic pathway for a diterminal alkane with the formation of a fatty alcohol.



3.1 Experimental Program

To evaluate the performance of the three-phase fluidized bed reactor for the treatment of wastewater contaminated with diesel, and the hydrodynamic properties and biofilm characterization, the experimental program was developed in four phases.

Phase I: Preparation of microorganisms inoculums and reactor start-up procedure.

Phase II: Reactor operation in intermittent mode.

Phase III: Reactor operation at steady state.

Phase IV: Validation of diesel biodegradation.

In Phase I, fresh biomass collected from the rotating biological contactor (RBC), located in the same laboratory, was inoculated in the fluidized bed. The reactor was set to work in batch conditions to ensure immobilization of the microorganisms on the support particles.

The objective of Phase II is to evaluate the maximum concentration of diesel able to be removed in the reactor in intermittent mode.

In Phase III the reactor was set to work at steady state with respect to diesel biodegradation. The objective of Phase III is to obtain steady state data with respect to diesel biodegradation to enable process scale-up.

The objective of Phase IV is to evaluate the losses of diesel due to volatilization and adsorption into the packing material.

3.2 Experimental Facilities

The experiments were conducted at the “Water and Wastewater Treatment Technologies” laboratory at Ryerson University. A schematic drawing of the experimental system is shown in Figure 3.1. The experimental unit consisted of a column, a feedwater tank, a feeding pump, a flow meter, an air flow meter, valves and circulation pipes. The system can be operated as a batch or continuously with or without recycle. A brief description of the equipment and instrumentation used in this research are summarized in Table 3.1.

The vial samples for the measurements of the concentration of diesel in the wastewater and in the liquid effluent were taken to the “Ryerson University Analytical Center ” for gas chromatograph analysis.

The bioparticles samples were taken to the “Advanced Microscopy Facilities” at the Department of Applied Chemistry and Biology for microscopy inspection.

EQUIPMENT	DESCRIPTION
Column (Fluidized Bed)	170 mm diameter, 3.0 m in height, 73 L capacity
Feedwater Tank	200 L capacity
Liquid Flow Meter	1.0 - 6.0 L/min
Air Flow Meter	4 - 45 L/min
Feedwater Pump	½ HP, 1725 RPM
DO Meter's Probe	YSI Model 5739 Probe
DO Meter	YSI Model 58
Colorimeter	Orbeco-Hellige 975 MP (Water Analysis System)
COD Heater Block	1-15 Tube heater block
Turbidity Meter	Turbidity model 800
Gas Chromatography	Perkin/Elmer AutoSystem XL Gas Chromatograph, Turbomass Software
Microscopy	Renishaw Raman imaging Microscope WiRe™ (Windows-based Raman Environment)
pH Meter	HI 9025C pH Meter
pH Electrode	HI 1230B pH Electrode
Furnace	General-Purpose Furnace FB 1300 Model.

TABLE 3.1 DESCRIPTION OF THE EQUIPMENTS USED IN THIS RESEARCH

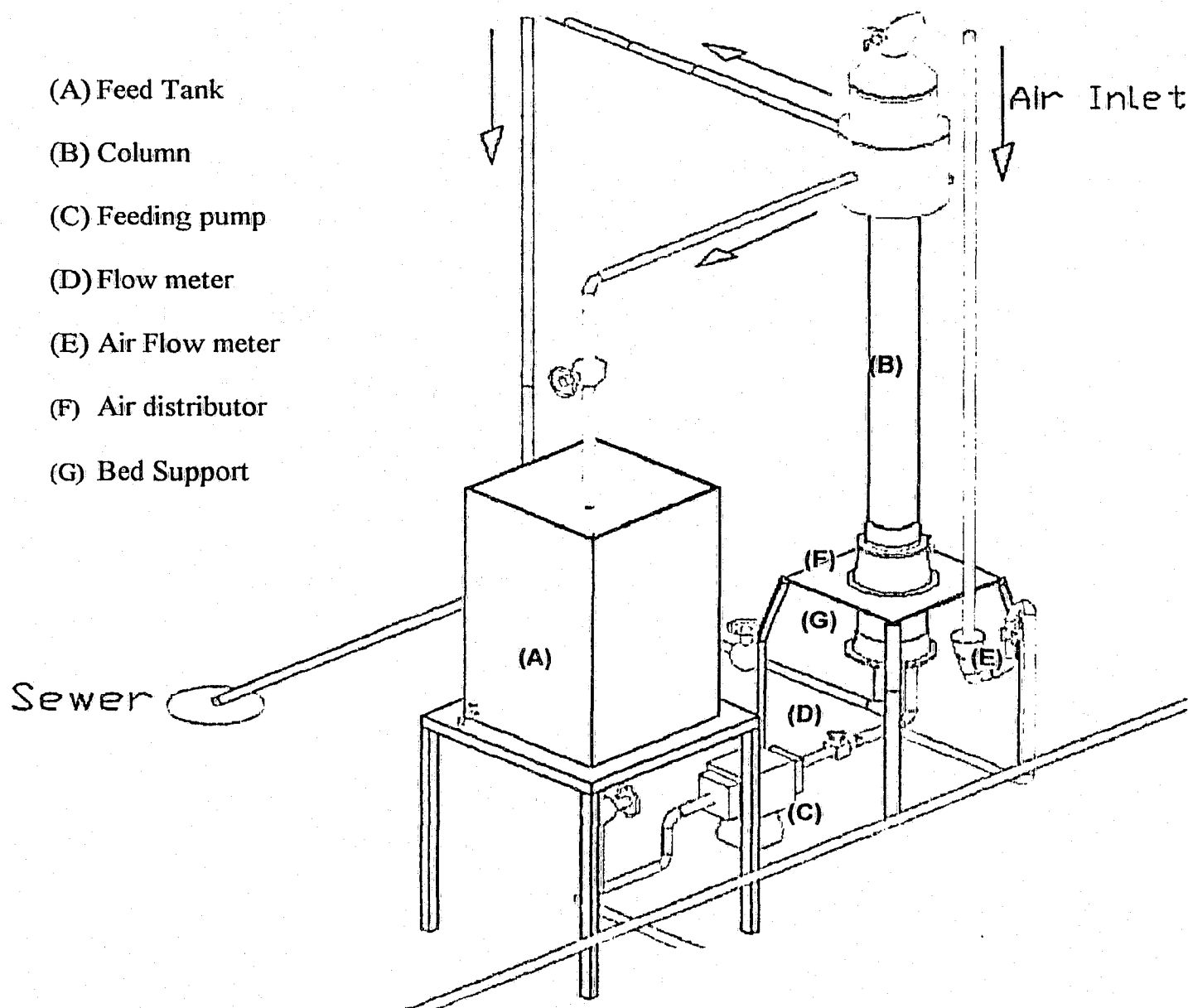


FIGURE 3.1 SCHEMATIC OF THE THREE-PHASE FLUIDIZED BED REACTOR SET-UP

3.2.1 Three-Phase Fluidized Bed Bioreactor

A pilot-scale fluidized bed bioreactor shown in Figure 3.3 was employed to obtain required experimental data. The reactor was divided into different parts including: liquid inlet, air inlet, air distributor, column, liquid drain, air outlet and recycle pipe.

The liquid inlet was located at the bottom of the reactor. This device is made of PVC with pipes for the liquid exits. The liquid is pumped from the feedwater tank through a pump connected to a 20 mm (internal diameter) PVC pipe. The liquid flow rate was adjusted using a liquid flow meter from 1 to 6 L/min.

Compressed air was injected into the bioreactor, directly from the bottom of the bed, through a U-turn pipe, which was necessary to prevent back flow of liquid into the air flow meter, in case of power failure. A central air compressor, situated in the basement of the Ryerson University building, supplied the air necessary for the experiments.

Figure 3.2 shows an actual picture of the air-liquid device to distribute air and liquid into the column. The system was made of a PVC material, with exception of the copper tubing device (13 mm of internal diameter) used for the injection of air. Liquid entered the column through a PVC pipe 50 mm diameter. The liquid flows into the distributor and mixes with the air that is injected into the column. An air distributor plate (135 mm of diameter) was placed at the end of the air inlet. The air distributor plate was perforated with 1.9 mm holes that produced small and smooth air bubbles. The air leaves at the top of the column through an 80 mm pipe.

The reactor consists of a straight constant diameter column made up of Pyrex glass with an inner diameter of 170 mm, 3.0 m in height, and 73 L capacity, with sampling ports installed

along the column length to remove liquid and bioparticles samples. The body of the column has a cross-sectional area of 0.0227 m^2 .

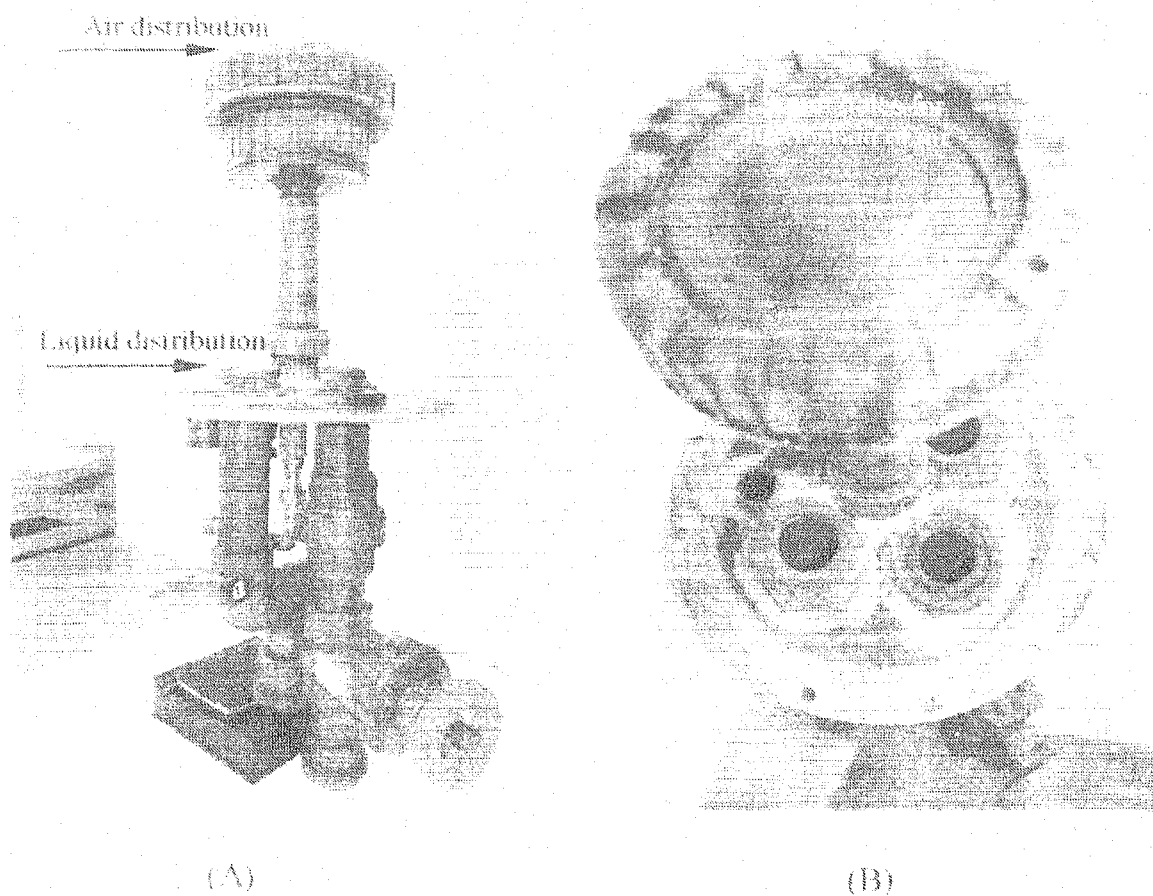


FIGURE 3.2 AIR AND LIQUID DISTRIBUTION IN THE REACTOR

(A) FRONT VIEW

(B) TOP VIEW

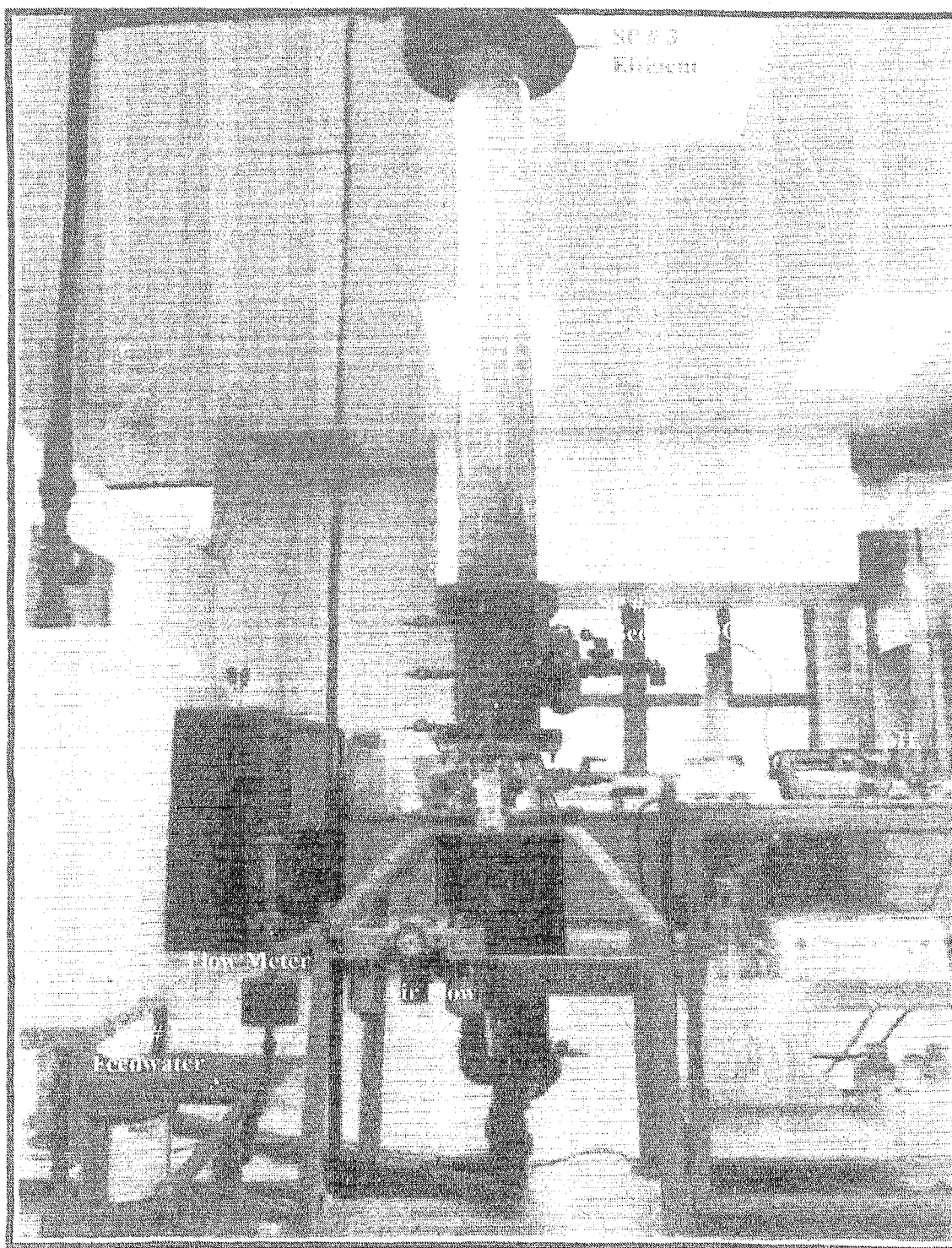
The liquid leaves the column through a 39 mm PVC recycling pipeline that returns to the feed tank to be recycled. The liquid also leaves the system through a 32 mm outlet located at the top of the reactor. Another drainage pipeline was located at the bottom of the reactor and it is used both to wash the column and as a drain in emergency situations.

Meshes were put in place to prevent particles from getting into the tank or falling to the lower part of the column. The top of the column was covered with an iron mesh to retain the solids from getting into the feeding tank. The lower part of the column was covered with a stainless steel golden mesh filter to retain the 600 μm particles used for microorganisms immobilization.

There were 8 sampling ports along the experimental unit from which liquid samples could be taken. However, only 3 sampling ports were used due to the configuration of the reactor. The sampling port # 1 (SP #1) was located at the bottom of the feeding tank and it was used to take liquid samples. The sampling port # 2 (SP #2) is located at 250 mm from the air distributor and it was used to take liquid and bioparticles samples. The sampling port # 3 (SP #3) was located at the top of the column and it was used for both liquid sampling and for bioparticles sampling from the upper part of the column.

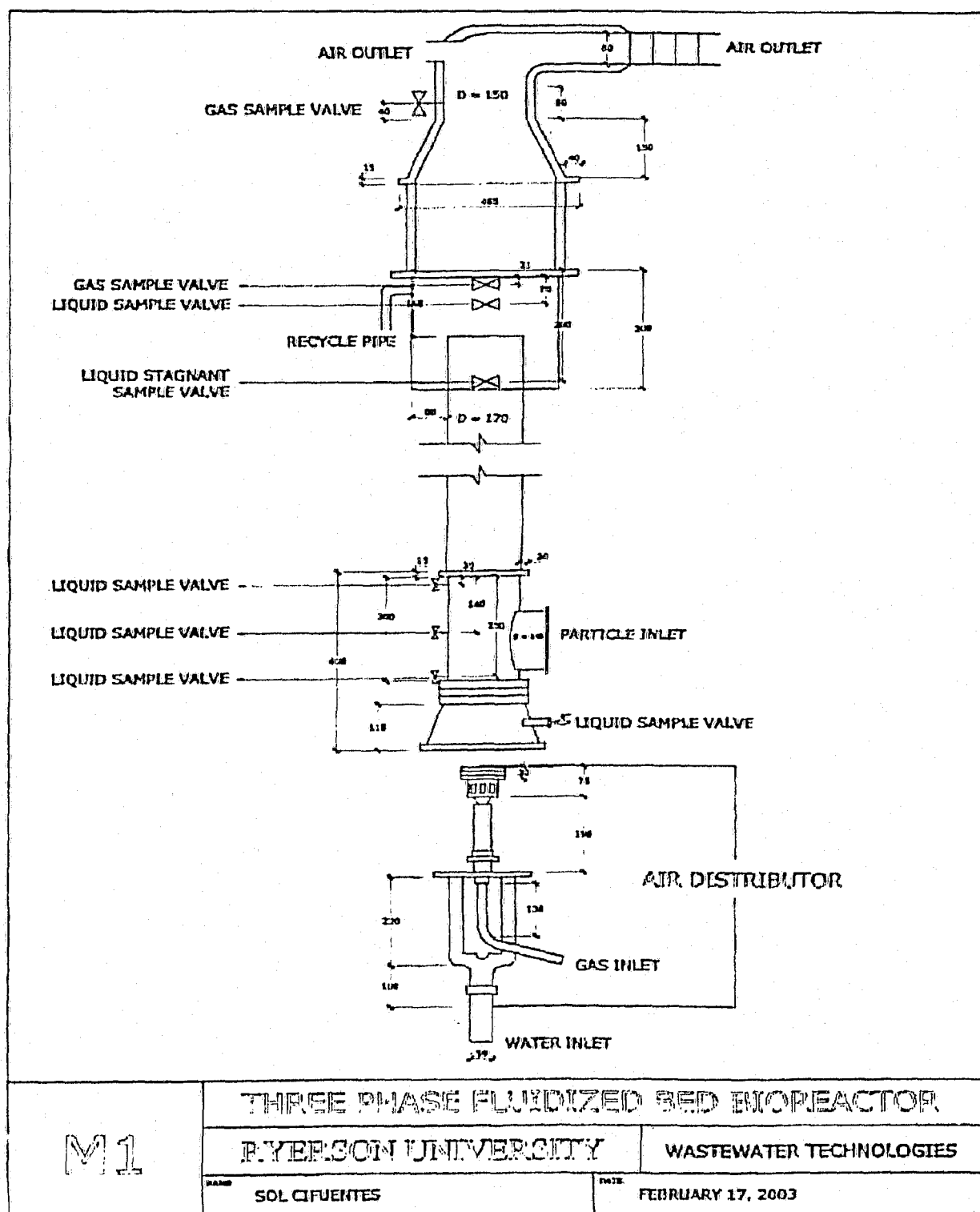
Dissolved oxygen meter, pH meter and turbidity meter were placed in a table near the experimental unit for fast measurements. Liquid samples were taken from SP #1, SP #2 and SP #3 at fixed time intervals every day during operation.

Full-scale view of the experimental facilities and a detailed description of the three-phase fluidized bed dimensions are shown in Figure 3.3 and Figure 3.4 respectively.



Note: SP (Sampling Port)

FIGURE 3.3 THE FULL-SCALE EQUIPMENT USED FOR THE
EXPERIMENTAL RESEARCH



(Adapted from Cifuentes, 2003)

FIGURE 3.4 THREE-PHASE FLUIDIZED BED DIMENSIONS

3.2.2 Biofilm Support

The biofilm support used in this research was lava rock. Lava rock was mechanically crushed at the engineering facilities at Ryerson University prior to sieving to obtain an average particle diameter of 600 μm . The solids were washed with distilled water and dried overnight at 103°C, and then added into the fluidized bed. A photograph of the support particles used in the fluidized bed is shown in Figure 3.5 and properties of the lava rock are shown in Table 3.2.

PARAMETERS	VALUE
Average diameter, d_p (μm)	600
Particle density ^a ρ_p (Kg/m^3)	1790
Total particle weight, W_{pt} (g)	1000
Minimum fluidization velocity ^b (cm/s)	0.3
Porosity ^c (%)	35.6

^a Cifuentes, 2003

^b Measured in water

^c Taken as volcanite material. Adapted from Melin et al. 1998

TABLE 3.2 LAVA ROCK CHARACTERISTICS

It is important to point out that lava rock was selected as the support particles due to the advantages that it gives for bacteria immobilization. Properties such as a high porosity, adequate density and low cost were prioritized for the selection of the support particle.



FIGURE 3.5 LAVA ROCK PHOTOGRAPH

3.2.3 Instrumentation

Dissolved oxygen, temperature, pH and turbidity were constantly monitored during this research.

The dissolved oxygen was measured using an YSI Model 58 oxygen meter that was connected to the fluidized bed by a plastic tube. The oxygen concentrations were measured in mg/L. The probe was constantly calibrated with saturated air. Magnetic stirrers were placed into the container that containing the liquid to obtain homogeneous sampling and accuracy in the measurements. The type of meter used in this research can be adjusted to atmospheric pressure and ambient conditions. A picture of the dissolved oxygen meter used in this research is shown in Figure 3.6.

Temperature in $^{\circ}\text{C}$ were measured in the same meter with a relative error of ± 0.1 . Temperature was controlled in the feeding tank at $20 \pm 0.5^{\circ}\text{C}$ and it was also measured at the liquid effluent.

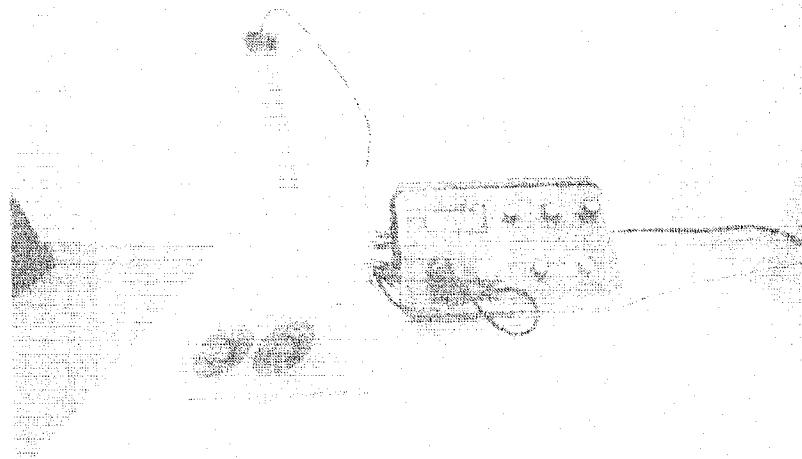


FIGURE 3.6 DISSOLVED OXYGEN METER AND PROBE USED IN THIS RESEARCH

A Hanna HI 9025 pH meter was used to measure acidity/alkalinity of the medium. The pH was directly read from the screen. The probe was constantly calibrated with a buffer solution of pH 4. Magnets stirrer were used to obtain a homogeneous medium for sampling. Figure 3.7 shows a picture of the pH and turbidity meter used in this research.



FIGURE 3.7 PH METER (LEFT) AND TURBIDITY METER (RIGHT) USED IN THIS RESEARCH

Turbidity values were also monitored in this investigation. A Turbidity Meter Model 800 manufactured by VWR, INTERNATIONAL was used to measure the quality of the feedwater and the liquid effluent. The measured turbidity was assessed immediately after the sample was taken in order to prevent particle flocculation and sedimentation. The measurement unit was in NTU (nephelometric turbidity units). The turbidity meter was pre-calibrated with a solution of turbidity 0 and 10, respectively. The technique for the turbidity measurements follows the same protocols for 2130 Turbidity used by Standard Methods for the Examination of Water and Wastewater (APHA, 1998).

3.3 Analytical Methods

The performance of the TPFBR was evaluated using chemical oxygen demand determination, gas chromatograph technique, and suspended solids determination. Microscopy inspection was performed to determine the thickness of the biofilm for the estimation of the attached biomass concentration.

3.3.1 Chemical Oxygen Demand Determination

Chemical oxygen demand (COD) is defined as the amount of a specified chemical oxidant that reacts with the sample under certain conditions. The MICRO-COD test method developed by Bioscience, Inc. is used to determine COD of the liquid samples. This method is based on a colorimetric technique, where the sample is digested with a solution of dichromate ion ($\text{Cr}_2\text{O}_7^{2-}$) oxidizing COD material in the sample. The method used was Test Kit No. 975-62 for high range COD between 100–4500 mg/L. The twist-cap vials were

purchased from VWR, INTERNATIONAL. Figure 3.8 shows the set up for measuring the COD of the sample.

Samples were collected from SF 31 and SF 39 for COD characterization of the hardwater and liquid effluent respectively. 50 ml. samples were homogenizing for approximately 2 minutes to obtain a representative sample and 0.5 ml. was added to the vials. The twist-cap vials were placed in a COD heater block at $150 \pm 2^\circ\text{C}$ for 2 hours. After two hours, the vials were removed and allowed to cool down for 10 minutes. The COD was directly read in mV/L using an Orionco-Hellige 975 MP colorimeter.

It is important to point out that this test was used over the BOD (biochemical oxygen demand) because the COD test can be completed in about 2.5 hours compared with 5 days for the BOD test.

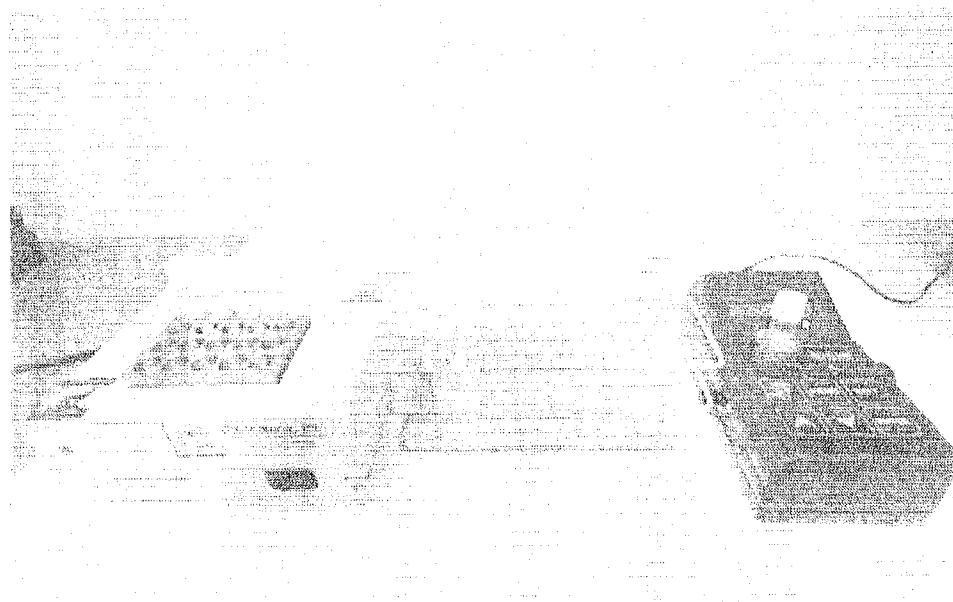


FIGURE 3.8 COLORIMETER AND HEATER BLOCK SET UP FOR THE MEASUREMENTS OF COD.

3.3.2 Liquid-liquid extraction and Gas Chromatography Technique

To assess a gas chromatography technique liquid-liquid extraction was performed to extract diesel from the liquid phase using a solvent. The liquid-liquid extraction technique follows similar protocol used by Environmental Protection Agency (EPA Method 8041). The solvent used for the extractions was dichloromethane (DCM), also known as ethylene chloride. To determine the unknown concentration of diesel it was necessary to establish a calibration curve with known concentrations of a modified Diesel Range Organics (DRO) and 5-Alpha Androstane as an internal standard (IS). Refer to Appendix A for a series of chromatographs used at different diesel concentrations to assess the calibration curve.

Samples of feedwater and liquid effluent were taken at the feeding tank (SP #1) and at the top of the column (SP #3) respectively. The samples were transferred to a 1 L separatory funnel where DCM was added. The separatory funnel was shaken for about 2 minutes. The lower organic layer was drawn from the bottom of the flask, after it rested for 15 minutes, and then passed through a funnel containing a plug of glass wool with 20 g of anhydrous sodium sulfate. The samples ready for gas chromatographic analysis were transferred to an auto sampler vials with twist tops. The amount of diesel isolated from feedwater and effluent samples was determined using a gas chromatograph coupled with a mass spectrometer. The total area of peaks between C_{10} to C_{20} was considered to represent the total of DRO.

3.3.3 Microscopy

Microscopy inspection was performed to determine the thickness of the biofilms. This parameter is used to calculate the attached biomass concentration in the reactor. A Renishaw

Raman imaging Microscope WiRe TM (Windows-based Environment) was used in this research to measure the thickness of the biofilm.

The bioparticles samples from SP #2 and SP #3 were placed in crystal slides and taken to the “Advanced Microscopy Facilities” at the Department of Applied Chemistry and Biology.

3.3.4 Total Suspended Solids Determination

Total suspended solids are defined as those solids that are retained by the filter and dried to constant weight at 103-105 °C, and it represent the suspended biomass in the reactor.

Measurement of the total suspended solid follows the same protocol used for Standard Method for the Examination of Water and Wastewater, 1998 (Test 2540). A well-mixed sample from SP # 3 is filtered through a standard GF/F glass fiber filter disk. The residue retained on the filter is transferred to an inert aluminum dish and dried to constant temperature at 103-105 °C in a general-purpose Furnace FB 1,000.

3.4 Experimental Procedure and Data Collection

Experiments were carried out in four phases as previously mentioned. Preparation of microorganism's inoculums and reactor start-up was carried out in Phase I. The first set of experiments was performed in Phase II to evaluate the maximum concentration of diesel able to be removed in the reactor in intermittent mode. The second set of experiments was performed in Phase III to obtain data with respect to diesel biodegradation in steady state conditions. The third set of experiments was carried out in Phase IV to evaluate losses of diesel due to volatilization and adsorption.

3.4.1 Phase I: Preparation of Microorganisms Inoculum and Reactor Start-Up Procedure

The experimental procedure used for microorganism's inoculums and reactor start-up is described as follows:

1. One kg of clean lava rock was placed at the bottom of the column.
2. Cold and hot water taps were opened simultaneously to create the desired water temperature. The water temperature was adjusted and kept constant throughout the experiment at 20 ± 5 °C.
3. The feeding tank was filled with tap water at the desired temperature; nutrients and 50 mg/L of diesel were added. The pH was set to 7.0 ± 0.3 with the addition of NaOH when it was required. The essential nutrients for bacterial growth are described in Table 3.3.
4. 5L of fresh biomass solids were collected from the first stage of the Rotating Biological Contactor (RBC), and added to the column through the device located in SP #2.
5. The start-up operation was set at a minimum fluidization velocity of 0.3 cm/s corresponding with a liquid volumetric flow rate of approximately 4 L/min. The injection of air at 1.0 cm/s (superficial velocity) increased the DO in the liquid phase. The system was set to work during batch conditions to ensure biofilm attachment into the support particles.
6. Every four hours, 1 L and 100 ml of samples was taken from SP #1 and SP #2 for DO and pH measurements.

7. Renewal of the feedwater was carried out approximately every three days. pH of the synthetic wastewater feed was set at 7.0 ± 0.2 with periodical addition of NaOH upon need.
8. Ten Particle samples were taken from the middle region of the fluidized bed (SP #2) for microscopy inspection every five days.

Biomass growth was visually observed as gray and sometimes light gray coatings on the support particles. At this point the fluidized bed was set to work at intermittent mode (Phase II) with periodical additions of diesel and nutrients.

NUTRIENT	AMOUNT (g)	NUTRIENT	AMOUNT (g)
NH ₄ Cl	15.4	KH ₂ PO ₄	6.1
CaCl ₂ .6H ₂ O	0.06	MgSO ₄ .7H ₂ O	1.2
MgCl ₂ .4H ₂ O	0.12	FeSO ₄ .7H ₂ O	0.06
Na ₂ HPO ₄	61.0	NaCl	30.5

**TABLE 3.3 ESSENTIAL NUTRIENTS ADDED INTO THE REACTOR FOR
BACTERIAL GROWTH OF DIESEL DEGRADING ORGANISMS**

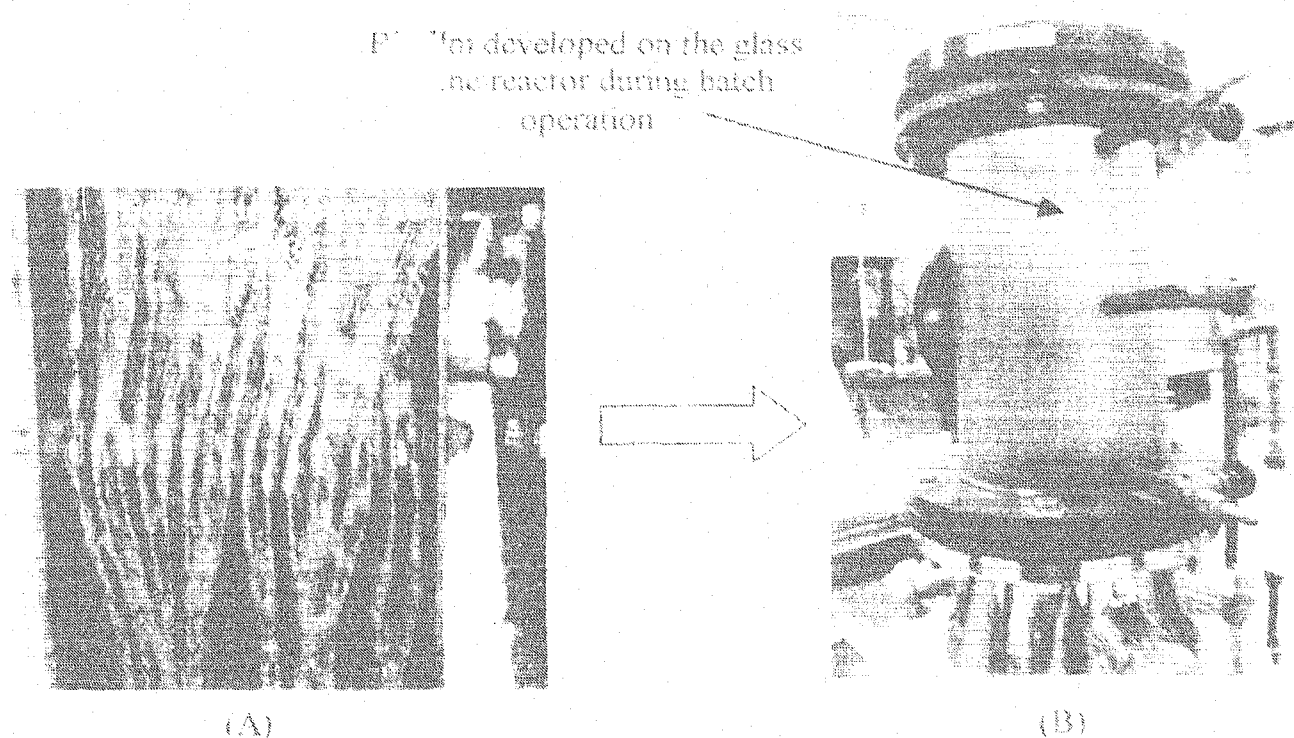


FIGURE 3.9 MICROORGANISMS INOCULUMS

(A) FIRST STAGE OF THE ROTATING BIOLOGICAL CONTACTOR (RBC)

(B) LOWER PART OF THE FLUIDIZED BED

3.4.2 Phase II: Reactor Operation in Intermittent Mode

At the end of the cultivation period, the system was set to work at intermittent mode without recycling and with daily additions of diesel and nutrients. In this phase diesel concentrations were gradually increased in order to assess the maximum diesel concentration that can be removed in the reactor. Every day the reactor was charged with fresh feedwater increasing the amount of diesel.

The experimental procedure is described as follows:

1. **Day one:** 75 mg/L of diesel and nutrients were added into the fluidized bed. The reactor was set to the new operating conditions of:
 - Liquid superficial velocity was set to 0.02 cm/s corresponding to a flow rate of 0.3 L/min.
 - Air superficial velocity was kept to 1 cm/s.
 - The experimental unit was set to work at once-through process at the hydraulic detention time of approximately 4 hours.
2. Samples of 100 ml, 50 ml, 1L, and 100 ml were taken from the feedwater (SP #1) for determining diesel concentrations, COD, DO and pH measurements respectively.
3. After two hours of operation, 1 L and 100 ml samples were taken from SP #2 for DO and pH inspection, respectively. This procedure was repeated one hour later.
4. After five hours of operation 100 ml, 50 ml, 1 L, and 100 ml samples were taken from the liquid effluent (SP #3) for determination of diesel concentrations, COD, DO and pH measurements, respectively.
5. **Day two:** 140 mg/L of diesel and also nutrients were added into the system following the same operating conditions and the same nutrient composition. The sampling followed the same procedure explained from point 2 to 4.
6. **Day three:** The same amount of 140 mg/L of diesel and nutrients were added into the reactor. Diesel concentrations in the feedwater were gradually increased up to 700 mg/L during 12 days of intermittent operation. The sampling procedure was same as that explained from point 2 to 4 for day one of operation.

Figure 3.10 shows the diesel concentrations during the 12 days of intermittent operation. These concentrations were chosen based on the RBC performance during treatment of wastewater contaminated with diesel.

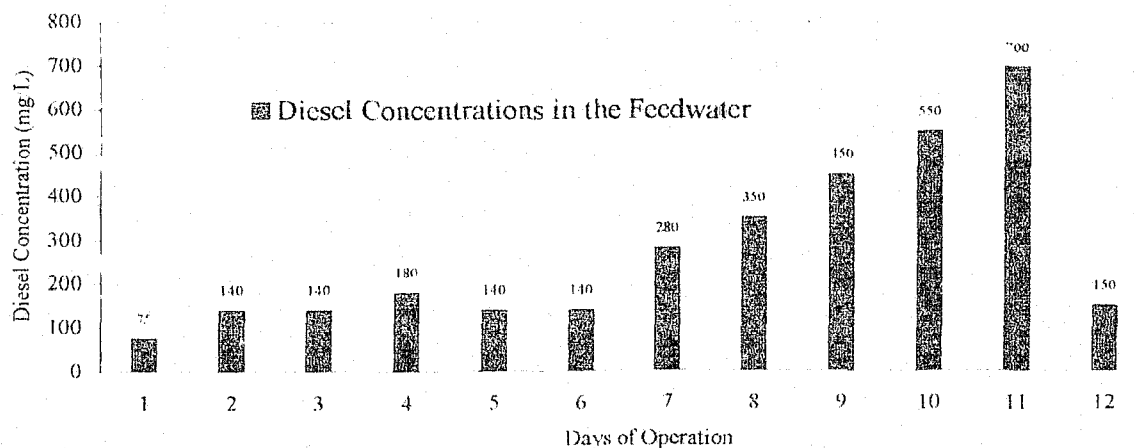


FIGURE 3.10 DIESEL CONCENTRATIONS DURING INTERMITTENT MODE

The maximum diesel concentration that can be removed in the reactor at the operating conditions and with the biofilm formed is experimentally determined during intermittent mode.

3.4.3 Phase III: Reactor Operation at Steady State

The fluidized bed was set to work at steady state with daily addition of the maximum concentration of diesel that can be removed in the reactor (determined in Phase II). To obtain steady state data (hydrodynamic and biofilm parameters) the experimental procedure is described as follow:

1. The reactor was set to treat the maximum concentration of diesel that the reactor could remove at the following operating conditions:

-Liquid superficial velocity of 0.02 cm/s.

-Air superficial velocity was kept to 1 cm/s (superficial velocity)

-Hydraulic detention time of 4 hours.

2. Diesel concentrations, COD, DO, pH and temperature were monitored following the same procedure explained from point 2 to 4 in intermittent mode.
3. For the microscopy measurement of biofilm thickness, ten bioparticles were taken from both the middle region of the fluidized bed and from the top of the reactor (SP #2, SP #3).
4. To determine the total suspended solids, 100 ml of the liquid sample were taken from SP #3. The turbidity was determined by taking 100 ml of the feedwater and the liquid effluent (SP #1 and SP #3).
5. This experiment was repeated for 5 days of steady state following the same operating conditions and repeating the same procedure explained from 2 to 4.

3.4.4 Phase IV: Validation of Diesel Biodegradation

To examine the amount of diesel that could be volatilized in the reactor, four experiments were run following the same operating conditions than in intermittent mode. During the performance of these experiments, the fluidized bed reactor was operated as follows:

1. Initially, one Kg of clean lava rock was placed at the bottom of the column. No microorganisms were added into the reactor.
2. Cold and hot water taps were opened simultaneously to create the desired water temperature of 20 ± 5 °C. The operating conditions were set at:

-Liquid superficial velocity of 0.02 cm/s

- Air superficial velocity of 1 cm/s.
 - Hydraulic detention time of 4 hours.
 - Dissolved oxygen concentrations were kept in the same range of operation during intermittent mode (4 -8 mg/L).
3. A known amount of diesel (100 mg/L) was added to the reactor every day during six weeks to achieve equilibrium between adsorption of the diesel into the lava rock.
 4. After six weeks, a set of four experiments was carried out varying the diesel concentrations in the feedwater. Samples were taken for gas chromatography inspection from both the feedwater and liquid effluent.



CHAPTER FOUR

INTERPRETATION AND DISCUSSION OF EXPERIMENTAL DATA

The experimental data were obtained when the acclimatizing period of the microorganisms was achieved and it was visually observed immobilized on the support particle. The experimental values were obtained from three groups of experiments.

- ⇒ **Group 1** refers to the experimental values obtained during Phase II of this research: Reactor operation in intermittent mode.
- ⇒ **Group 2** refers to the experimental values obtained during Phase III: Reactor operation at steady state.
- ⇒ **Group 3** refers to the experimental values obtained during Phase IV: Validation of the biodegradation of diesel.

Interpretation and discussion of the experimental data will follow the same order mentioned before.

4.1 Interpretation of the Experimental Results Obtained in Phase II: Reactor Operation in Intermittent Mode

The experimental data analyzed in this section correspond to the set of experiments carried out during the days 1 to 12 of intermittent mode. Following the 3-months batch acclimatizing period, diesel and bacterial nutrients were introduced in the reactor every day during 12 days. The diesel-loading rate during intermittent mode can be seen in Figure 4.1.

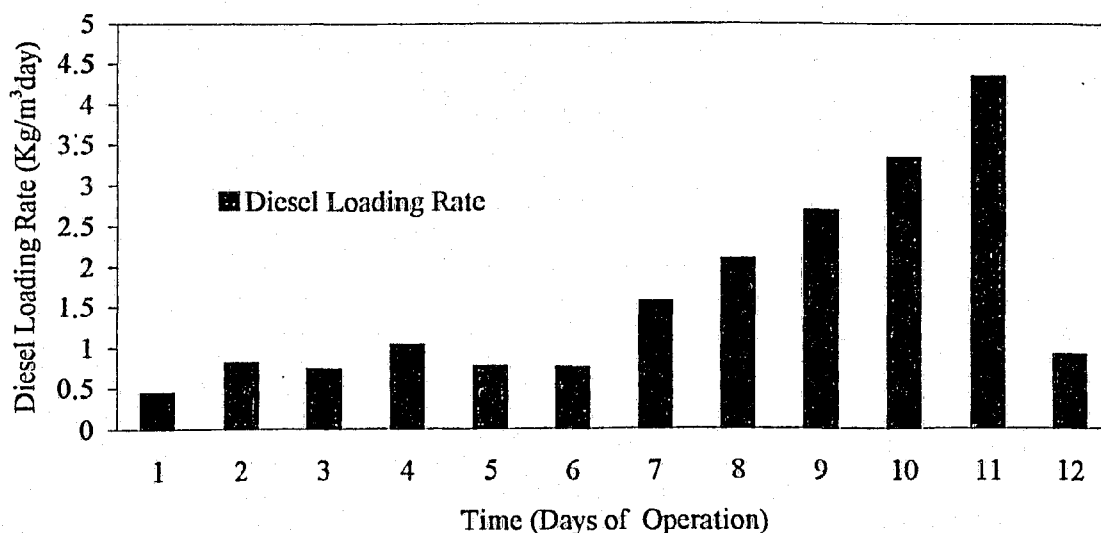


FIGURE 4.1 DIESEL LOADING RATES DURING THE 12 DAYS OF INTERMITTENT MODE

As a general remark related with the reactor start-up procedure, it should be pointed out that the nature of the inoculums and fluidization conditions govern the adhesion of microorganism into the lava rock. The duration of the 3 months acclimatizing period was considered excessive for industrial applications, where short start-ups are required. The reactor apparently showed good operational characteristics, but a power blackout in the Toronto area (August 2003) led to the shutdown of the reactor for 7 hours. As a result, the

reactor did not receive enough oxygen and septic conditions occurred in the reactor. This problem was overcome with the injection of two liters of fresh biomass collected from the rotating biological contactor and the re-establishment of the injection of air. The favorable conditions for microorganism's growth were reached after two weeks of the shutdown.

The diesel was fed at an initial loading rate of 0.43 Kg diesel/m³ day (69 mg/L of diesel at a flow rate of 0.3 L/min) and was gradually increased throughout 12 days of continuous operation until the diesel loading rate reached a value of 4.33 Kg diesel/m³ day (693 mg/L of diesel). The objective of these experiments was to investigate the maximum concentration of diesel that could be removed with the biofilm formed and at the operating conditions shown in Table 4.1.

PARAMETER	VALUE
U_L	0.02 cm/s
U_g	1 cm/s
τ	4 hours
Diesel Load Range	0.43-4.33 Kg diesel/m ³ day
COD Concentration Range	550-4000 mg/L

TABLE 4.1 OPERATIONAL CONDITIONS DURING INTERMITTENT MODE

Figure 4.2 shows the percent of diesel removed versus the diesel-loading rate during 12 days of intermittent mode. Removal efficiencies up to 100% were achieved, when the diesel loading rate varied between 0.4–1.2 Kg diesel/m³ day corresponding to diesel concentrations in the range of 70-200 mg/L. Within the range of the aforementioned concentrations the

operation of the experimental facility was very stable and the diesel concentration in the liquid effluent was always lower than 0.5 mg/L. Breakthrough of diesel was detected in the effluent after 6 days at a diesel-loading rate of 1.5 Kg diesel/m³day. At a higher diesel-loading rate of 2.0-4.3 Kg diesel/m³day, corresponding to a diesel concentration in the range of 350-700 mg/L, the removal efficiencies dropped up to 10%. At higher concentrations, the operation in the reactor became unstable and the diesel concentrations and chemical oxygen demand increased progressively. As an important remark, it should be pointed out that very high diesel removal efficiencies of 100% were achieved at a very low hydraulic detention time of 4 hours.

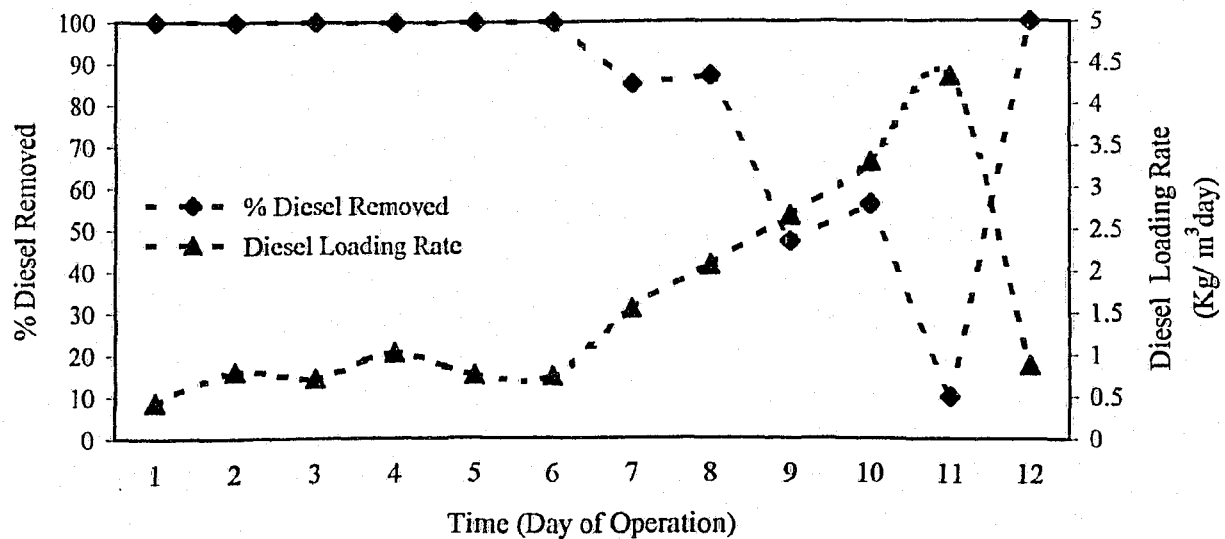


FIGURE 4.2 PERCENT OF DIESEL REMOVED AND DIESEL LOADING RATE DURING INTERMITTENT MODE

Higher concentrations of diesel in the liquid phase and in the biofilm surrounding could lead to a metabolic inhibition of the cells decreasing the specific conversion rate (Rittmann and McCarty, 2001 and Lai and Shieh, 1997). Inhibitors can affect either an enzyme active for substrate utilization or it can affect cell function such as respiration. This phenomenon can

cause reduced biomass levels that may slow degradation of the substrate. Rittman and McCarty (2001) have indicated that self-inhibition is a common type of inhibition for microorganisms in the presence of high concentrations of aromatic hydrocarbons.

The formation of white-foam products known as soluble microbial products (SMP), observed near the distributor of the fluidized bed, was taken as a sign of biodegradation processes. Lai and Shieh (1997) agree that microorganisms besides consuming substrate and producing new biomass will also generate SMP that can cause a white color or foam in the reactor.

Overall removal efficiency as a function of the chemical oxygen demand concentrations of the feedwater is presented in Figure 4.3.

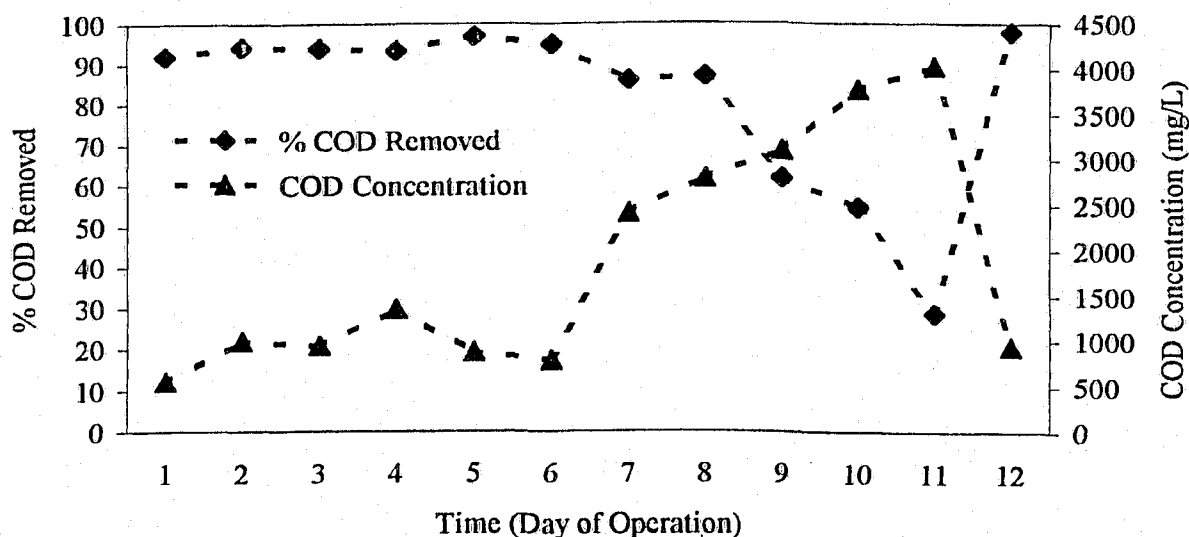


FIGURE 4.3 PERCENT OF COD REMOVED AND COD CONCENTRATIONS DURING INTERMITTENT MODE

The COD of the feedwater is mainly composed of nutrients and diesel. As shown in Figure 4.3, removal efficiencies around 90 % were achieved when the COD of the feedwater ranged between 500 and 2500 mg/L. The COD removal efficiency dropped up to 30 % for COD values around 4000 mg/L. As noted earlier, the COD removal efficiencies were obtained at a low hydraulic detention time of 4 hours.

Biological aerobic oxidation of hydrocarbons is a complex process that can be affected by various parameters such as dissolved oxygen concentrations, pH and temperature.

It is well known that the DO concentrations ranging between 2 and 4 mg/L are favorable for aerobic processes. MetCalf and Eddy, 2003 and Rittmann and McCarty, 2001, support this statement. In this research DO concentration in the feedwater was kept above 8 mg/L to ensure that enough dissolved oxygen is available for aerobic biological oxidation of the substrate.

Figure 4.4 shows the dissolved oxygen variation during intermittent mode. As we can see, DO concentration drops considerably at the lower section of the fluidized bed suggesting both dissolved oxygen utilization for oxidation of the substrate (diesel) and an increase in aerobic biological activity. The oxygen concentrations increase again at the liquid effluent due to the injection of air near the distributor. Diesel biological oxidation and the COD utilization during Phase I was observed at DO concentration between 4-10 mg/L. Thus, the oxygen was not a limiting factor for microbial activity during the degradation of the diesel and during COD utilization. These results are in agreement with Karapinar and Kargi (1996) and Metcalf and Eddy, 2003 who believe that this is one of the main advantages of the TPFBR, which overcomes oxygen transfer problems encountered in both activated sludge processes and tricking filters.

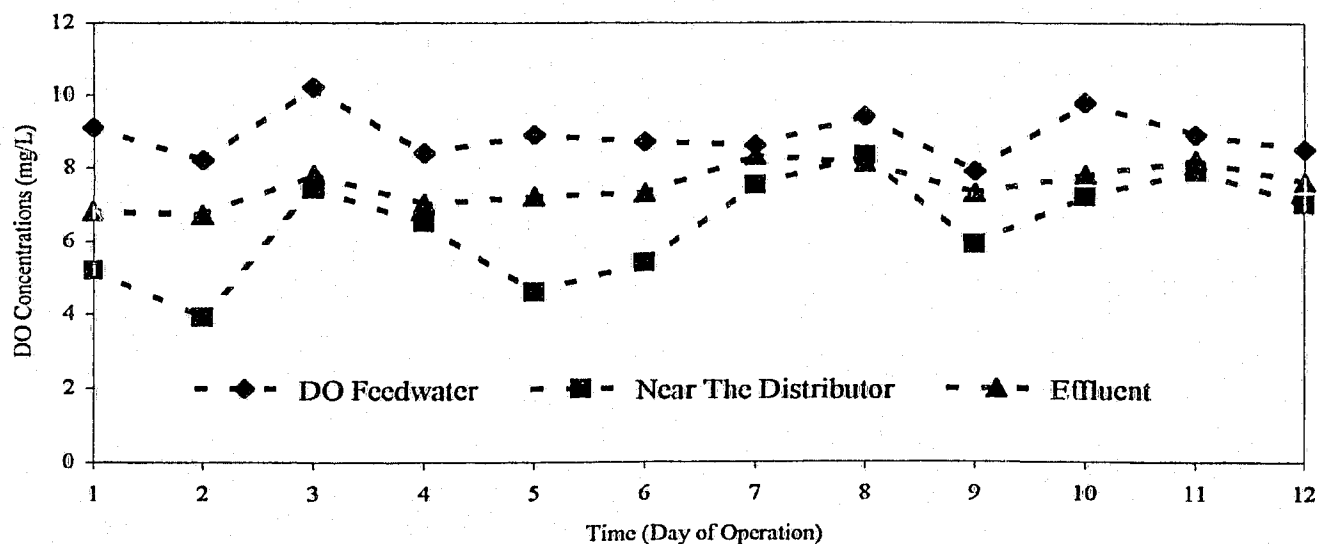


FIGURE 4.4 DISSOLVED OXYGEN DURING INTERMITTENT MODE

It should be also noted that the DO concentrations of the liquid effluent are above 6 mg/L. This indicates that the discharge of this effluent into rivers or estuaries is not considered to be a hazard for aquatic life because it is not depleted of oxygen.

Another important factor to consider in aerobic biological oxidation is the pH. Figure 4.5 shows the pH of the feedwater and the liquid effluent during the 12 days of intermittent mode. The pH was controlled at 7.5 ± 0.3 in the feedwater and it was found to decrease along the reactor.

It is important to point out that complete biological aerobic oxidation tends to increase the pH in fluidized biofilm process, and in other processes where biofilm technology is applied. The results obtained in this research suggest the presence of extracellular products like fatty acids resulting from the microbial utilization of straight-chain hydrocarbons (Atlas, 1984).

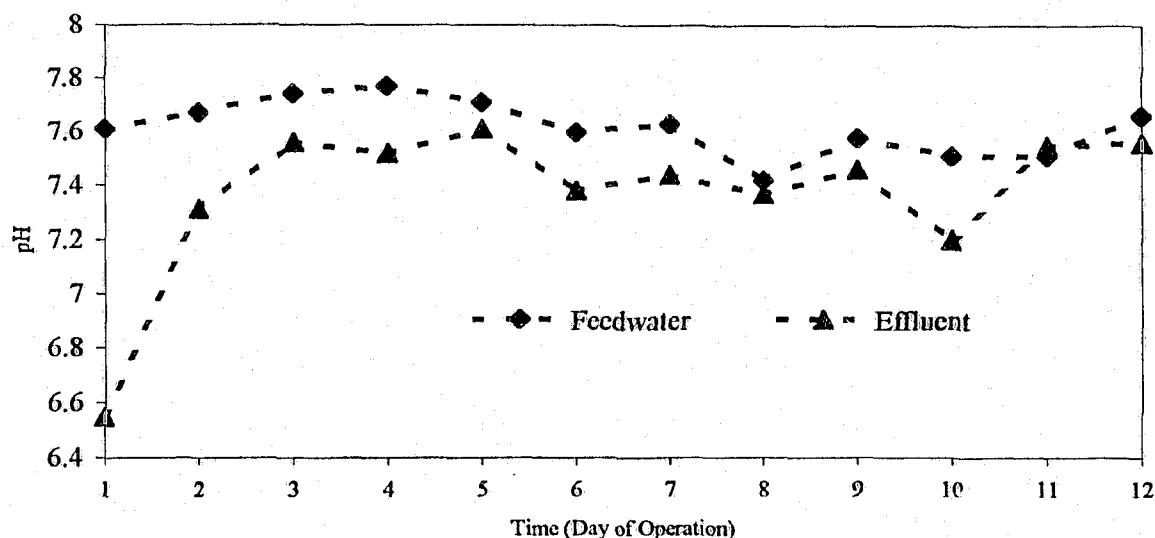


FIGURE 4.5 PH DURING INTERMITTENT MODE

Metcalf and Eddy (2003) have suggested that for treated effluent discharged to the environment the allowable pH range varies from 6.5 to 8.5. In this investigation the pH of the liquid effluent is still within the aforementioned recommendation that is between 6.5 and 7.5. This effluent is not considered to be hazardous to the environment.

The temperature is another factor to count in aerobic processes. MetCalf and Eddy (2003) have indicated that the most favorable temperature range for aerobic oxidation lies between 15 to 30 °C. During this experiment, the temperature was always kept above 15 °C up to 25 °C.

It was well established that 1.2 Kg diesel/m³day (200 mg/L) was the maximum load that could be removed in the reactor with no detectable diesel concentration in the effluent.

4.2 Interpretation of the experimental results obtained in Phase III: Reactor Operation at Steady State

To collect both steady-state data on diesel biodegradation, and to evaluate biofilm thickness to estimate the attached biomass concentration, the reactor was set to treat 200 mg/L of diesel (1.2 Kg diesel/ m³day) on day 13 through day 17. Diesel concentration, COD concentrations, DO concentration, pH, total suspended solids, turbidity and biofilm thickness were measured in every run. A constant rate of diesel was added to the feedwater, and diesel concentrations in the effluent showed 100% of removal at all times (Figure 4.6). Also, the COD values in this phase were around 1200 mg/L. The COD removal efficiencies were higher than 95 %. The percent of diesel removed and the percent of COD removed are shown in Figure 4.6 and 4.7 respectively. In this phase, steady state conditions prevail, that is the processes in the biofilm (endogenous metabolism, cell maintenance, cell losses due to shear) are balanced.

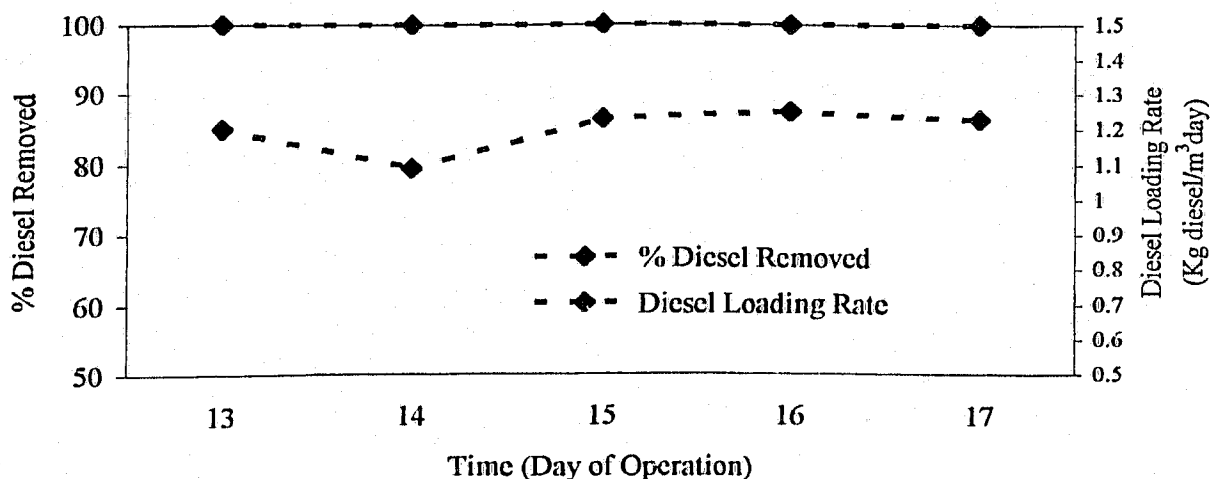


FIGURE 4.6 PERCENT DIESEL REMOVED AND DIESEL LOADING RATE DURING STEADY STATE

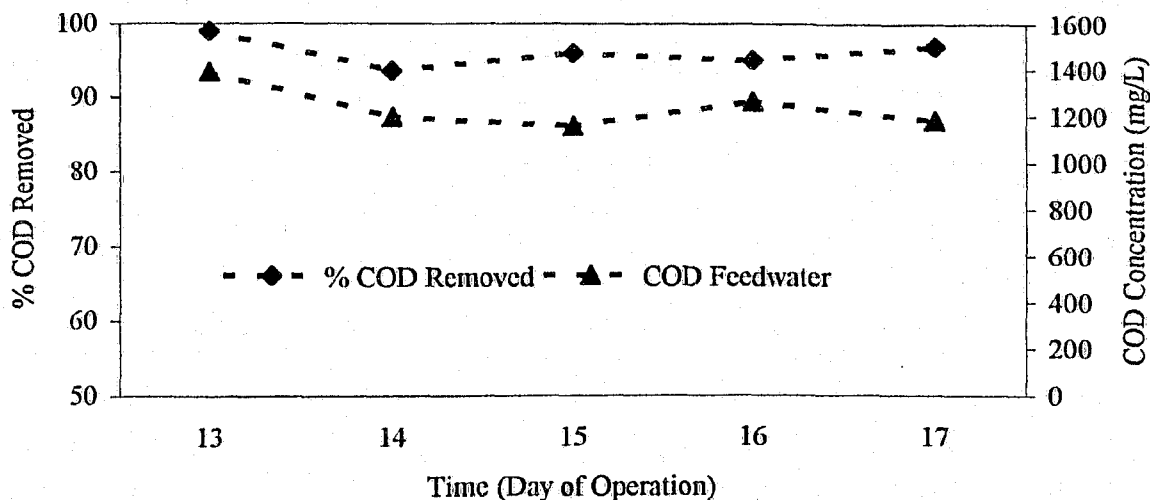


FIGURE 4.7 PERCENT COD REMOVED AND COD CONCENTRATIONS DURING STEADY STATE

The dissolved oxygen concentration follows the same trend than in Phase II. Figure 4.8 shows the DO concentrations versus height of the reactor on day 13 trough days 17. In this figure, SP #2 and SP #3 are considered to be at 25 cm and 280 cm above the distributor respectively.

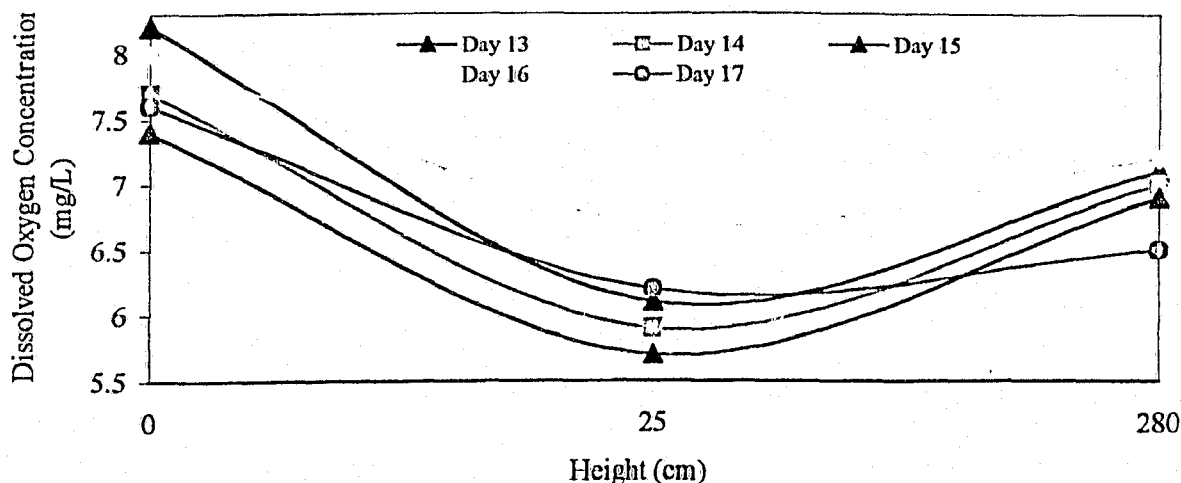


FIGURE 4.8 DISSOLVED OXYGEN VERSUS HEIGHT OF THE REACTOR

Dissolved oxygen concentrations around 7.5 mg/L were kept in the feedwater, and it dropped near the distributor (SP #2) due to an increase in aerobic biological activity. DO increased with high due to aeration. The effluent produced has approximately 7.0 mg/L of dissolved oxygen.

The fluidized bed does not behave as an activated sludge processes where the biomass is suspended in the liquid phase; in this experiment the biomass was visually observed attached to the solid support. This statement can be seen in the total suspended solids values that were collected from the effluent. Values of total suspended solids can be seen in Figure 4.9. As we can see in this figure, suspended solids average of 0.9 g/L were found in the effluent. The low production of suspended biomass, suspended flocs and sludge represent one of the main advantages of this technology over other attached biomass processes.

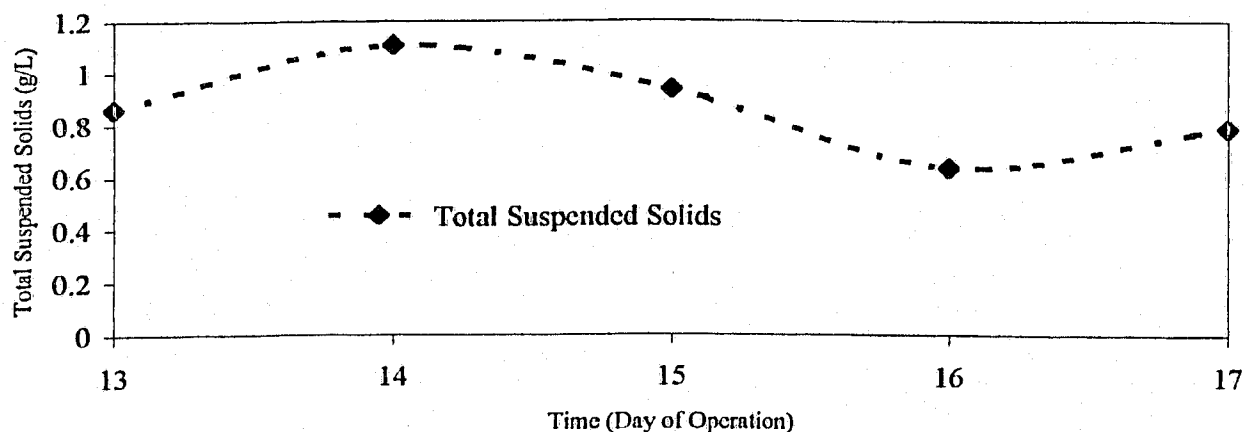


FIGURE 4.9 TOTAL SUSPENDED SOLIDS AT STEADY STATE

The turbidity values measured as NTU (nephelometric turbidity units) were collected at the feedwater and liquid effluent during days 13 through 17 and it is shown in Figure 4.10. The maximum value of turbidity for an effluent to be discharged into the environments is around

10 NTU. In this investigation was observed a good quality effluent with average value of turbidity of 5 NTU. This effluent does not constitute a potential hazard for the environment.

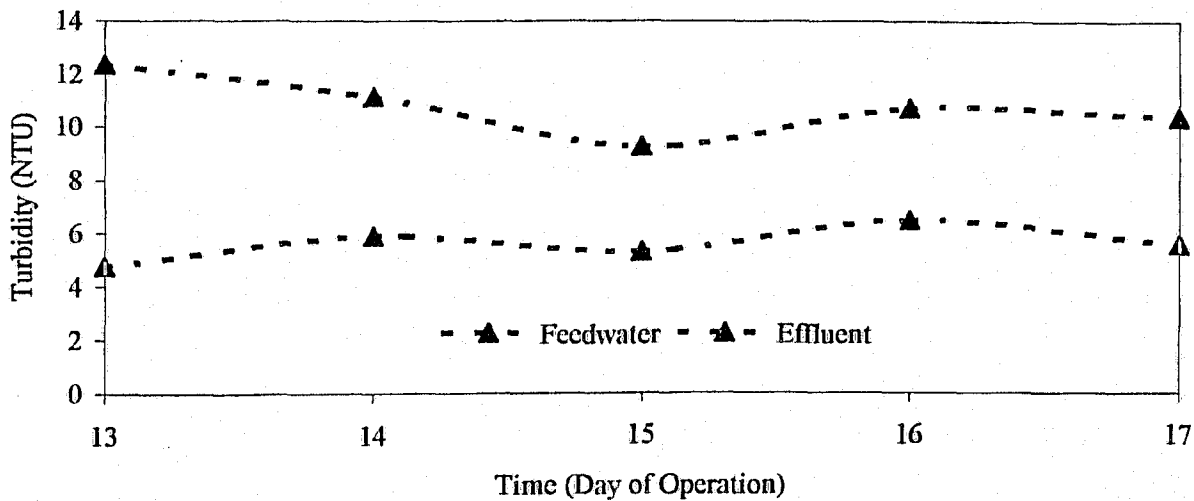


FIGURE 4.10 TURBIDITY VALUES DURING STEADY STATE

In general, the bed of bioparticles did not show homogeneous biofilm thickness in every section of the reactor. Particles with thicker biofilm were observed at the top of the reactor and particles with thinner biofilm were observed at the bottom of the reactor. Thus, it appears that turbulence, shear stress, and high particle collisions in the lower part of the reactor, could cause the formation of thin biofilms. This phenomenon was observed by Schreyer and Coughlin (1999) and Trinet et al. (1991). The expanded height of the fluidized bed gradually increased throughout the first 12 days of continuous operation showing different region depending on the biofilm thickness.

Biofilm with a thickness between 50-700 μm (average) were observed microscopically. A microscopy photograph of the bioparticles can be observed in Figures 4.11 and 4.12. Figure 4.11 shows a microscopic view of active biofilms developed in the lower part of the reactor.

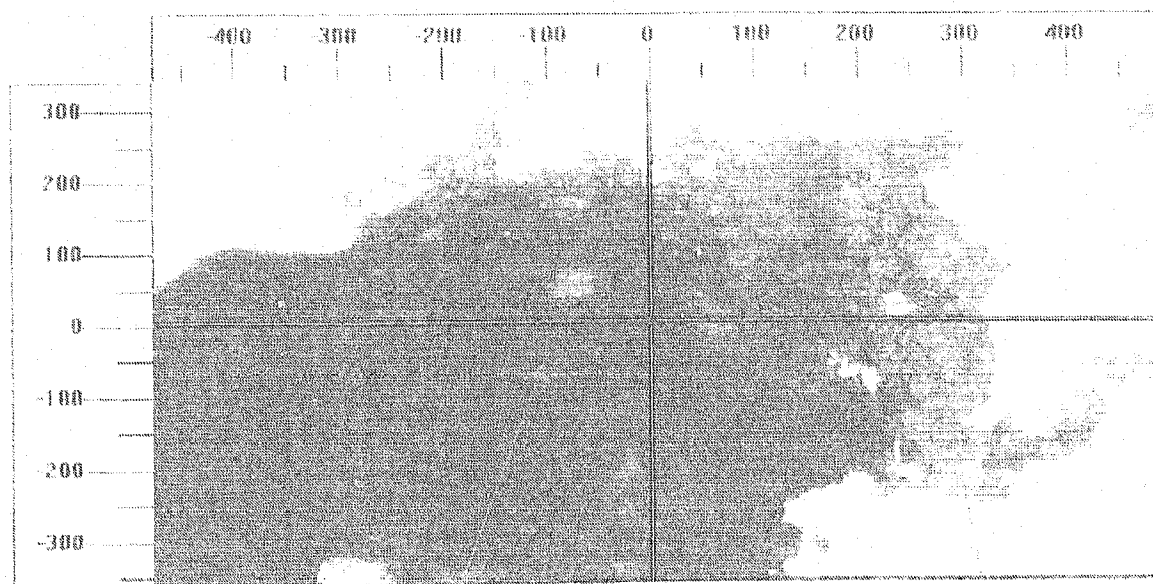
Figure 4.12 shows a microscopic view of active biofilms developed in the upper part of the reactor. The nature of the biofilm and their microbial composition is not covered in this study. However, it is important to note that aerobic attached growth processes have more complex microbial ecology than the activated sludge processes (MetCalf and Eddy, 2003).

At steady state, values of biofilm thickness, total suspended solids and turbidity were collected. As we can see in Table 4.2 bioparticles with a thickness between 50-700 μ m, treated approximately 1.2 kg diesel/m³day, with no detectable diesel concentrations at the liquid effluent. The COD is reduced from 1300 mg/L to 65 mg/L within a hydraulic detention time of 4 hours. Good quality effluent, with turbidity value around 5 NTU and a low production of suspended solids of 0.9 g/L were achieved at steady state.

PARAMETER	STEADY-STATE VALUE
Bioparticle thickness (average)	50-700 μ m
Total Suspended Solids (average)	900 mg/l
Diesel Loading rate	1.2 kg diesel/m ³ d
Feed Diesel Concentration (average)	190 mg/L
Effluent Diesel Concentration	ND ^a
Hydraulic Detention Time	4 hours
NTU Effluent (average)	5.4
COD Feedwater (average)	1300 mg/l
COD Effluent (average)	65 mg/l
Diesel Removed	100 %

^a (ND: not detected)

TABLE 4.2 BIOFILM PROPERTIES AND HYDRODYNAMIC PARAMETERS AT STEADY STATE OPERATION



SUPPORT PARTICLE

BIOFILM

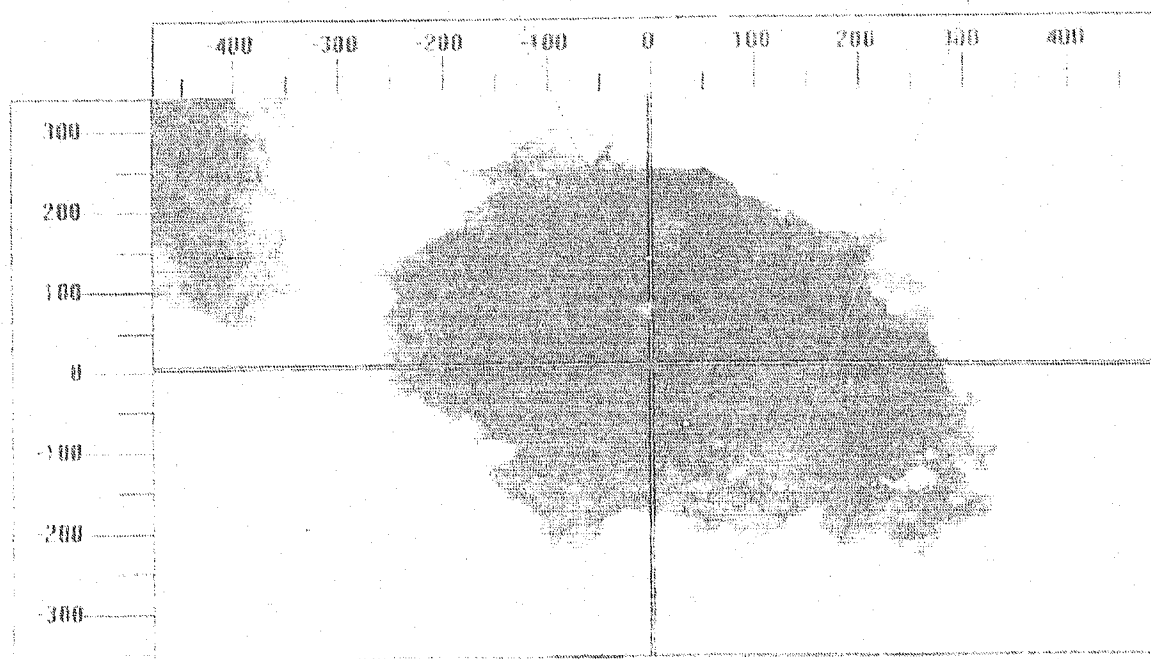
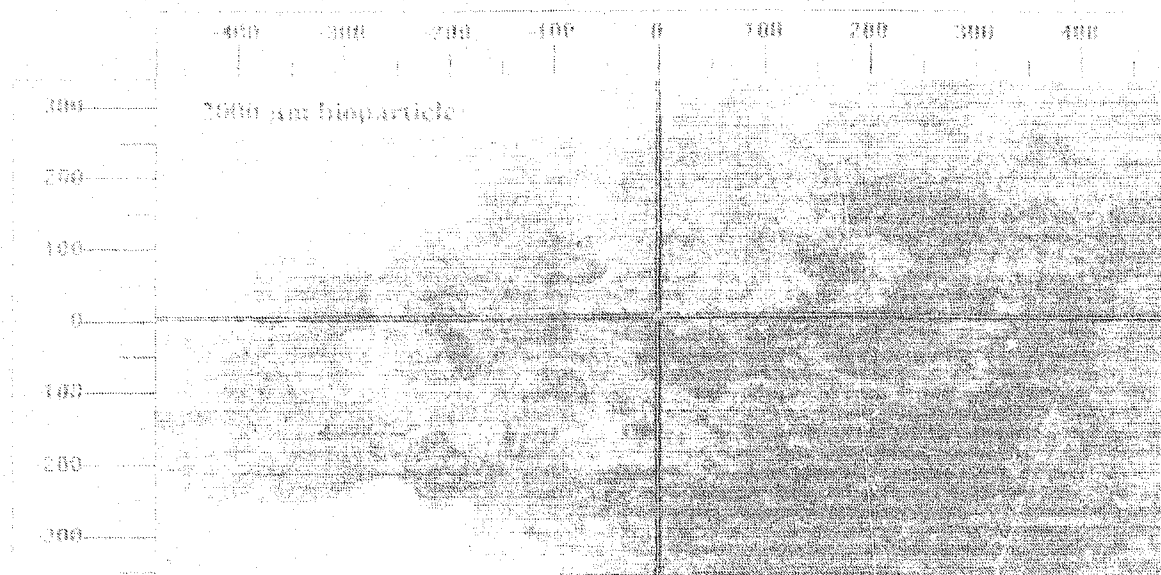


FIGURE 4.11 MICROSCOPY PHOTOGRAPH OF ACTIVE BIOFILM
DEVELOPED IN THE LOWER PART OF THE REACTOR



SECTION OF BIOFILM ON A PARTICLE SAMPLED IN THE
UPPER PART OF THE REACTOR

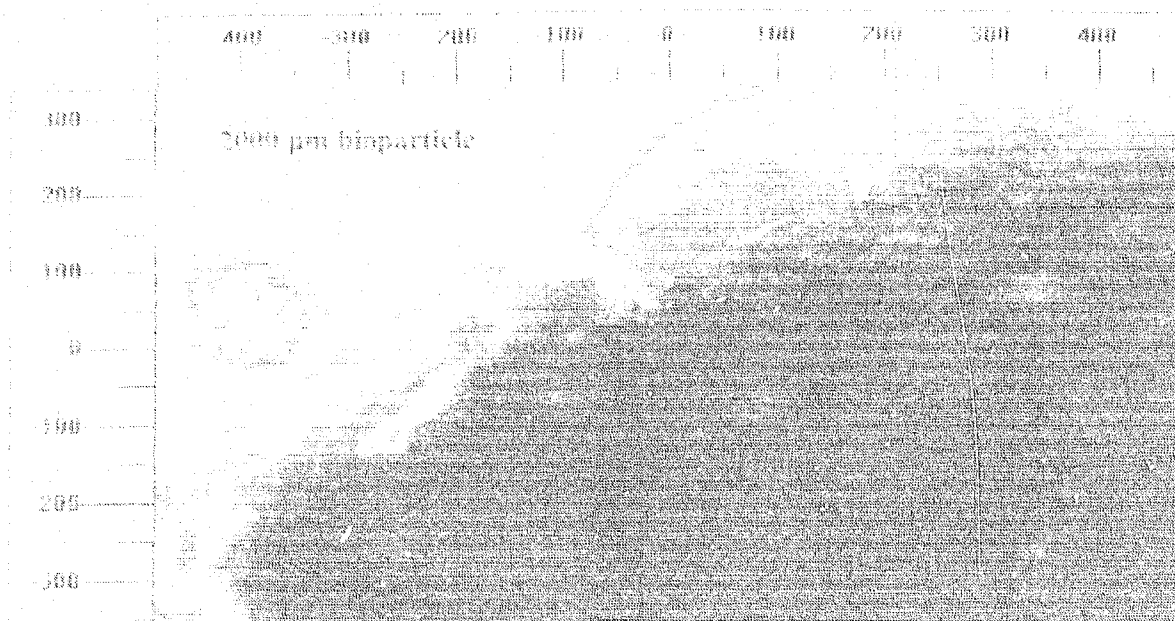


FIGURE 4.12 MICROSCOPY PHOTOGRAPH OF ACTIVE BIOFILM
DEVELOPED IN THE UPPER PART OF THE REACTOR

As mentioned before, bioparticles stratified in the fluidized bed, this phenomenon lead to the formation of three visible regions along the column.

1. Region I: Dense Bed
2. Region II: Stratified Bed
3. Region III: Dispersed Bed

A photograph of the reactor in operation and the formation of these regions can be seen in Figure 4.13. This figure also displays the regions' length, visible bioparticles, flocs, and air bubbles developed in the reactor.

The Region I, located above the air distributor up to 25-30 cm along the column, is characterized by particles sparsely covered by biofilm and it had the appearance of no biofilm immobilized on it. Particles with thinner biofilm and the highest settling velocity were observed in this region, where shear stress, turbulence, and particles collisions were present. The thickness of these bioparticles was found to be around 50 μm (average).

In Region II, the particles were noticeably larger and the biofilm was visually observed as dark and light coating in the lava rock. In this region lava rock appears to be completely covered by a large layer of biofilm. In this region the turbulence was lower and it could have permitted much thicker biofilm to develop on the lava rock. However, sampling was not possible in this region due to the characteristics of the column (glass wall).

It was visually noticed in Region III, at the upper part of the reactor, larger bioparticles, flocs and biofilm covering the glass of the column. Particles with thicker biofilm and lowest settling velocity were observed in this region. The thickness of these bioparticles was found to be around 700 μm . The lower shear at the top of the bed permitted the formation of large biomass flocs containing embedded particle grains. These large flocs of particles were most

susceptible to washout because of their large cross-sectional area. When particles washed out of the column, they returned to the feedwater tank, and then returned into the column through pumping.

Although particles were considered spheres, irregularities on the shape could lead to a formation of filamentous in the biofilm as observed in the microscopic photograph in Figure 4.11. In general, the bed behavior was dominated by an unstable stratification due to solids mixing. This phenomenon is undesirable in the reactor because it tends to even out the film thickness throughout the bed.

It is important to note that although uniform holes (1.9 mm) in the air distributor system were used a multi-bubble system was observed. Bubbles of near the distributor region were small and smooth. As the bubbles rose, they coalesced and broke-out forming a bigger bubble size of lower interfacial area. Accurate and simple predictions of bubble-rise velocity and size distribution proved to be complex during the operating conditions established in this study (low gas hold-up for optimal liquid-solids contact). Table 4.3 shows the characteristics of the regions formed in the TPFBR.

PARAMETER	REGION I	REGION II	REGION III
Bed Height	250-300 mm	NA	NA
Characteristics	Biofilm: Not visually observed Bubbles: Small and Smooth	Biofilm: Visually observed Bubbles: Larger than Region I	Biofilm: Visually observed Bubbles: Larger than Region I and Region II
Biofilm Thickness (μm)	50	NA	700

Note: NA, not available

TABLE 4.3 CHARACTERISTICS OF THE REGIONS FORMED IN THE REACTOR

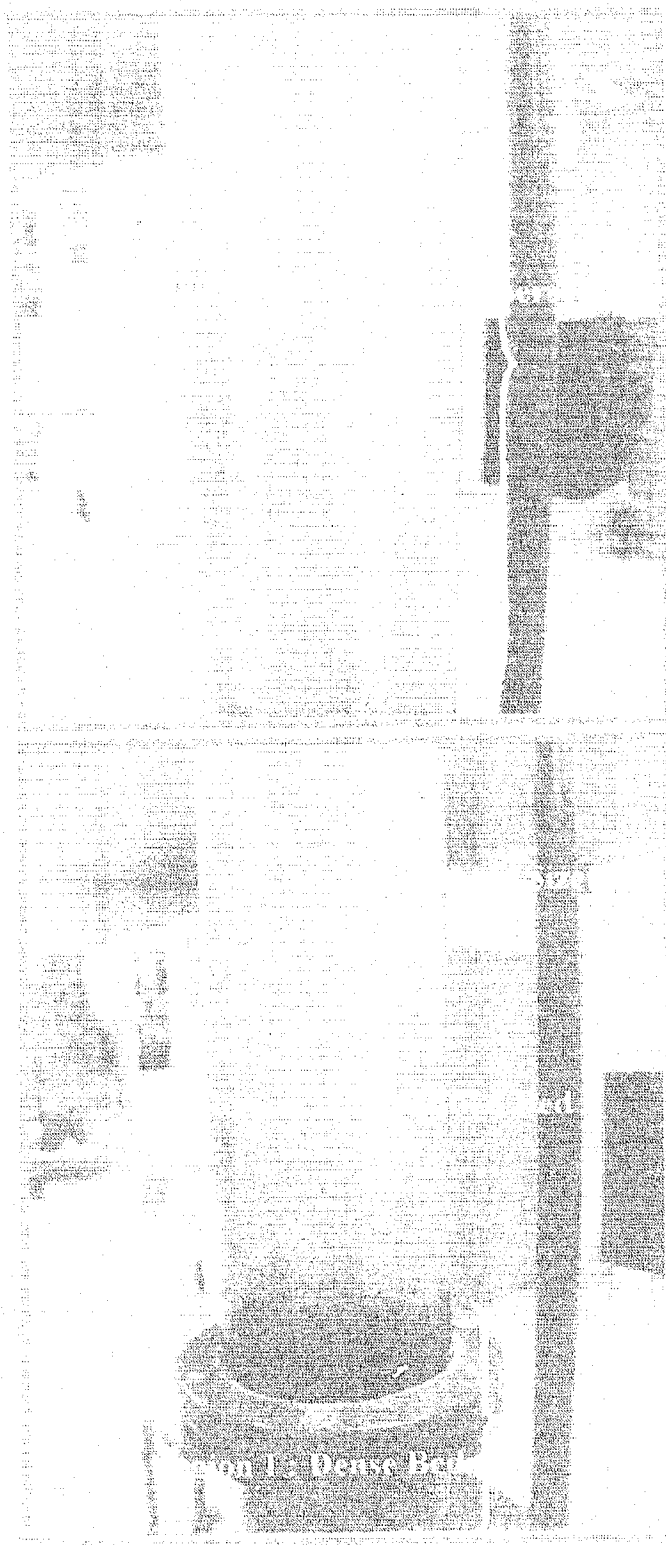


Figure 1: Dense Bar

THESE ARE THE RESULTS OF THE ANALYSIS OF THE DATA.

4.2.1 Estimation of the Attached Biomass Concentration Using Larachi's Model

The simflui3p software developed by Larachi et al. (2000) was used for predicting bed porosity and hold-ups of solids, liquid and air. The attached biomass concentration was predicted once Larachi's Model was validated.

The parameters used for the estimation of the hold-ups (ϵ_s , ϵ_L , ϵ_g) and biomass concentration in the fluidized bed is summarized in Table 4.4.

PARAMETER	VALUE	SYMBOL
Column Cross Sectional Area (m ²)	0.0227	A
Biofilm Thickness (m)	Variable	δ
Biofilm Wet density (Kg/m ³)	1020	ρ_{wb}
Biofilm Dry Density (Kg/m ³)	1170	ρ_{db}
Clean Particle Density (Kg/m ³)	1790	ρ_p
Sphericity Factor of Bioparticles (-)	1	π
Type of System (-)	Foaming (2)	(-)
Clean Particle Diameter (m)	0.0006	d_p
Weight of Clean Particles (Kg)	1	W_{pt}
Superficial Gas Velocity (m/s)	0.01	U_g
Superficial Liquid Velocity (m/s)	0.0002	U_L
Liquid Surface Tension (Kg/s ²)	0.072	σ_L
Liquid Viscosity (Kg/m.s)	0.001	μ_l
Liquid Density (Kg/m ³)	1000	ρ_l
Gas Viscosity (Kg/m.s)	0.0000125	μ_g
Gas Density (Kg/m ³)	1.2	ρ_g

**TABLE 4.4 PARAMETER USED IN SIMFLUI3P AND FOR PREDICTION OF
THE BIOMASS CONCENTRATION**

Following the procedure discussed in section 2.2.5

The bioparticle diameter using 50 and 700 μm thickness of biofilm is:

$$d_{bp} = d_p + 2\delta \quad (7)$$

$d_{bp} = 0.0007\text{m}$ for bioparticles with 50 μm of thickness and,

$d_{bp} = 0.002\text{ m}$ for bioparticles with 700 μm of thickness

And the bioparticle density was estimated as:

$$\rho_{bp} = \rho_p (1 + 2\delta/d_p)^{-3} + \rho_{wb} [1 - (1 + 2\delta/d_p)^{-3}] \quad (6)$$

$\rho_{bp} = 1505.74\text{ Kg/m}^3$ for bioparticles with 50 μm of thickness and,

$\rho_{bp} = 1040.79\text{ Kg/m}^3$ for bioparticles with 700 μm of thickness

These results seem to agree with the postulate that the biomass growth decreases the overall density of the particles. Bioparticles with density of 1040.79 Kg/m^3 migrate to the top of the bed, although the high solids mixing modified this tendency making them return to the middle part of the column.

The hydrodynamic parameters obtained by simflui3p are presented in Table 4.5 and in Appendix E.

PARAMETER	BIOPARTICLES OF 50 μm OF THICKNESS	BIOPARTICLES OF 700 μm OF THICKNESS	UNIT
Bed Porosity (ϵ)	0.856	0.758	(-)
Gas Hold-up (ϵ_g)	0.355	0.179	(-)
Liquid Hold-up (ϵ_L)	0.501	0.579	(-)
Solids Hold-up (ϵ_s)	0.144	0.242	(-)

TABLE 4.5

HYDRODYNAMIC PARAMETERS

To validate the parameters obtained by simflui3p (hold-ups ϵ_s , ϵ_L , ϵ_g), the estimated ϵ_s is compared with the ϵ_s that can be calculated from the observed fluidized height for Region I, using the following equation:

$$\epsilon_s = (W_{pt} / H \rho_p A) (1 + 2\delta/d_p)^3 \quad (4)$$

Particles in Region I formed a bed of fluidized particles between 25 and 30 cm from the air distributor. The estimated and experimental solids hold-up (ϵ_s) for bioparticles from Region I is shown in Table 4.6.

BIOPARTICLE DIAMETER	ESTIMATED ϵ_s	EXPERIMENTAL ϵ_s
700 μm	0.144	0.156

TABLE 4.6 ESTIMATED AND EXPERIMENTAL SOLIDS HOLD-UP

The estimated ϵ_s is in accordance with the experimental ϵ_s with a relative error of 8%. The fluidization parameters developed by Larachi's Model are capable of predicting the bed porosity with good accuracy.

The simulated bed porosity for both bioparticles with 700 and 2000 μm of diameter is used for the calculation of the attached biomass concentration in the reactor. The procedure used to predict the biomass concentration in the reactor was discussed in section 2.2.5 and it is also shown in Figure 2.4 (Flow chart to predict the biomass concentration in the three-phase fluidized bed bioreactor).

The biomass concentration, X , which is defined as dry weight of biomass per unit volume of bed, is predicted using the following equation.

$$X = \rho_{db} (1 - \epsilon) [1 - (d_p/d_{bp})]^3 \quad (5)$$

Minimum and maximum thickness of 50 μm and 700 μm produce a total biomass concentration (attached) between 0.50 and 97 g/L respectively. Based on the results displayed before, it can be assumed that an average biomass concentration of 49 g/L is found along the reactor column. The total biomass concentration (attached) of 49 g/L is higher than the total suspended solid (0.9 g/L) found for steady state during phase III of this research. This result shows a good reactor performance where obviously diesel degradation was mainly performed by the attached biomass.

Table 4.7 lists total biomass concentrations values determined from several biofilm systems treating different types of wastewaters. Trinet et al. (1991) found biofilm thickness of 1.8 and 12 μm that produced a 14-212 g/L of biomass concentrations with approximately 6500 of clean particles. In other studies, including this one, the biomass concentrations were found to be strongly dependent of the density of the bioparticles and the operating conditions. Ozturk et al. (1994) also encountered this problem.

REFERENCE	BIOMASS CONCENTRATIONS (g/l)	COMMENTS
Trinet et al. (1991)	14-212	$W_{pt}=6661$, COD removal. Thickness of 1.8 and 12 μm
Hermanowicz and Cheng (1983)	4-24	Denitrification with support particles of $d_p=0.5$ mm
Ozturk et al. (1994)	3-23	COD removal treating 1960-3500 mg/L, thickness of 9-108 μm

TABLE 4.7 BIOMASS CONCENTRATION DETERMINED BY OTHER INVESTIGATORS

4.3 Interpretation of the Experimental Results Obtained in Phase IV: Validation of Diesel Biodegradation

A set of four experiments was performed, with clean particles and without microorganism following the same operating conditions, to validate diesel volatilization in presence of diffusive air. It was considered that losses in the system occur by air stripping due to injection of the air at 0.01 m/s. Adsorption of diesel into the packing material was considered negligible due to the reactor was working during 3 months with periodical addition of diesel. Furthermore after this time the support particle became saturated with diesel.

The results (Figure 4.14) show that for diesel concentration of 255 mg/L there is a 120 mg/L of diesel at the liquid effluent, showing that 50 % of the diesel was volatilized in the presence of air. For higher concentration of diesel in wastewater (1038 and 1051 mg/L), there is a 37 % of diesel volatilized in the system.

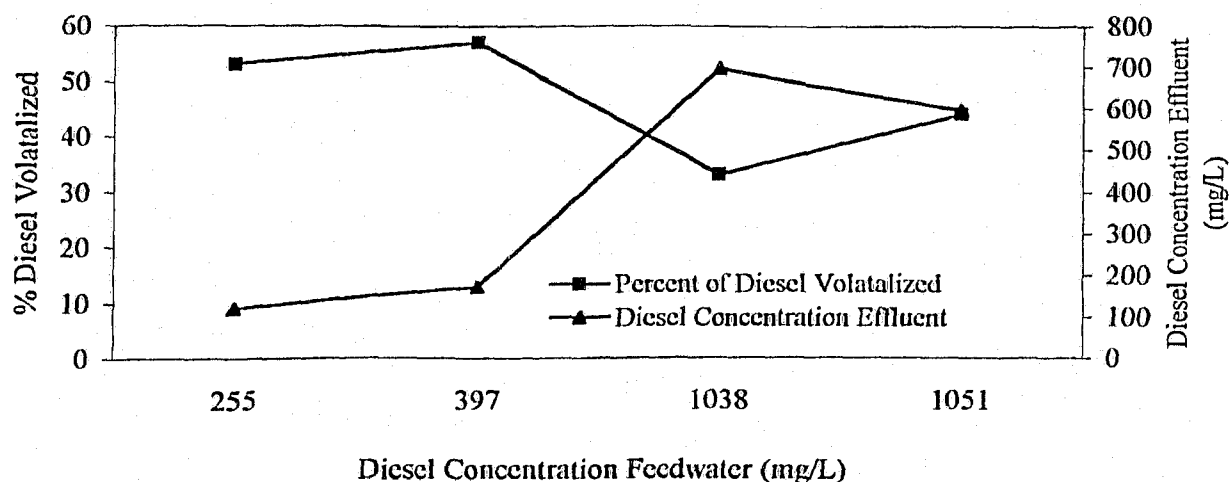


FIGURE 4.14 DIESEL VOLATILIZATION IN THE REACTOR

The results show that average 45 % of the diesel is volatilized in the presence of diffusive air, and 55 % of the diesel is biodegraded along the reactor. The results obtained in this research are in accordance for the use of the three-phase fluidized bed aerobic reactor using volatilized component found by Flanagan (1998) and Gonzalez et al. (2001).

As a summary of this research, it is important to note that bioparticles with a diameter between 700-2000 μm produced an average biomass concentration of 49 g/L. The reactor treated approximately 1.2 kg diesel/ m^3day , with no detectable diesel concentrations at the liquid effluent. The COD was reduced from 1300 mg/L to 65 mg/L at a hydraulic detention time of 4 hours. A good quality effluent, with turbidity value around 5.4 NTU and low production of suspended solids of 0.9 g/L were achieved. The diesel removed due to biodegradation and volatilization was 100 %. The diesel removed due to biodegradation processes was 55 %. A Summary of selected parameters for steady state operation can be seen in Table 4.8.

PARAMETER	STEADY-STATE VALUE
Bioparticle Diameter (average)	700-2000 μm
Total Suspended Solids (average)	900 mg/l
Fluidized Height of Bioparticles (stable)	25-30 cm
Feed Flow Rate	0.3 L/min
Diesel Loading Rate	1.2 kg diesel/m ³ d
Feed Diesel Concentration (average)	190 mg/L
Effluent Diesel Concentration	ND
Hydraulic Detention Time	4 hours
Superficial Air velocity	1.0 cm/s
Superficial Liquid velocity	0.02 cm/s
NTU Effluent (average)	5.4
COD Feedwater (average)	1300 mg/L
COD Effluent (average)	65 mg/L
Biomass Concentration (estimated)	49 000 mg/L
Diesel Removed	100 %
Diesel Biodegraded	55 %

Note: ND, not detected

TABLE 4.8 SUMMARY OF SELECTED PARAMETERS OF STEADY STATE OPERATION

4.4 Sources of Errors

During the collection of the experimental data, sources of variability were identified in the COD measurements and the liquid-liquid extraction technique.

COD measurements were taken by triplicate and samples varied approximately 10 %, a mean value was taken as a representative value. This variability is due to the characteristics of the sample.

Liquid and Liquid extraction showed efficiencies of approximately 17 %. The extracted diesel samples were not stored due to its volatility; losses of diesel could be present during the handling and procedure.

There are parameters that could affect the accuracy of the estimated bed porosity and phase's hold-ups for bioparticles. These include:

1. Inaccuracy in the measurements of biofilm thickness.
2. Inaccuracy in the measurement of fluidized height of bioparticles.

The above sources of error could be quite significant and their elimination will require further research. However, the agreement between measured and predicted values is certainly acceptable for quality work. The deviation between predicted and measured value is 8%.



5.1 CONCLUSIONS

A three-phase fluidized bed bioreactor was used for the aerobic remediation of diesel-contaminated wastewater. The following conclusions can be drawn from this research.

- 1 A good reactor performance and good quality effluent with no detectable diesel concentration was achieved in the reactor. Low turbidity values (5.4 NTU), low chemical oxygen demand (65 mg/l) and low production of suspended solids (0.9 g/L) were attained.
- 2 Biofilm properties and hydrodynamic parameters at steady-state can be used for industrial scale up fluidized beds for treating diesel-contaminated wastewater.
- 3 Diesel removal efficiencies of 100 % were obtained at a very low hydraulic detention time of 4 hours.
- 4 55 % of diesel is removed due to biodegradation processes.
- 5 An average of 49 g/L of biomass was developed in the reactor. This value is higher than that found in activated sludge.

- 6 The diesel biodegradation rate appeared to be limited by microbial inhibition rather than oxygen availability, suggesting that there may be opportunities for process improvement.
- 7 The microorganisms used in the fluidized bed can successfully carry out biodegradation of diesel and it could be extended for remediation of hydrocarbon-contaminated sites.
- 8 The dynamic behavior of the three-phase fluidized bed reactor was simulated by combining simfluid3p software and well known biofilms correlation. The procedure developed in this research was capable of predicting the biomass concentration in the reactor with good accuracy. The relative error is 8 %.

5.2 RECOMMENDATIONS AND FUTURE WORK

Three-phase fluidized bed bioreactors are a relatively new technology when applied to wastewater treatment technologies. The recommendation presented in this research can be used successfully for future work.

1. The time for biomass adaptation and biomass immobilization of 3 months was considered excessive for industrial applications and it is suggested an aggressive diesel loading soon after inoculation.
2. Proper choice of the support particles could increase the reactor stability and performance to overcome stratification and therefore particles elutriation.
3. Cost-effective operation of fluidized beds can be obtained with uniform and low-density particles (e.g. activated carbon) achieving bed homogeneity at lower gas flow rates.
4. Diesel volatilization can be reduced by considering pre-oxygenated fluidized bed or the use of emulsifiers in the wastewater for a better partitioning of diesel fuel in the water phase.
5. Future work has to be done to have a better understanding in modeling the substrate utilization in the three-phase fluidized bed bioreactor.

BIBLIOGRAPHY

1. Abdul-Aziz, M. and Asolekar, S. R., (2000). "Modeling of biological particle mixing in a fluidized-bed biofilm reactor". *Water Environment Research*. Vol. 72, No. 1, pp. 105-114.
2. Alvarez-Cuenca, M. (2003). *Fundamentals, Design and Operation of Small Wastewater Treatment Plants Class Notes*, Department of Chemical Engineering. Ryerson University, Toronto, Canada.
3. Alvarez-Cuenca, M. (2004). "Rudimentary Wastewater Treatment Technologies Hurt the Bottom Line". *Water and Wastewater Europe 2004 Conference*. Barcelona, Spain.
4. Andrews, G., and Trapasso, R., (1985). "The optimal design of fluidized bed bioreactors". *Journal WPCF*. Vol. 57, No. 2, pp. 143-150.
5. APHA (1998). "Standard Methods for the Examination of Water and Wastewater". 20th Edition. American Public Health Association, Baltimore.
6. Arcangeli, J-P, and Arvin, E., (1995). "Biodegradation rates of aromatic contaminants in biofilm reactors". *Wat. Sci. Tech*. Vol. 31, pp. 117-128.
7. Arvin, E., and Harremoes, P., (1990). "Concepts and modeling for biofilm reactor performance". *Wat. Sci. Tech*. Vol. 22, No.1/2, pp. 171-192.
8. Atlas, R. (1985). "Petroleum biodegradation and oil spill bioremediation". *Marine Pollution Bulletin*. Vol. 31, No 4-12, pp. 178-182.
9. Atlas, R. (1984). "Petroleum Microbiology". Macmillan Publishing Company, New York.

10. Badot, R., Coulom, T., Longeaux, N., Badard, M., and Sibony, J., (1994). "A fluidized-bed reactor: The biolift process". *Wat. Sci. Tech.* Vol. 29, No. 10-11, pp. 329-338.
11. Bignami, L., Eramo, B., Gavasci, R., Ramadori, R., Rolle, E., (1991). "Modeling and experiments on fluidized-bed biofilm reactors". *Wat. Sci. Tech.* Vol. 24, No.7, pp. 47-58.
12. Boaventura, R. A., and Rodrigues, A. E. (1988). "Consecutive reactions in fluidized bed biological reactors: Modeling and experimental study of wastewater denitrification". *Chemical Engineering Science.* Vol. 43, No. 10, pp. 2715-2728.
13. Briens, L., Briens, C., Margaritis, A., and Hay, J., (1997). "Minimum liquid fluidization velocity in gas-liquid solids fluidized beds of low-density particles". *Chemical Engineering Science.* Vol. 52, No. 21/22, pp. 4231-4238.
14. Bryers, J. D. (2000). "Biofilm II: Process Analysis and Applications". John Wiley & Sons, Inc, New York.
15. Buchtman, C., Kies, U., Deckwer, D., and Hecht, V. (1997). "Performance of three-phase fluidized bed reactor for quinoline degradation on various supports at steady state and dynamic conditions". *Biotechnology and Bioengineering.* Vol. 56, No. 3, pp. 295-302.
16. Cassidy, D., and Irvine, R., (1997). "Biological treatment of a soil contaminated with diesel fuel using periodically operated slurry and solid phase reactors". *Wat. Sci. Tech.* Vol. 35, No. 1, pp. 185-192.

17. Chang, H., Rittmann, B. E., Amar, D., and Lesty, Y., (1991). "Biofilm detachment mechanisms in a liquid-fluidized bed". *Biotechnology and Bioengineering*, Vol. 38, pp. 499-506.
18. Chang, H. and Rittmann, B. E., (1994). "Predicting bed dynamics in three-phase fluidized bed biofilm reactors". *Wat. Sci. Tech*, Vol. 29, No. 10-11, pp. 231-241.
19. Cifuentes, S. (2003). "Oxygen Transfer in a Three-Phase Fluidized Bed Reactors". *Bachelor in Engineering Thesis Report*. Ryerson University. Toronto, Canada.
20. Coelho, I. Boaventura, and Rodrigues, A., (1992). "Biofilm reactors: An experimental and modeling study of wastewater denitrification in fluidized-bed reactors of activated carbon particles" *Biotechnology and Bioengineering*. Vol, 40, pp. 625-633.
21. Cohen, M., Williams, J., and Yamasaki, H., (2002). "Biodegradation of diesel fuel by an *Azolla*-derived bacterial consortium". *Journal of Environmental Science and Health*. Vol. A37, No. 9, pp. 1593-1606.
22. Diez-Blanco, V., Garcia Encina, P., and FDZ Polanco, F., (1995). "Effects of biofilm growth, gas and liquid velocities on the bed expansions of an anaerobic fluidized bed reactor (AFBR)". *Wat. Res.* Vol. 29, No. 7, pp. 1649-1654.
23. Dowd, R. M. (1994)., "Leaking underground storage tanks". *Environ. Sci. Technol.* Vol. 18, No. 10. pp 309-310.
24. Eggers, E., and Terlouw, T., (1979). "Biological denitrification in a fluidized bed with sand as carrier material". *Wat. Res.* Vol. 13, pp. 1079-1090.
25. Environment Canada, 2002. " Canadian Environmental Quality Guidelines". URL: <http://www.ec.gc.ca/water/index.htm>. Last update: January 2002.

26. Erikson, M., Swartling, A., and Dalhammar, G., (1998). "Biological degradation of diesel fuel in water and soil monitored with solid-phase micro-extraction and GC-MS". *Appl. Microbiol Biotechnol.* Vol. 50, pp. 129-134.
27. Fan, L-S. (1989). "Gas-Liquid-Solid Fluidization Engineering". Butterworth Publisher, Stoneham, MA.
28. Flanagan, W. P. (1998). "Biodegradation of dichloromethane in a granular activated carbon fluidized-bed reactor" *Water Environment Research.* Vol. 70, No. 1, pp 60-66.
29. Gao, B., Yang, L., Wang, X, Zhao, J., and Sheng, G., (1999). "Influence of modified soils on the removal of diesel fuel oil from water and the growth of oil degradation microorganisms". *Chemosphere.* Vol. 41, pp. 419-426.
30. Gonzales, G., Herrera, G., Garcia, Ma.T and Pena, M., (2001) " Biodegradation of phenolic industrial wastewater in a fluidized bed bioreactor with immobilized cells of *Pseudomonas putida*". *Bioresource Technology.* Vol. 80, pp. 137-142.
31. Harada, H., Ando, H., and Momonoi, K., (1987). "Process analysis of fluidized bed biofilm reactor for denitrification". *Wat. Sci. Tech.* Vol. 19, pp. 151-162.
32. Hermanowicz, S. W and Cheng, Y.W., (1983). "Biological fluidized bed reactor: Hydrodynamics, biomass distribution and performance". *Wat. Sci. Tech.* Vol. 22, No.1/2, pp. 193-202.
33. Hermanowicz, S. W and Ganczarczyk, J. J. (1990)., "Some fluidization characteristics of biological beds". *Biotechnology and Bioengineering.* Vol. 25, pp 1321-1330.

34. Hosaka, Y., Kaihou, M., and Hirata, A., (1985). "Biological treatment of phenolic wastewater in a three-phase fluidized bed". Wat. Sci. Tech. Vol. 17, pp. 1437-1439.
35. <http://www.gch.ulaval.ca/bgrandjean/ulmf/ulmf.html>
36. Karapinar, I., and Kargi, F. (1996). "Effect of particle number density on wastewater treatment performance of a fluidized-bed bioreactor". Enzyme and Microbial Technology. Vol. 19, pp. 140-144.
37. Lai, B., and Shieh, W. K. (1997) "Substrate inhibition kinetics in a fluidized bioparticles" Chemical engineering Journal. Vol. 65, pp. 117-121.
38. Larachi, F., Iluta, I., and Rival, O. (2000). "Prediction of minimum fluidization velocity in three-phase fluidized-bed reactors". Ind. Eng. Chem. Res. Vol 39, pp. 563-572.
39. Lazarova, V., and Manem, J. (1994). "Advances in biofilm aerobic reactors ensuring effective biofilm activity control". Wat. Sci. Tech. Vol. 29, No. 10-11, pp. 319-327.
40. Lazarova, V., Pierzo, V., Fontvielle, D, and Manem, J., (1994). "Integrated approach for biofilm characterization and biomass activity control". Wat. Sci. Tech. Vol. 29, No. 7, pp. 345-354.
41. Lecomte, P., and Mariotti, C. (1997). "Handbook of Diagnostic Procedure for Petroleum- contaminated Sites" John Wiley & Sons, Inc, New York.
42. Lewandowski, Z., Stoodley, P., Altobelli, S., and Fukushima, E., (1994). "Hydrodynamic and kinetics in biofilm systems- recent advance and new problems". Wat. Sci. Tech. Vol. 29, No. 10-11, pp. 223-229.

43. Margesin, R., and Schnner, F., (1998). "Low-temperature bioremediation of a wastewater contaminated with anionic surfactants and fuel oil". *Appl Microbiol Biotechnol.* Vol. 49, pp. 482-486.
44. Marquez-Rocha, F., Hernandez, V., and Lamela, T., (2001). "Biodegradation of diesel oil in soil by a microbial consortium". *Water, Air and Soil Pollution.* Vol. 128, pp 313-320.
45. Melin, E. S., Jarvinen, K. T., and Puhakka, J. A. (1998). "Effects of temperature on chlorophenol biodegradation kinetics in fluidized-bed reactors with different biomass carriers". *Wat. Res.* Vol. 32, No.1, pp. 81-90.
46. MetCalf & Eddy, Inc. (2003). "Wastewater Engineering: Treatment and Reuse". 4th Edition, Mc Graw- Hill, New York.
47. Mishra, P. N., and Sutton, P. M. (1990)., "Biological fluidized bed for water and wastewater treatment: A state of-the-art review". *Biodeterioration and Biodegradation* (Edited by Rossmore H. W), pp. 340-357. Elsevier Science, New York.
48. Mulcahy, L. T and Shieh, W. K., (1987). "Fluidization and reactor biomass characteristics of the denitrification fluidized bed biofilm reactor". *Wat. Res.* Vol. 21, No. 4, pp. 451-459.
49. Ngian, K., and Martin, W., (1980). "Biologically active fluidized beds: mechanistic considerations". *Biotechnology and Bioengineering.* Vol. XXII, pp. 1007-1014.
50. Nicolella C., Chiarle, S., Di Felice, R., and Rovatti, M., (1997). " Mechanisms of biofilm detachment in fluidized bed reactors". *Wat. Sci. Tech.* Vol. 36, No. 1 pp. 229-235.

51. Nicolella C., Di Felice, R., and Rovatti, M., (1996). "An experimental model of biofilm detachment in liquid fluidized bed biological reactors". *Biotechnology and Bioengineering*. Vol. 51, pp. 713-719.
52. Nicolella, C., Converti, A., Di Felice, R., and Rovatti, M (1995). "The estimation of the solid size and density in liquid fluidized-bed biological reactors". *Shorter communication. Chemical Engineering Science*. Vol. 50. No.6, pp. 1059-1062.
53. Nicolella, C., Loosdrecht, M. C., Di Felice, R., and Rovatti, M., (1998). "Terminal settling velocity and bed-expansion characteristics of biofilm-coated particles". *Biotechnology and Bioengineering*, Vol. 62, No. 1, pp. 62-70.
54. Ochieng, A., Ogada, T., Sisenda, W., and Wambua, P., (2002). "Brewery wastewater treatment in a fluidized bed bioreactor". *Journal of Hazardous Materials*. Vol. B90, pp. 311-321.
55. Ozturk, I., Turan, M. and Idris, A. H. (1994). "Scale-up and biomass hold-up characteristics of biological fluidized bed reactors" *Wat. Sci. Tech*. Vol. 29, No. 11, pp. 353-360.
56. Paul, T. and Edward, J. (1992)., "Contaminated Soil: Diesel Fuel Contamination". *Lewis Publishers, Michigan*.
57. Perryman, J. (2003)., "Degradation of diesel in a rotating biological contactor". *Bachelor in Engineering Thesis Report. Ryerson University. Toronto, Canada*.
58. Picioreanu, C., Loosdrecht, M., Heijnen, J., (1999). "A theoretical study on the effect of surface roughness on mass transport and transformation in biofilm". *Biotechnology and Bioengineering*. Vol. 68, No. 4, pp. 355-361.

59. Picioreanu, C., Loosdrecht, M., Heijnen, J., (2000). "Two- dimensional model of biofilm detachment caused by internal stress from liquid flow". *Biotechnology and Bioengineering*. Vol. 72, No. 2, pp. 205-218.
60. Polanco, F., Real, F. J., and Garcia, P. A. (1994). "Behavior of an anaerobic/aerobic pilot scale fluidized bed for the removal of carbon and nitrogen". *Wat. Sci. Tech.* Vol.29, No. 10-11, pp. 339-346.
61. Rahman, K., and Rahman T., (2002). "Occurrences of crude oil degrading bacteria in gasoline and diesel station soils". *J. Basic Microbiol.* Vol. 42, pp. 284-291.
62. Richard, J., and Vogel, T., (1999). "Characterization of a soil bacterial consortium capable of degrading diesel fuel". *International Biodeterioration & Biodegradation*. Vol. 44, pp. 93-100.
63. Rittmann, B., and McCarty, P., (1982). "Comparative performance of biofilm reactor types". *Biotechnology and Bioengineering*. Vol. XXIV, pp. 1341-1370.
64. Rittmann, B., and McCarty, P., (1980-a). " Evaluation of steady-state biofilm kinetics". *Biotechnology and Bioengineering*. Vol. XXII, pp. 2359-2373.
65. Rittmann, B., and McCarty, P., (1980-b). " Model of steady-state biofilm kinetics". *Biotechnology and Bioengineering*. Vol. XXII, pp. 2343-2357.
66. Rittmann, B., and McCarty, P., (1981). " Substrate flux into biofilm of any thickness". *Journal of the Environmental Engineering Division*. Vol. 107, No 4, pp. 831-848.
67. Rittmann, B., and McCarty. (2001). "Environmental Biotechnology: Principles and Applications". Mc Graw-Hill, New York.

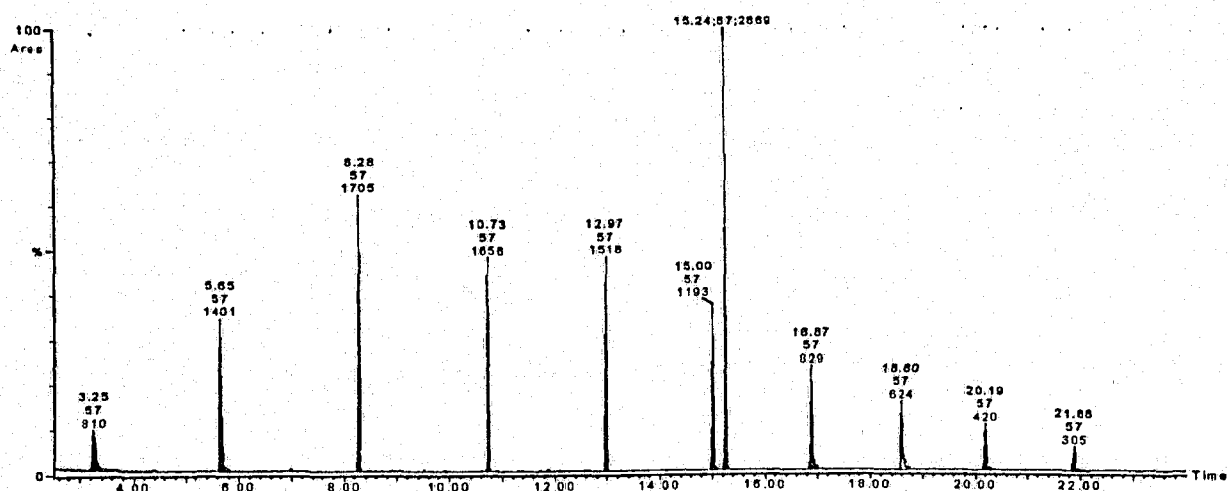
68. Ruggieri, B., Caire, G., Specchia, V., Sassi, G., Bosco, F., and Gianetto, A., (1994). "Determination of optimal biofilm activity in a biological fluidized bed (BFB) reactor". *Wat. Sci. Tech.* Vol. 29, No. 10-11 pp. 347-351.
69. Safferman, S. I., and Bishop, P. L., (1997). "Operating strategies for aerobic fluidized bed reactors". *Journal of hazardous materials.* Vol. 54, pp. 241-253.
70. Schreyer, H. B., and Coughlin, R. W., (1999). "Effect of stratification in a fluidized bed bioreactor during treatment of metal working wastewater". *Biotechnology and Bioengineering.* Vol. 63, No. 2, pp. 129-140.
71. Sepic, E., Trier, C., and Leskovšek, H., (1996). "Biodegradation studies of selected hydrocarbons from diesel oil". *Analyst.* Vol. 121, pp. 1451-1456.
72. Shieh, W. K., Sutton, P. M., and Kos, P., (1981). "Predicting reactor biomass concentration in a fluidized-bed system". *Journal WPCF.* Vol. 53, No. 11, pp. 1574-1584.
73. Smith, M., (1990). "The biodegradation of aromatic hydrocarbons by bacteria". *Biodegradation.* Vol. 1, pp. 191-206.
74. Song, C., Hsu, C., and Mochida, I. (2000). "Chemistry of diesel fuels". Taylor & Francis, New York.
75. Suidan, M., Rittmann, B., and Traegner, U., (1987). "Criteria establishing biofilm-kinetic types". *Wat. Res.* Vol. 24.No. 4, pp. 491-498.
76. Sutton, P. M, and Mishra, P. N., (1993). "Activated carbon based biological fluidized beds for contaminated water and wastewater treatment: A state of art review". *Wat. Sci. Tech.* Vol.29, pp. 309-317.

77. Sutton, P. M., and Mishra, P. N., (1990). "Fluidized bed biological wastewater treatment: Effects of scale-up on system performance". Wat. Sci. Tech. Vol. 22, No. 1/2, pp. 419-430.
78. Tavares, C. R. G., Sant'Anna, G. L., and Capdeville, B. (1995). "The effect of air superficial velocity in a three-phase fluidized bed reactors". Wat. Res. Vol. 29, No. 10, pp. 2293-2298.
79. Tsuneda, S., Auresenia, J., Morise, T., and Hirata, A., (2002). "Dynamic modeling and simulation of a three-phase fluidized bed batch process for wastewater treatment". Process Biochemistry. Vol. 38, pp. 599-604.
80. Trinet, F., Heim, R., Amar, D., Chang, H. T., and Rittmann, B. E., (1991). "Study of biofilm and fluidization of bioparticles in a three-phase liquid-fluidized-bed reactor". Wat. Sci. Tech. Vol. 23, pp. 1347-1354.
81. Wilson, G., Khodadoust, A. P., Suidan, M.T, Brenner, C., and Acheson., (1998). "Anaerobic-Aerobic biodegradation of pentachlorophenol using gas fluidized bed reactors: Optimization of the empty bed contact time" Wat. Sci. Tech. Vol. 38, No.7, pp. 9-17.
82. Wu, C., and Huang, J., (1996). "Bioparticle characteristics of tapered anaerobic fluidized-bed bioreactors". Wat. Res. Vol. 30, No. 1, pp. 233-241.
83. Yang, L., Lai, C., and Snieh, W., (2000). "Biodegradation of dispersed diesel fuel under high salinity conditions". Wat. Res. Vol. 34, No. 13, pp. 3303-3314.
84. Yu, H., and Rittmann, B. E., (1997). "Predicting bed expansion and phase holdups for three-phase fluidized-bed reactors with and without biofilm". Wat. Res. Vol. 31, No. 10, pp 2604-2616.

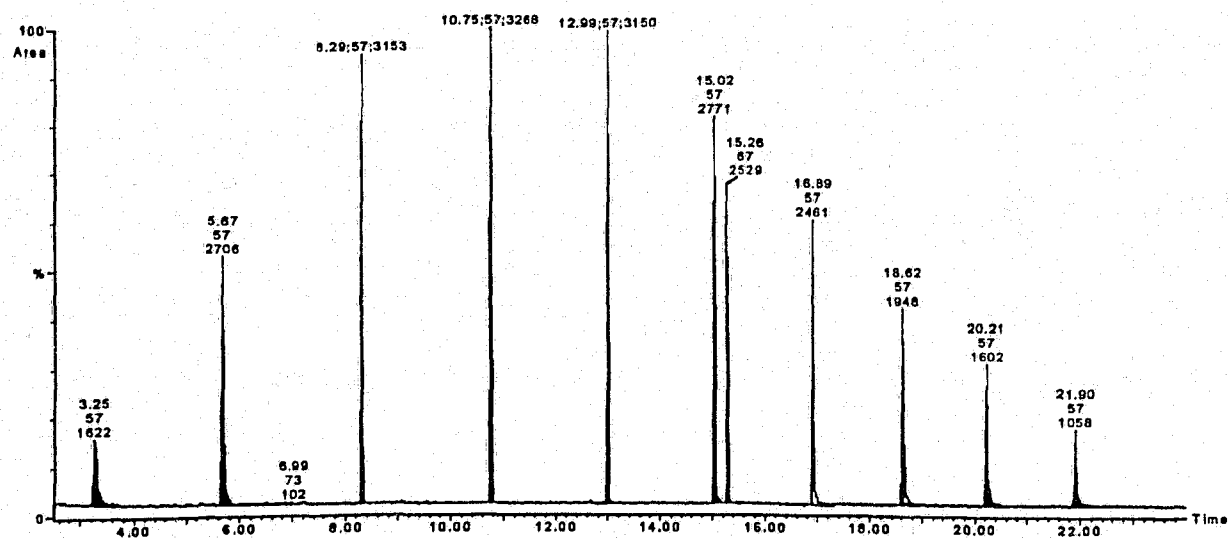
85. Zhang, T. C., and Bishop, P. L., (1993). "Structure, activity and composition of biofilm". Wat. Sci. Tech. Vol. 29, No. 7, pp. 335-344.
86. Zhang, T., Bishop, P. L., (1994). "Density, porosity, and pore structure of biofilm". Wat. Res. Vol. 28, No. 11, pp. 2267-2277.
87. Zhang, W., Bouwer, E., Wilson, L., and Durant, N., (1995). "Biotransformation of aromatic hydrocarbons in subsurface biofilms". Wat. Sci. Tech. Vol.31, No.1, pp. 1-14.

APPENDICES

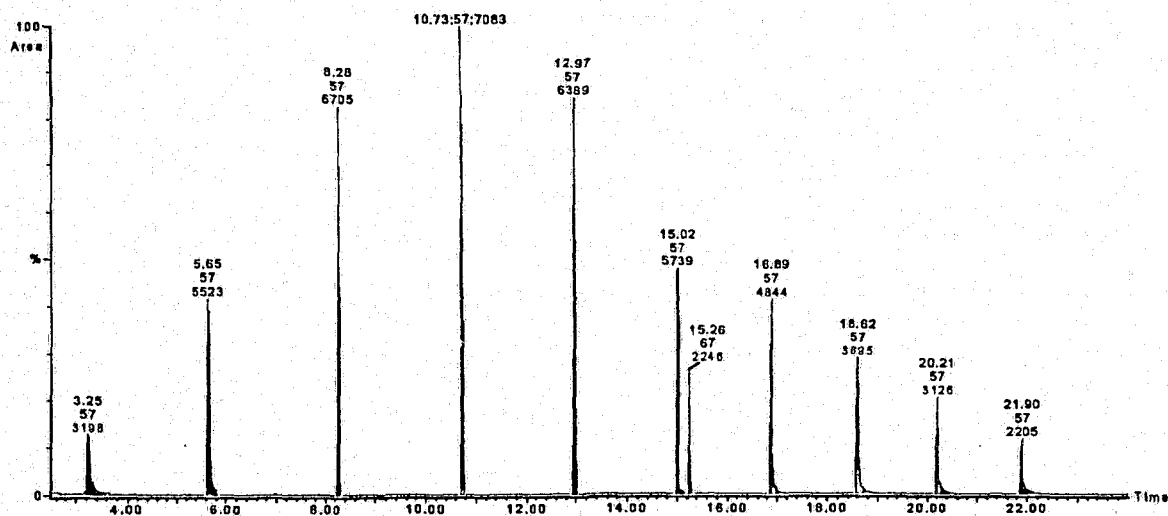
CALIBRATION CURVE GAS CHROMATOGRAMS



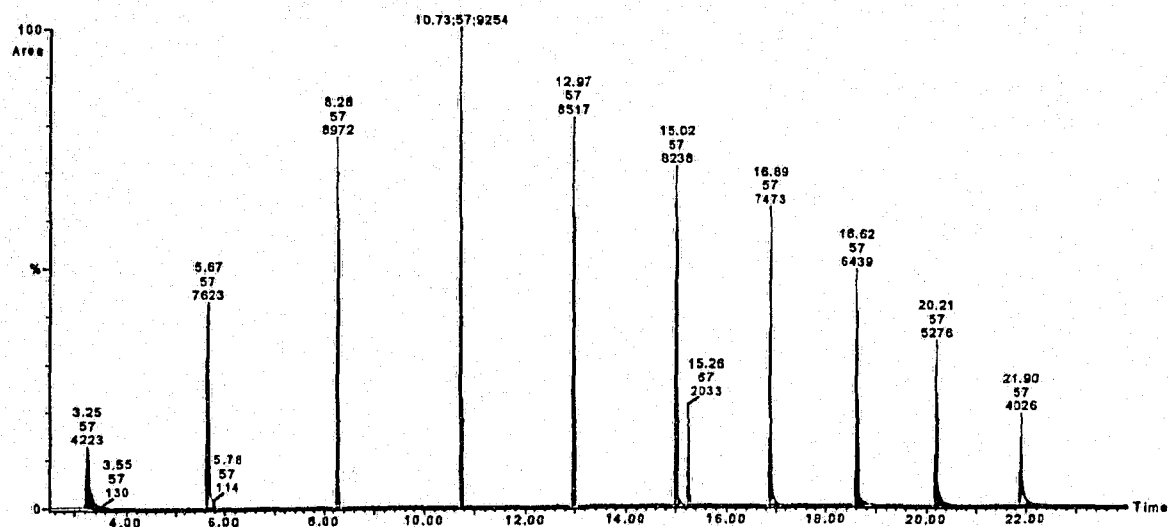
Gas chromatogram for the calibration curve (50 ppm of DRO)



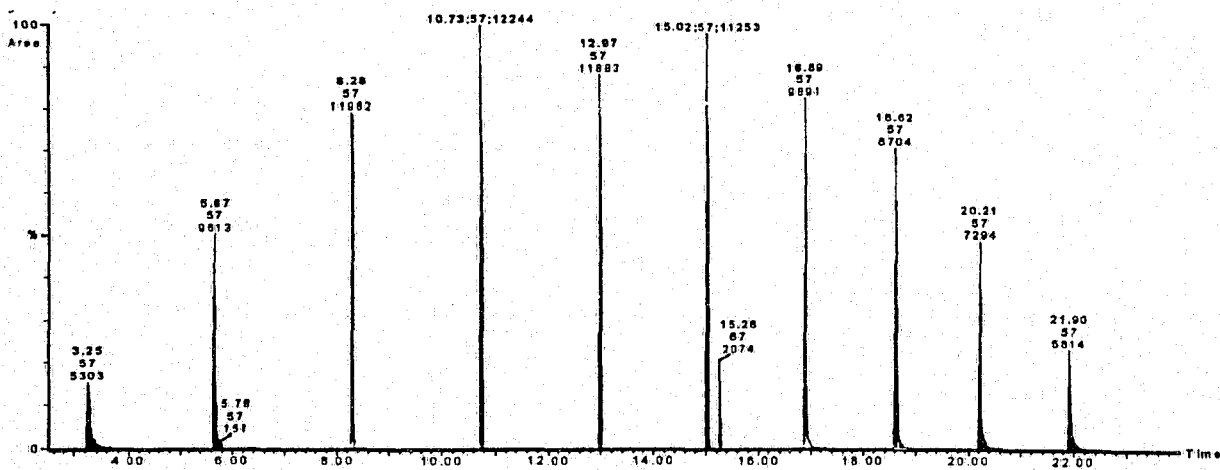
Gas chromatogram for the calibration curve (100 ppm of DRO)



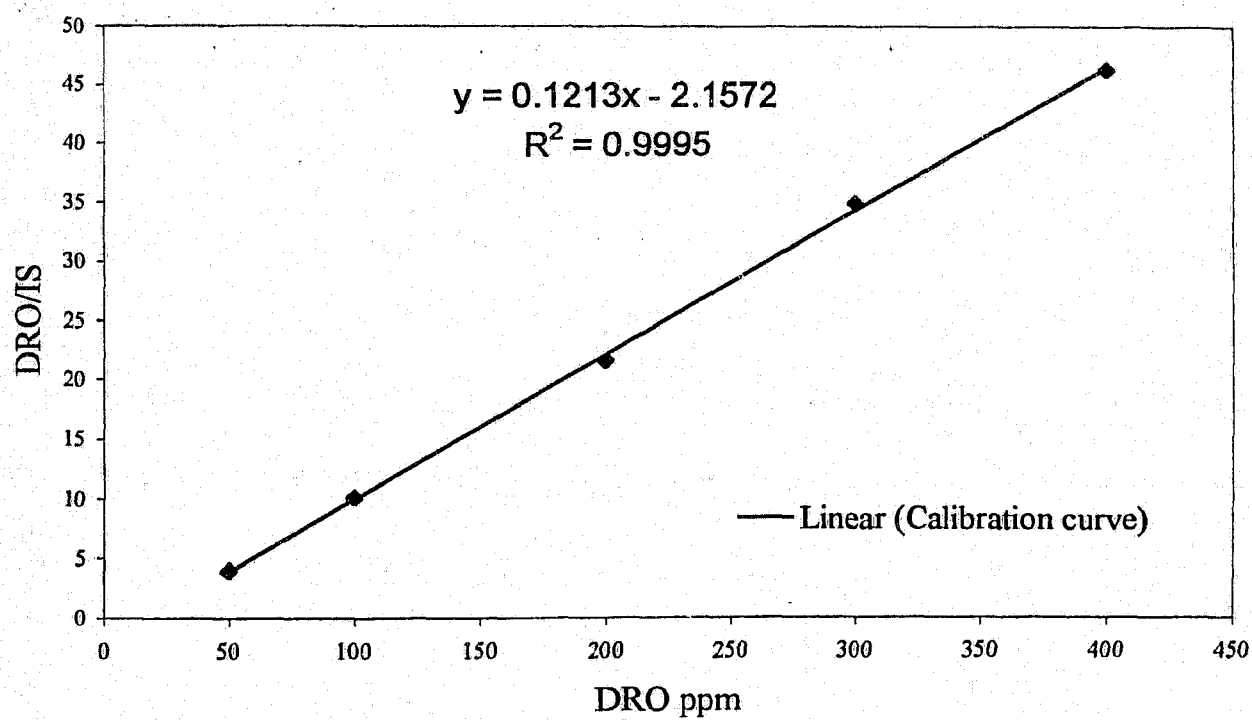
Gas chromatogram for the calibration curve (200 ppm of DRO)



Gas chromatogram for the calibration curve (300 ppm of DRO)



Gas chromatogram for the calibration curve (400 ppm of DRO)



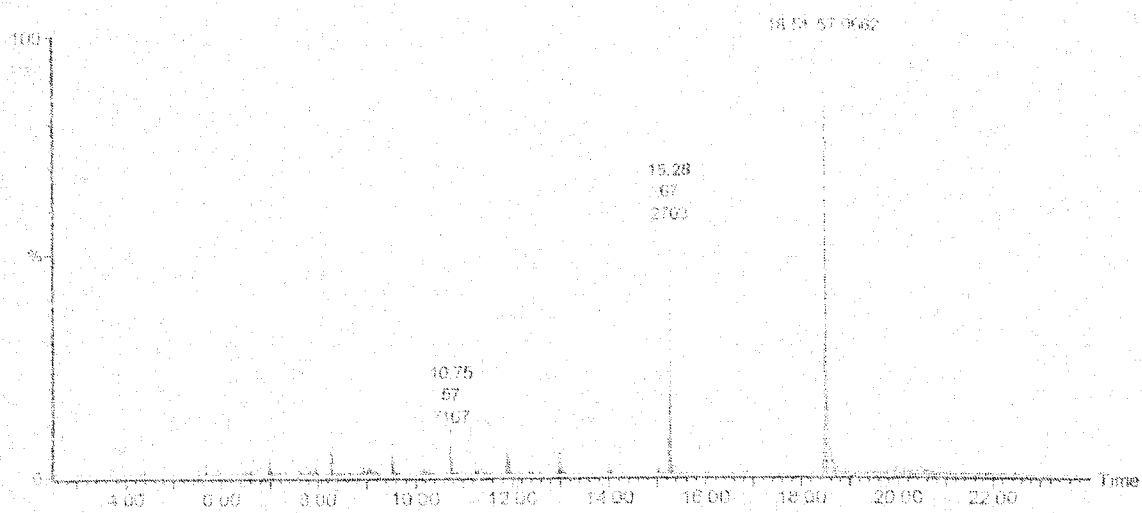
Gas chromatogram calibration curve

**RAW DATA AND GAS CHROMATOGRAMS FOR PHASE II: REACTOR
OPERATION IN INTERMITTENT MODE**

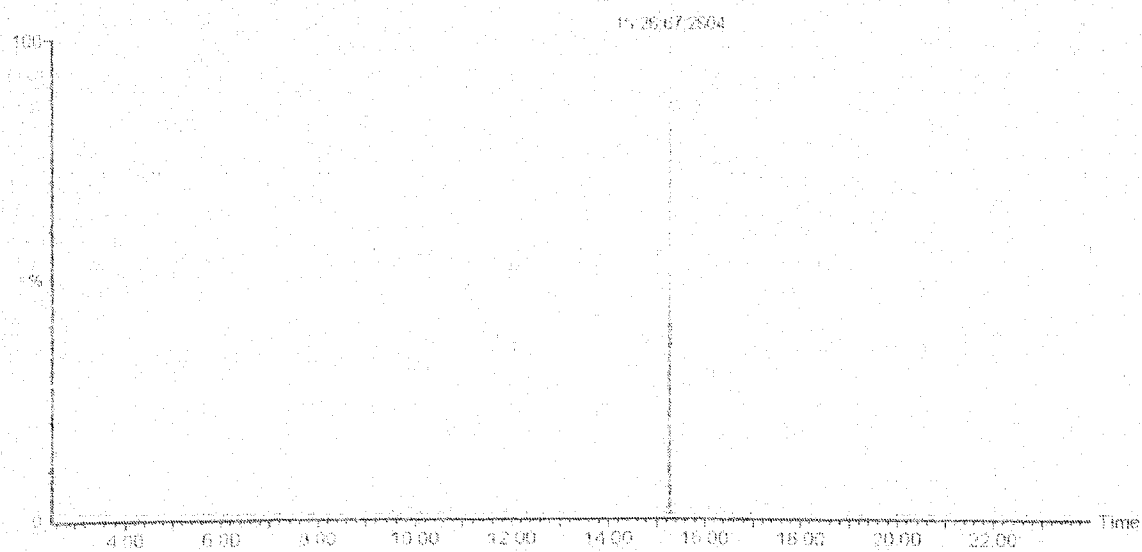
PARAMETER	DAY 1	DAY 2	DAY 3	DAY 4	DAY 5	DAY 6	DAY 7	DAY 8	DAY 9	DAY 10	DAY 11	DAY 12
Diesel Concentration Feedwater (mg/L)	69.0	128.0	116.0	166.0	122.0	119.0	248.6	332.0	427.0	530.0	693.0	141.0
COD Feedwater (mg/L)	547.0	980.3	937.7	1345.0	867.0	780.0	2400.8	2789.0	3100.6	3773.0	4025.0	934.0
pH Feedwater (-)	7.61	7.67	7.74	7.77	7.71	7.6	7.63	7.42	7.58	7.51	7.51	7.66
Temperature Feedwater (°C)	20.0	25.0	15.8	24.8	19.9	22.1	22.5	19.3	22.8	23.4	19.8	20.5
Dissolved Oxygen Feedwater (mg/L)	9.1	8.2	10.2	8.4	8.9	8.7	8.6	9.4	7.9	9.8	8.9	8.5
Dissolved Oxygen Bed (mg/L)	6.8	3.9	7.8	6.5	4.6	5.4	7.5	8.3	5.9	6.6	7.9	7.0
Diesel Concentration Effluent (mg/L)	ND	ND	ND	ND	ND	ND	37.0	43.0	228.0	233.0	626.0	ND
COD Effluent (mg/L)	37.6	46.7	56.8	59.6	27.6	34.7	345.9	362.5	1200.0	2156.0	2897	19.7
pH Effluent (-)	6.55	7.31	7.56	7.52	7.61	7.38	7.44	7.37	7.46	7.2	7.55	7.56
Temperature Effluent (°C)	23.5	25.6	16.5	25.4	21.4	23.7	23.2	20.4	23.5	24.2	20.3	21.2
Dissolved Oxygen Effluent (mg/L)	5.2	6.7	7.4	7.0	7.2	7.3	8.3	8.1	7.3	7.8	8.0	7.6

Note: ND Not Detected

Raw data for the 12 days of intermittent mode



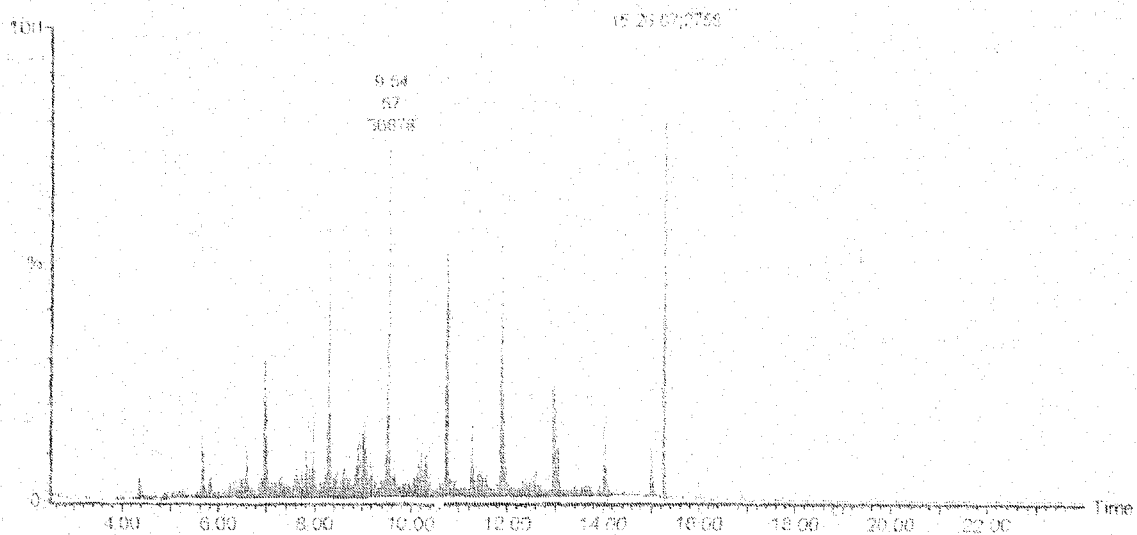
(A)



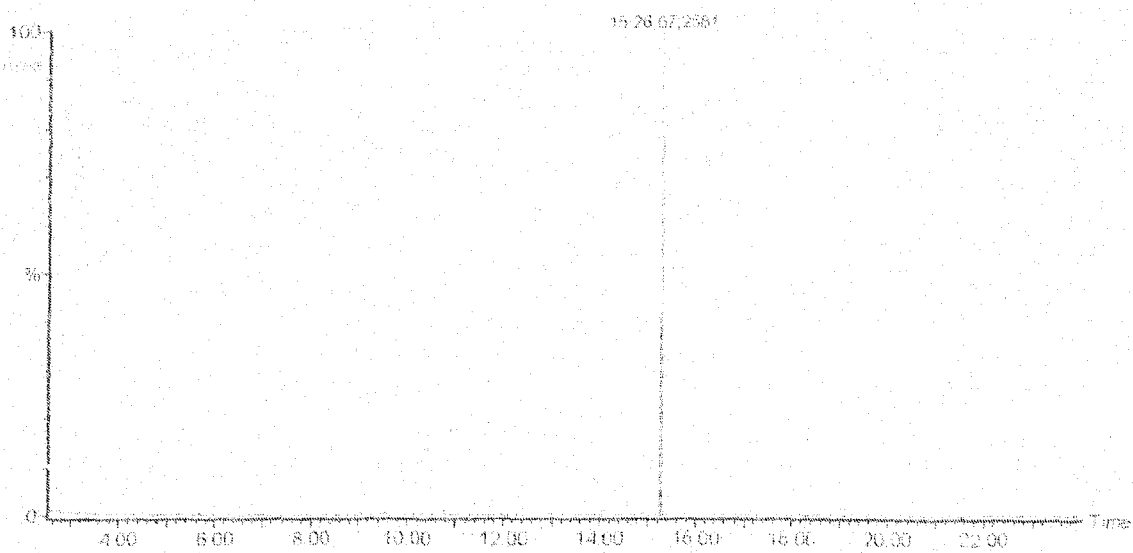
(B)

Gas Chromatogram for day 1 of operation

(A) Feedwater (B) Effluent



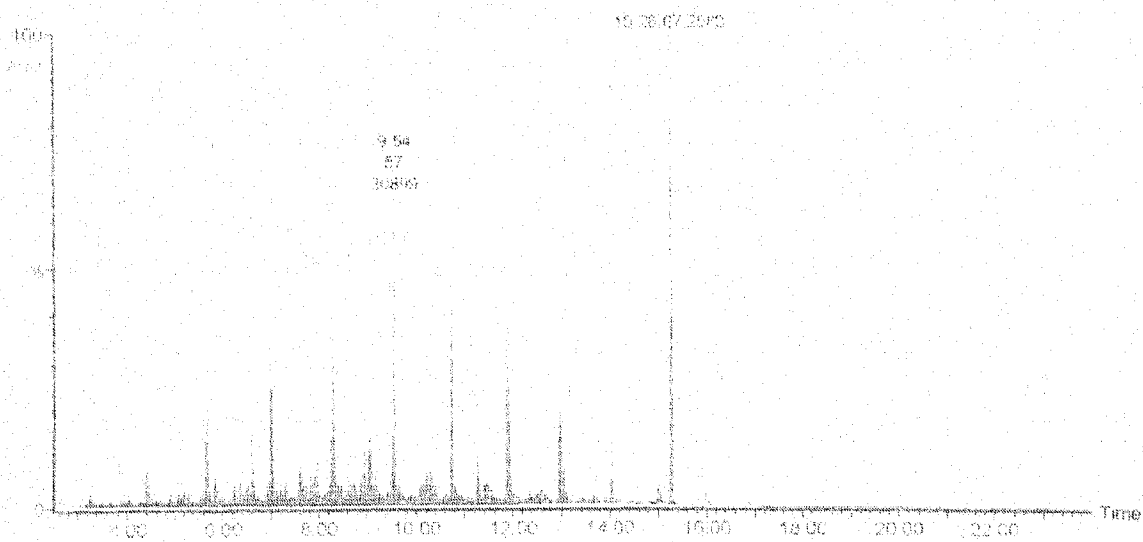
(A)



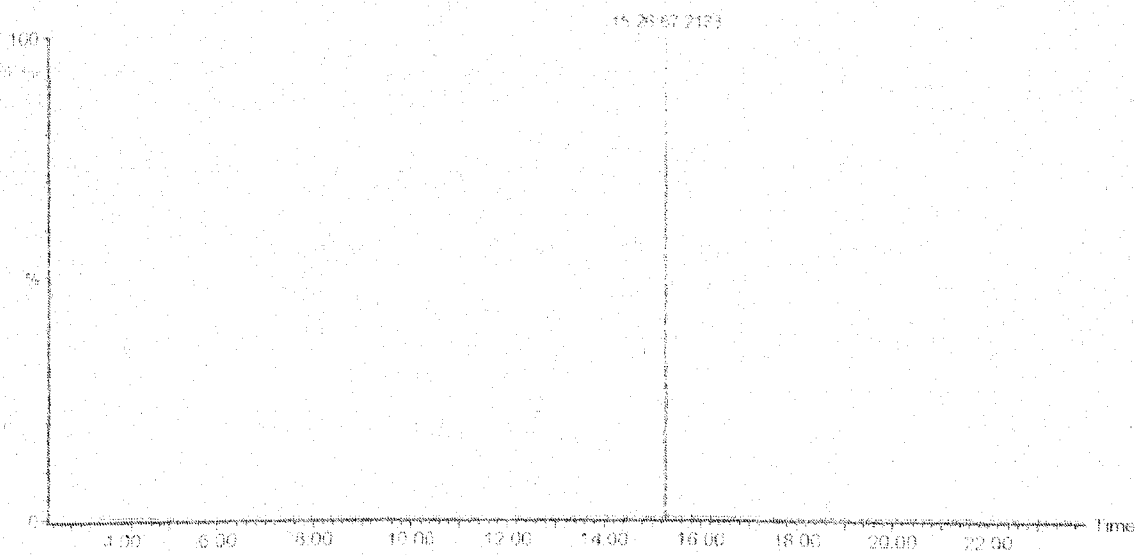
(B)

Gas Chromatogram for day 2 of operation

(A) Feedwater (B) Effluent



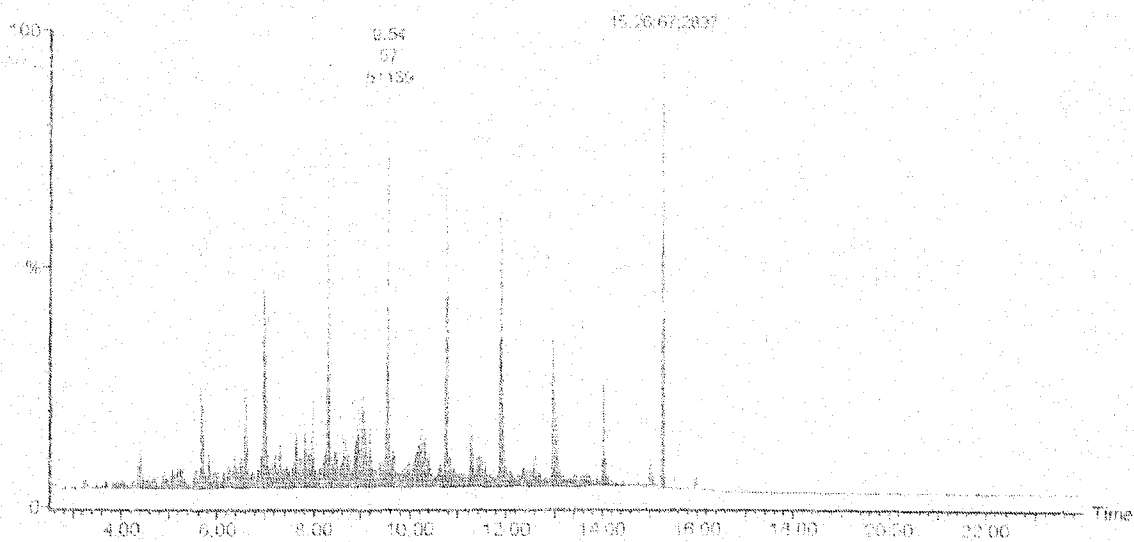
(A)



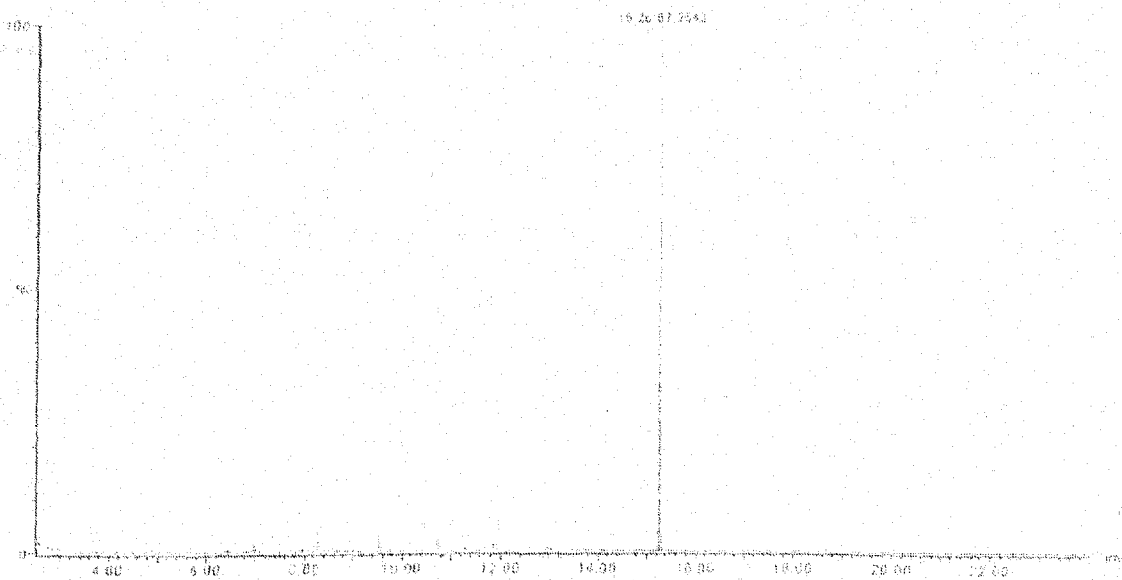
(B)

Gas Chromatogram for day 3 of operation

(A) Feedwater (B) Effluent



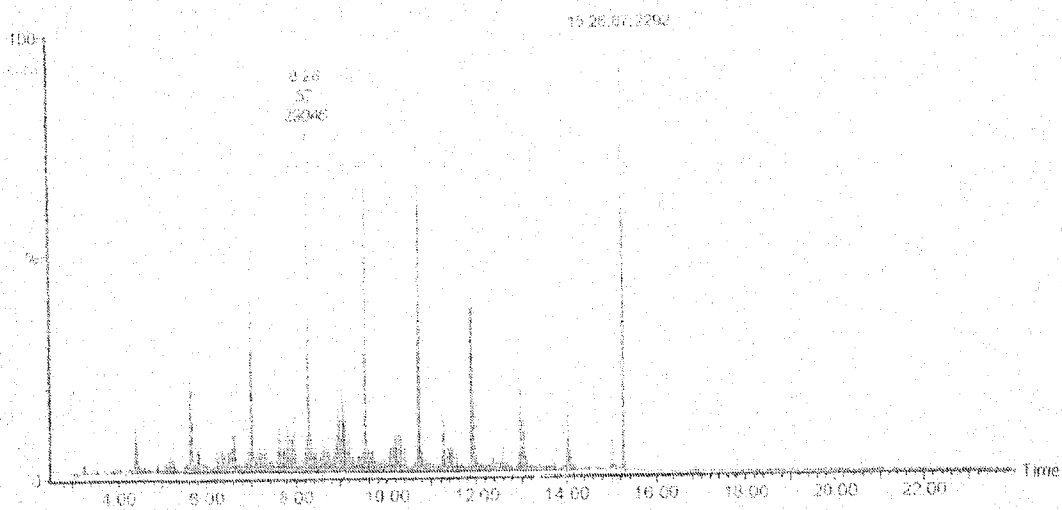
(A)



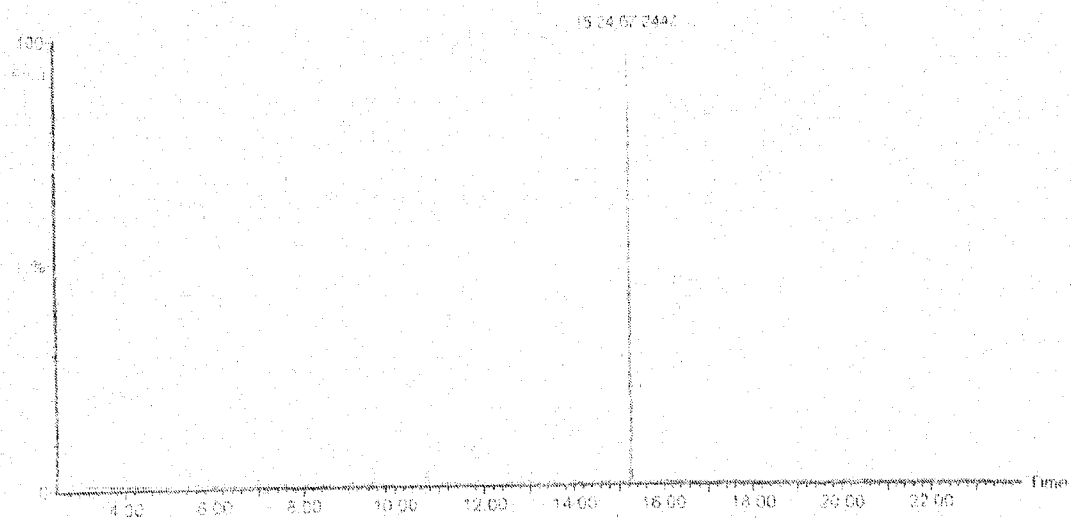
(B)

Gas Chromatogram for day 4 of operation

(A) Feedwater (B) Effluent



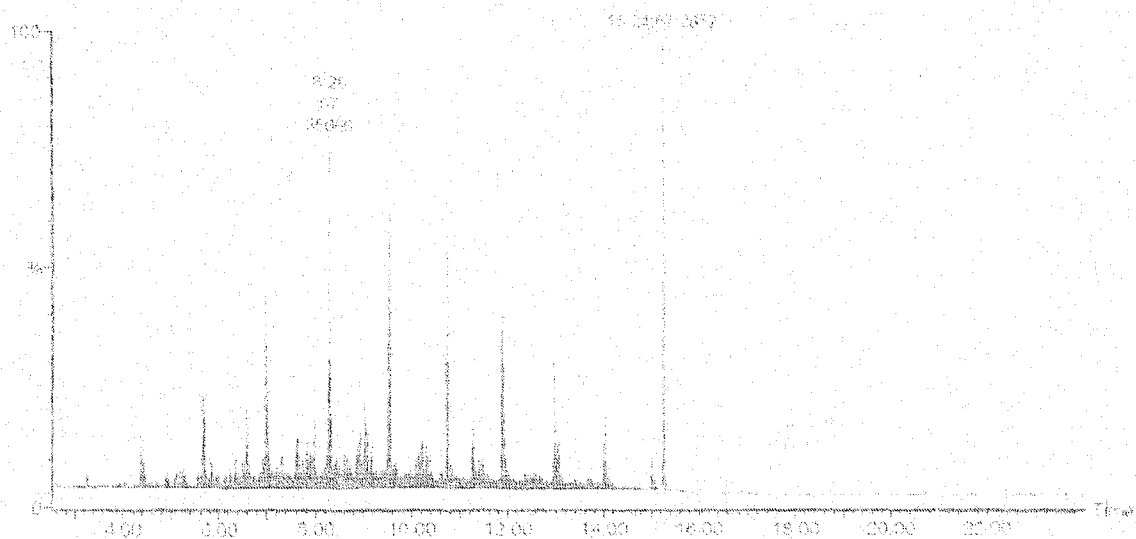
(A)



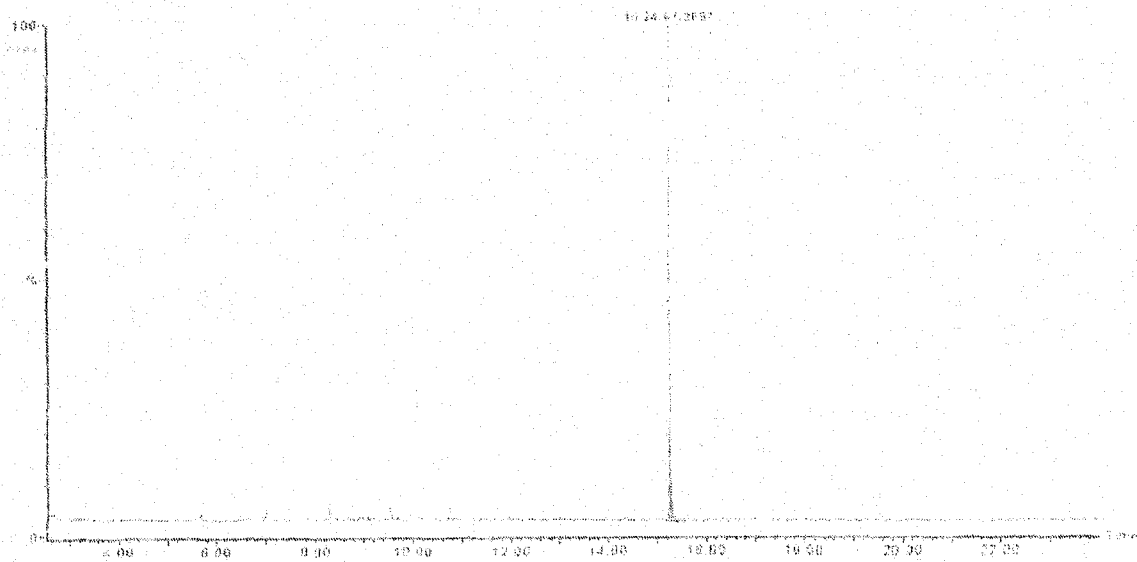
(B)

Gas Chromatogram for day 5 of operation

(A) Feedwater (B) Effluent



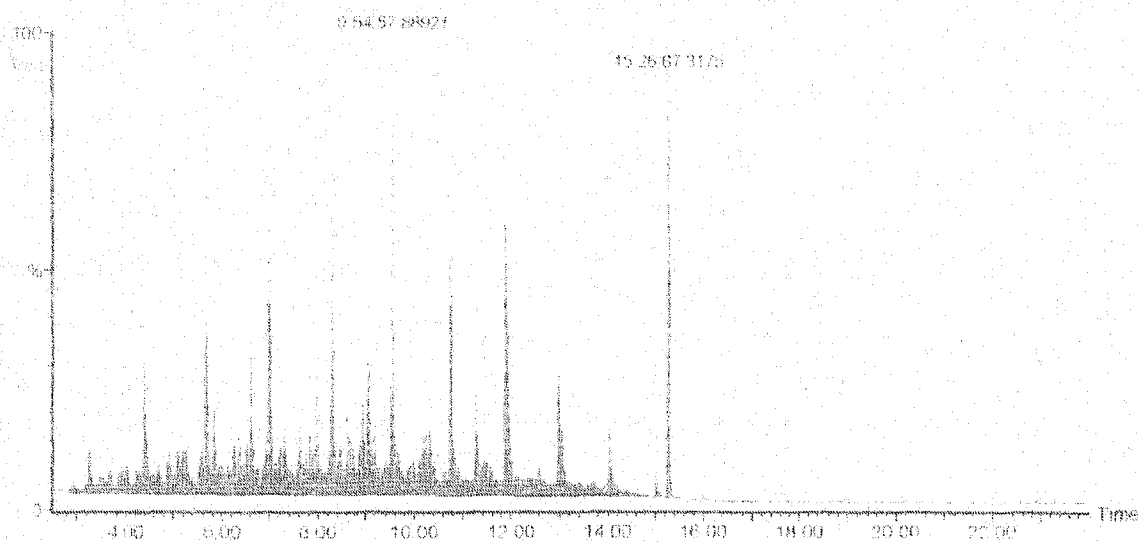
(A)



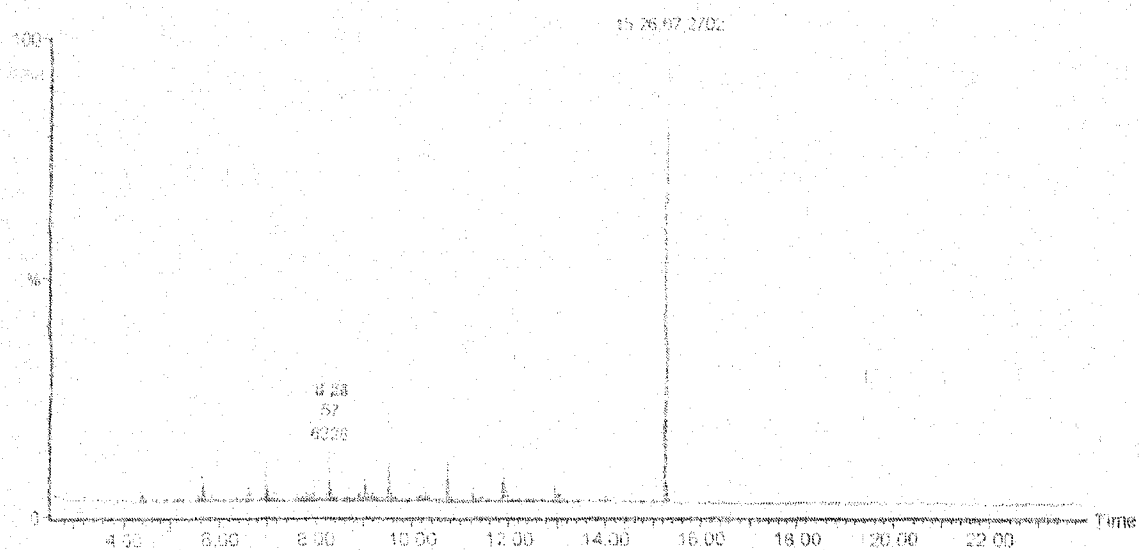
(B)

Gas Chromatogram for day 6 of operation

(A) Feedwater (B) Effluent



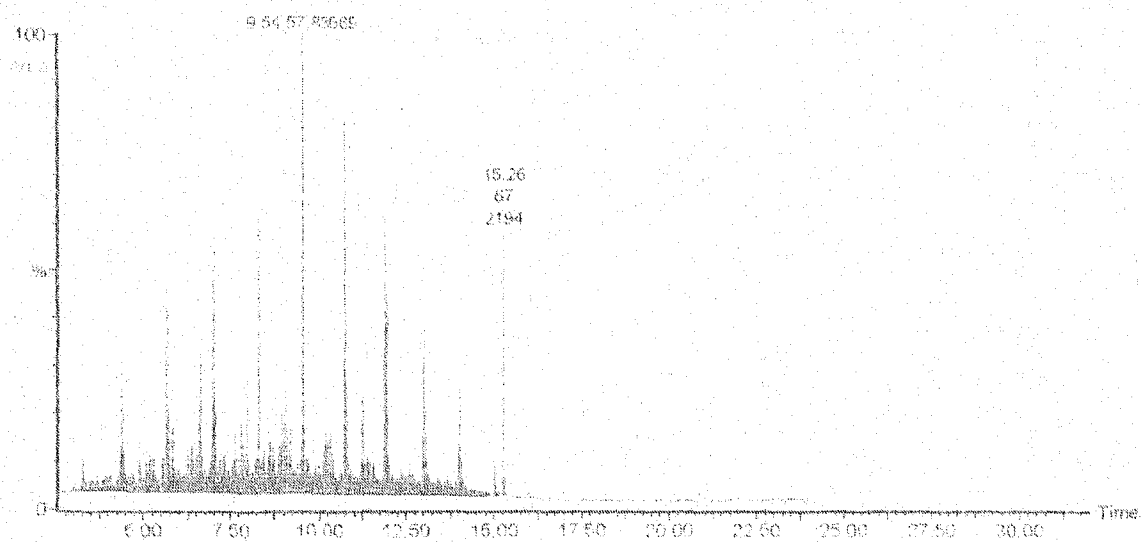
(A)



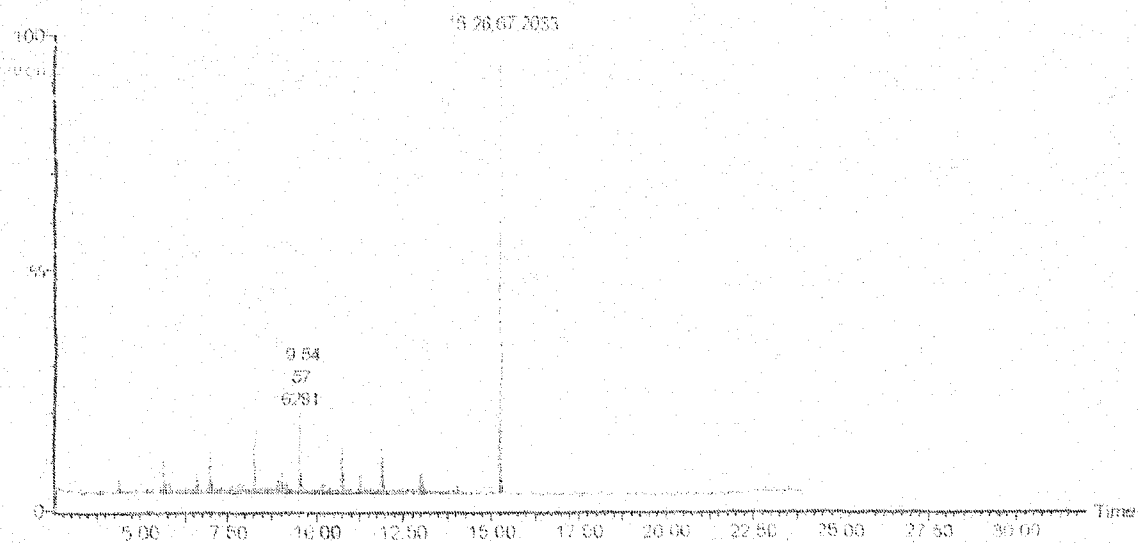
(B)

Gas Chromatogram for day 7 of operation

(A) Feedwater (B) Effluent



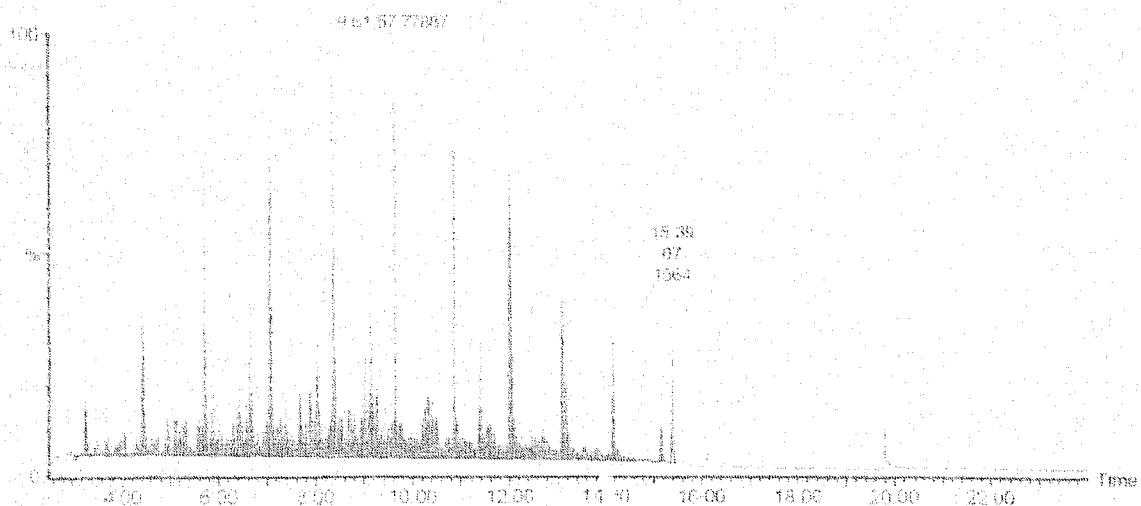
(A)



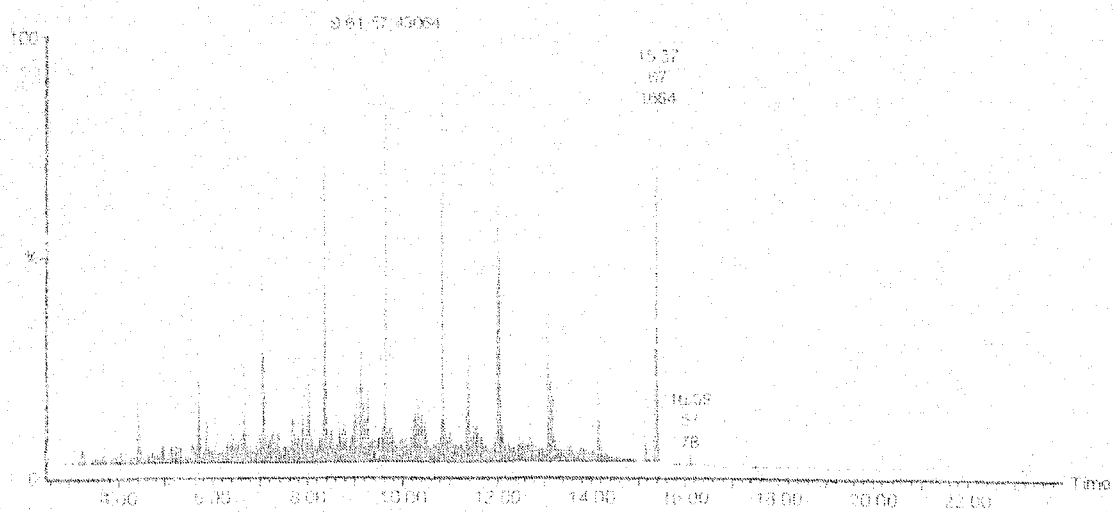
(B)

Gas Chromatogram for day 8 of operation

(A) Feedwater (B) Effluent



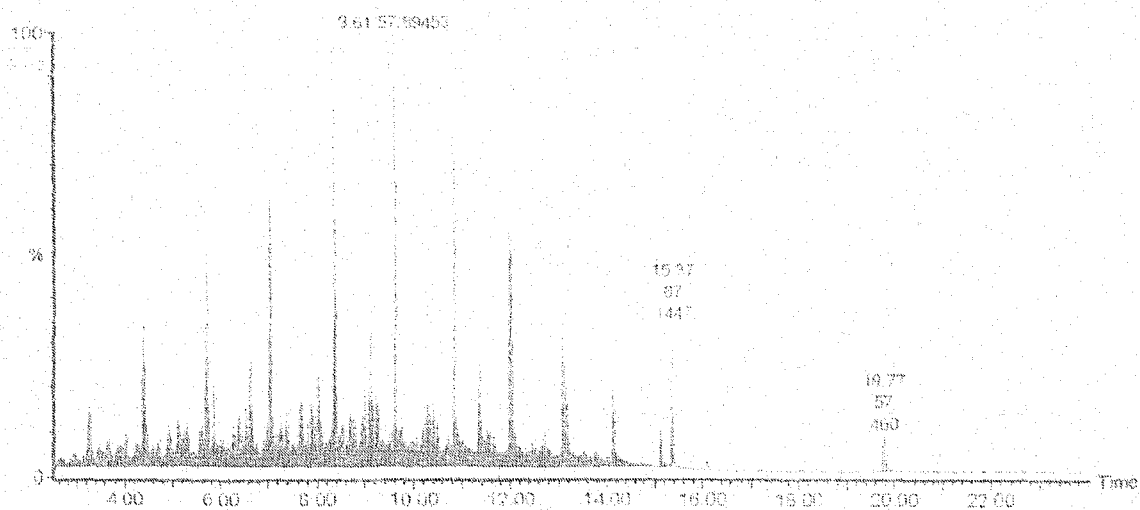
(A)



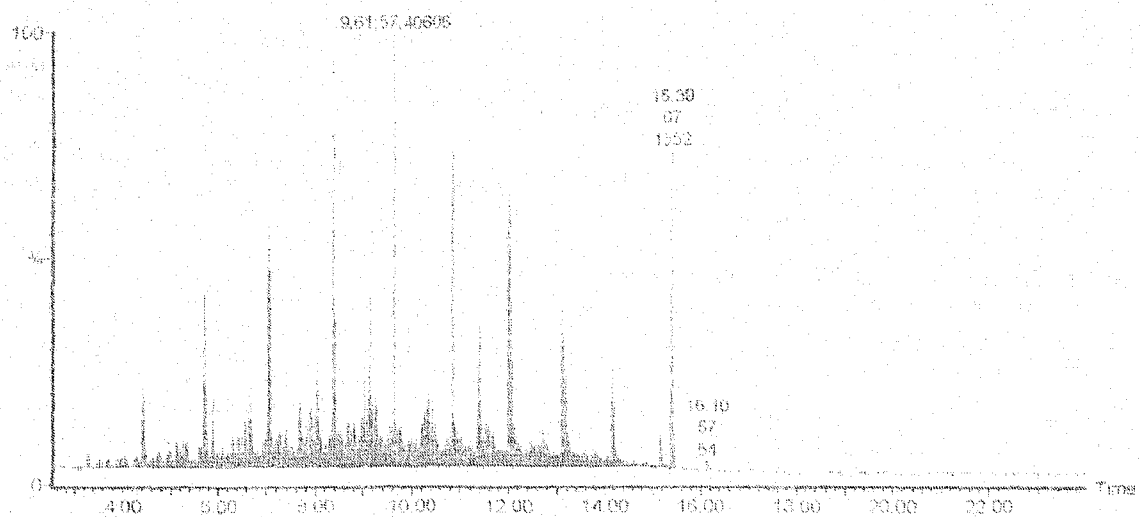
(B)

Gas Chromatogram for day 9 of operation

(A) Feedwater (B) Effluent



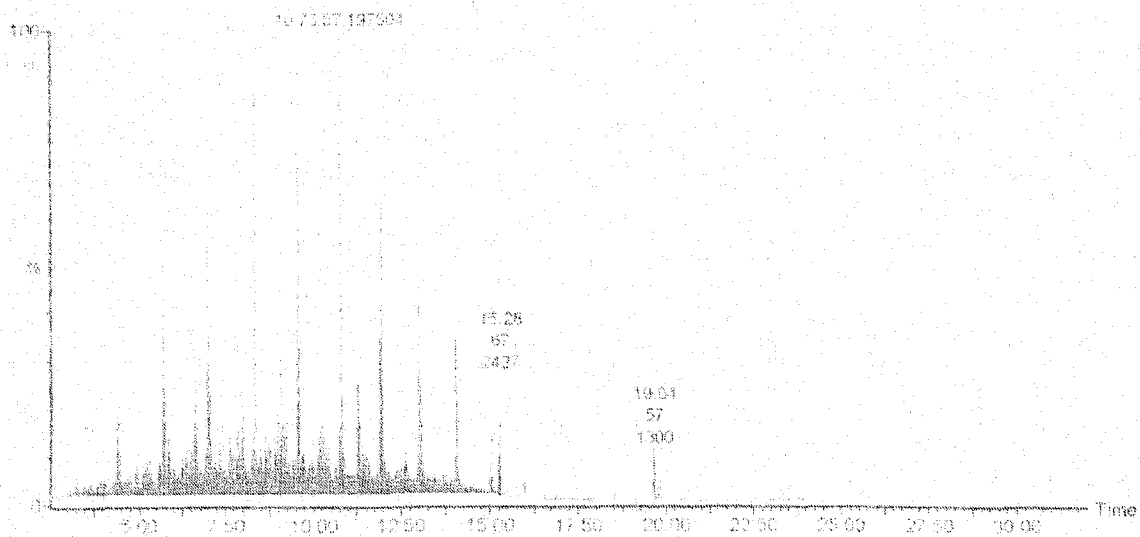
(A)



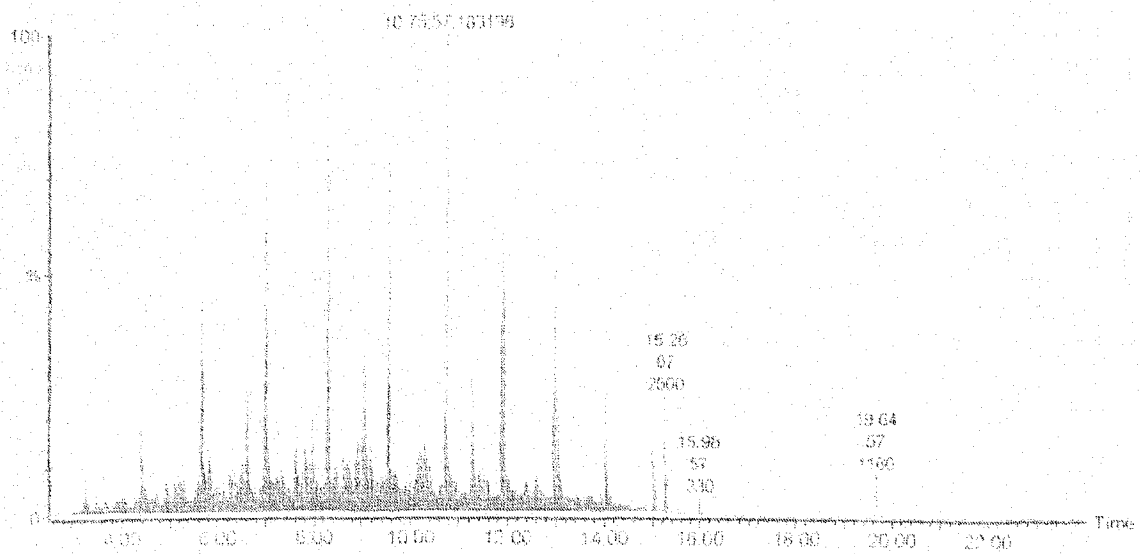
(B)

Gas Chromatogram for day 10 of operation

(A) Feedwater (B) Effluent



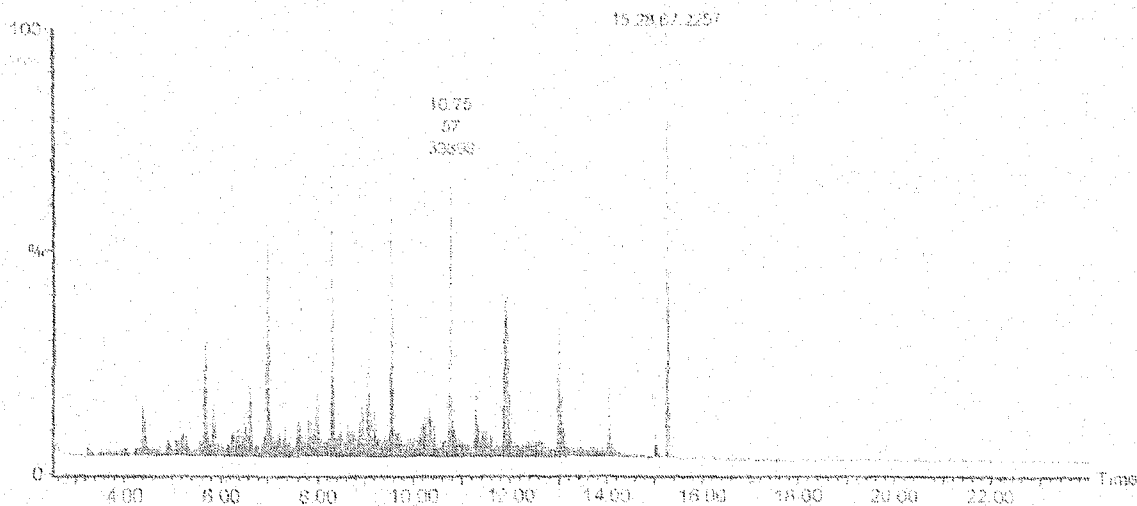
(A)



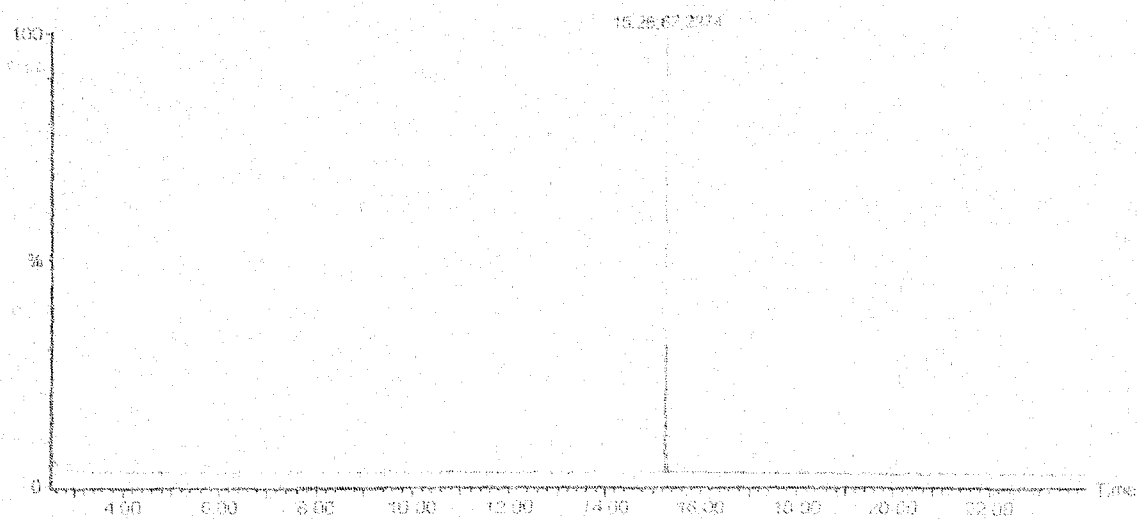
(B)

Gas Chromatogram for day 11 of operation

(A) Feedwater (B) Effluent



(A)



(B)

Gas Chromatogram for day 12 of operation

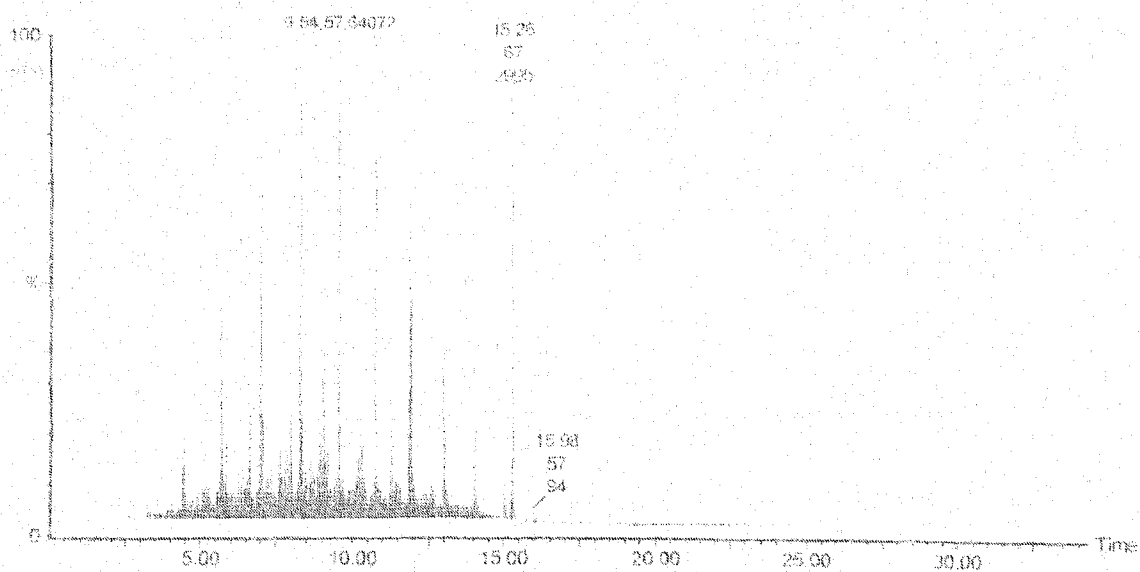
(A) Feedwater (B) Effluent

**RAW DATA AND GAS CHROMATOGRAMS FOR PHASE III: REACTOR
OPERATION AT STEADY STATE**

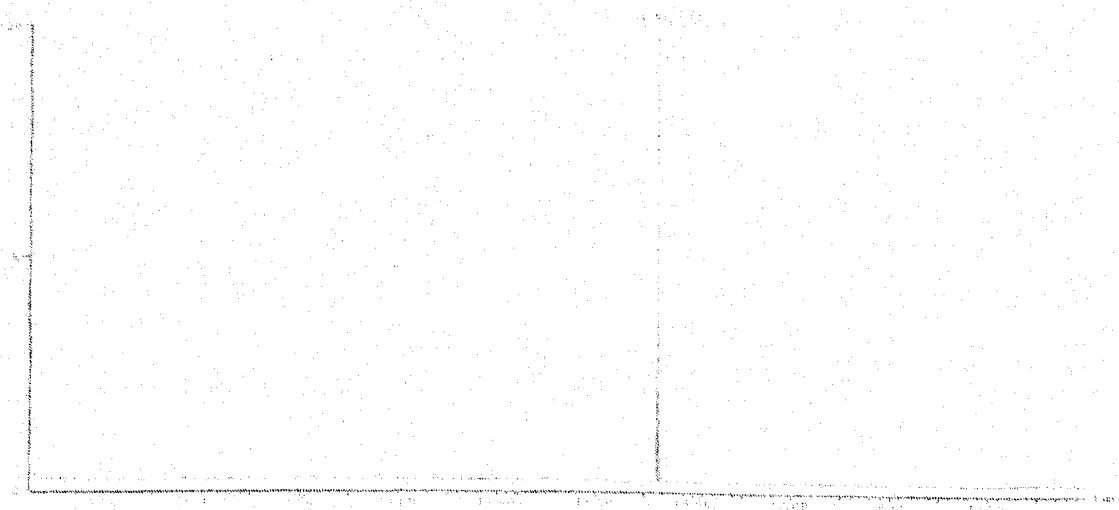
PARAMETER	DAY 13	DAY 14	DAY 15	DAY 16	DAY 17
Diesel Concentration Feedwater (mg/L)	193.0	175	198.0	200.0	198.0
COD Feedwater (mg/L)	1389.6	1195.0	1156.0	1262.0	1182.0
pH Feedwater (-)	7.52	7.5	7.57	7.49	7.54
Temperature Feedwater (°C)	20.4	22.7	23.2	19.2	22.1
Turbidity Feedwater (NTU)	12.35	11.13	9.23	10.7	10.36
Dissolved Oxygen Feedwater (mg/L)	8.2	7.7	7.4	8.0	7.6
Dissolved Oxygen Bed (mg/L)	6.1	5.9	5.7	6.7	6.2
Total Suspended Solids (mg/L)	0.86	1.12	0.94	0.64	0.79
Diesel Concentration Effluent (mg/L)	ND	ND	ND	ND	ND
COD Effluent (mg/L)	25.6	93.6	73.6	65.0	29.7
pH Effluent (-)	7.45	7.58	7.52	7.44	7.3
Temperature Effluent (°C)	22.3	22.9	23.8	20.4	23.4
Dissolved Oxygen Effluent (mg/L)	7.1	7.0	6.9	7.2	6.5
Biofilm thickness (µm)	NA	60-700	70-800	40-700	50-700
Turbidity Effluent (NTU)	4.75	5.9	5.3	6.5	5.6

Note: ND (Not Detected), NA (Not Available)

Raw data for day 13 through day 17 of steady state operation.



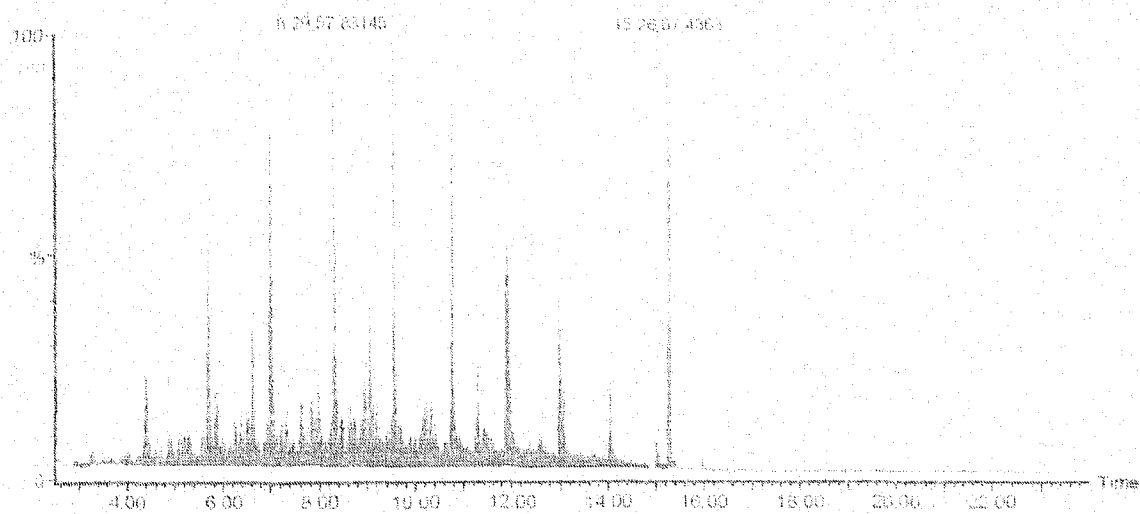
(A)



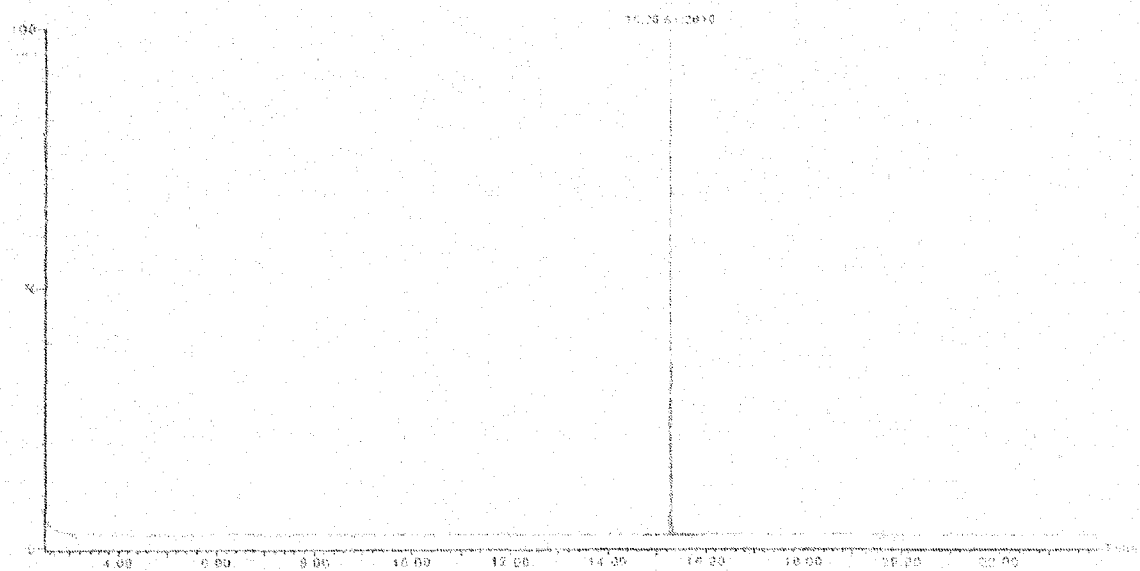
(B)

Gas Chromatogram for day 13 of operation

(A) Feedwater (B) Effluent



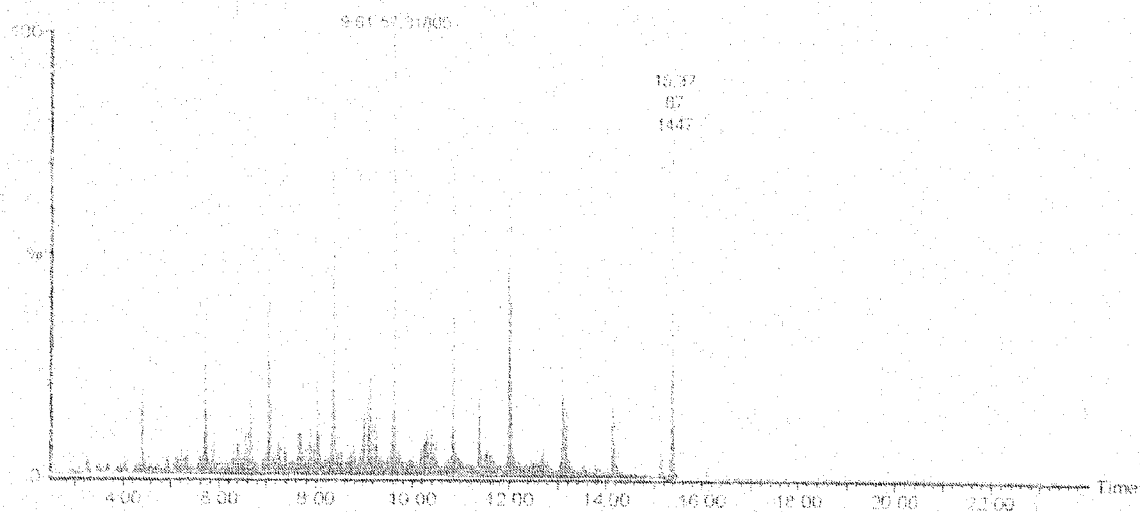
(A)



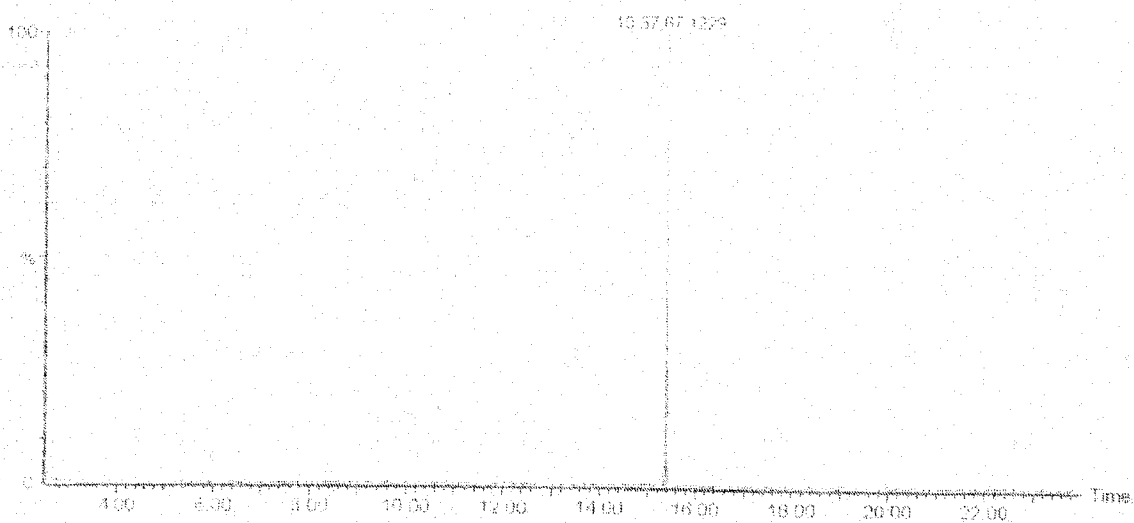
(B)

Gas Chromatogram for day 14 of operation

(A) Feedwater (B) Effluent



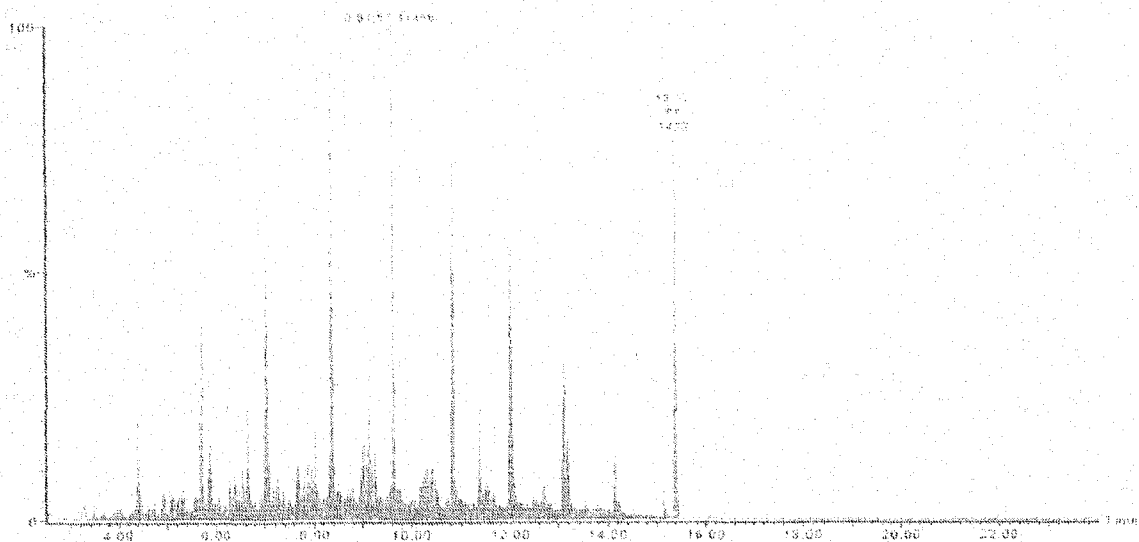
(A)



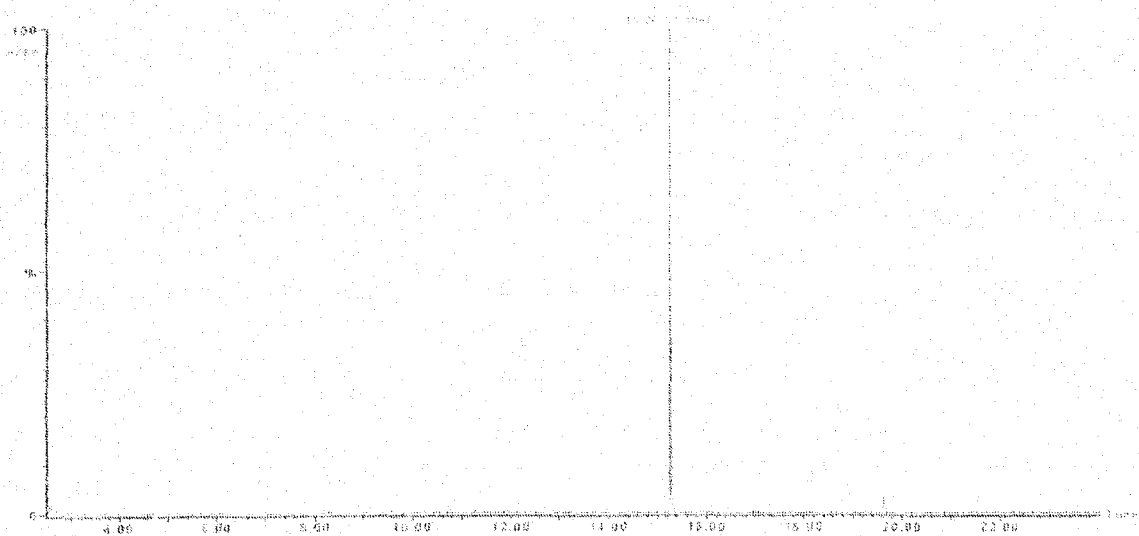
(B)

Gas Chromatogram for day 15 of operation

(A) Feedwater (B) Effluent



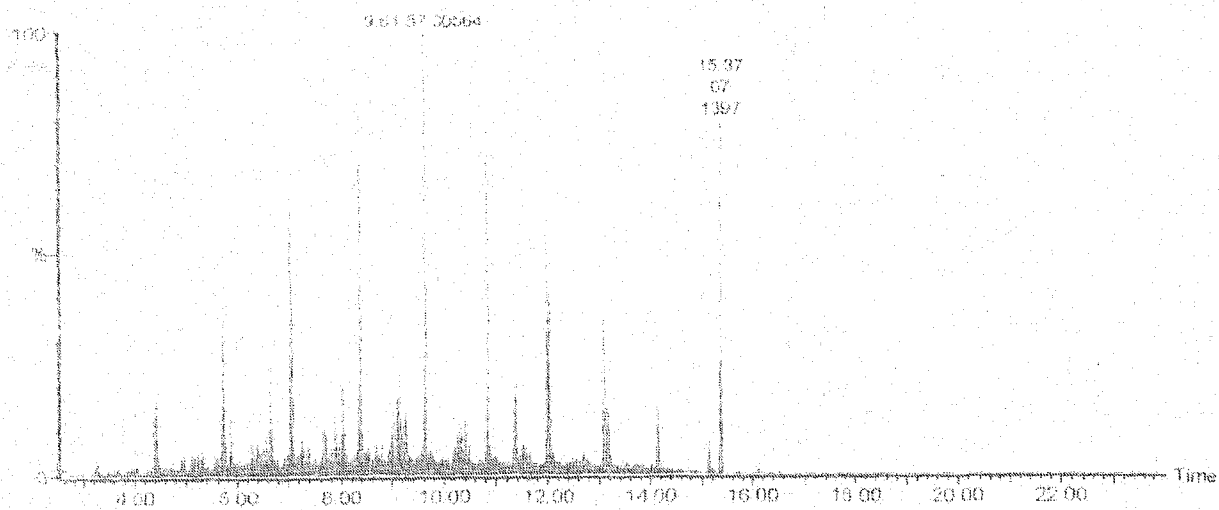
(A)



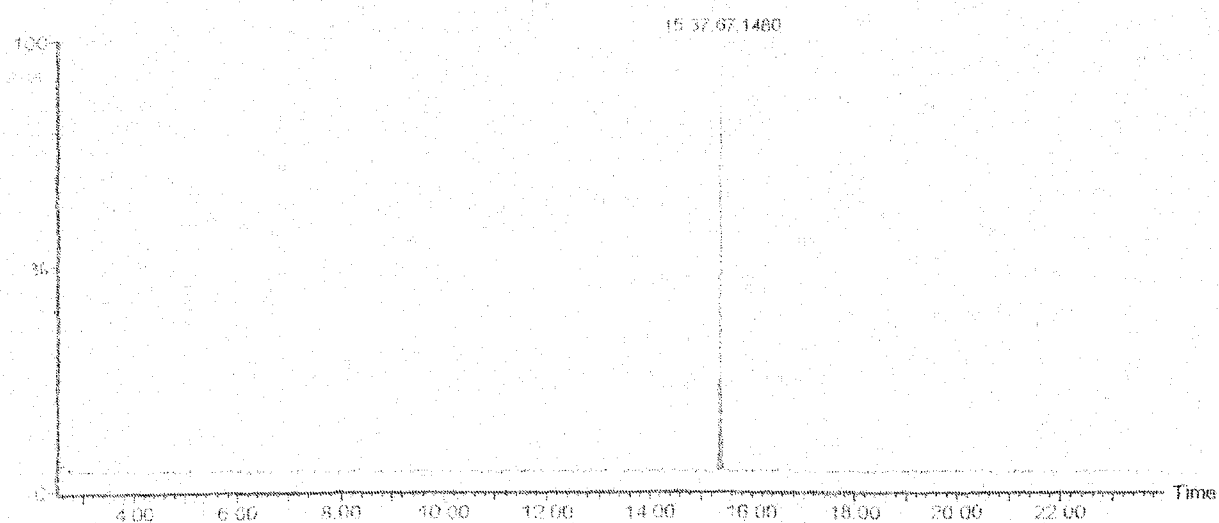
(B)

Gas Chromatogram for day 16 of operation

(A) Feedwater (B) Effluent



(A)



(B)

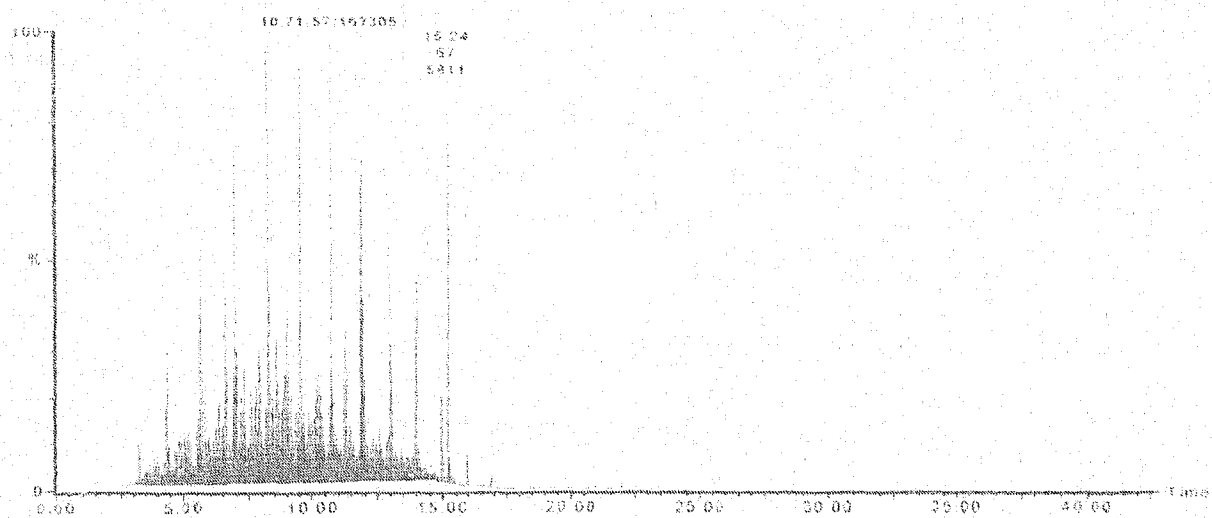
Gas Chromatogram for day 17 of operation

(A) Feedwater (B) Effluent

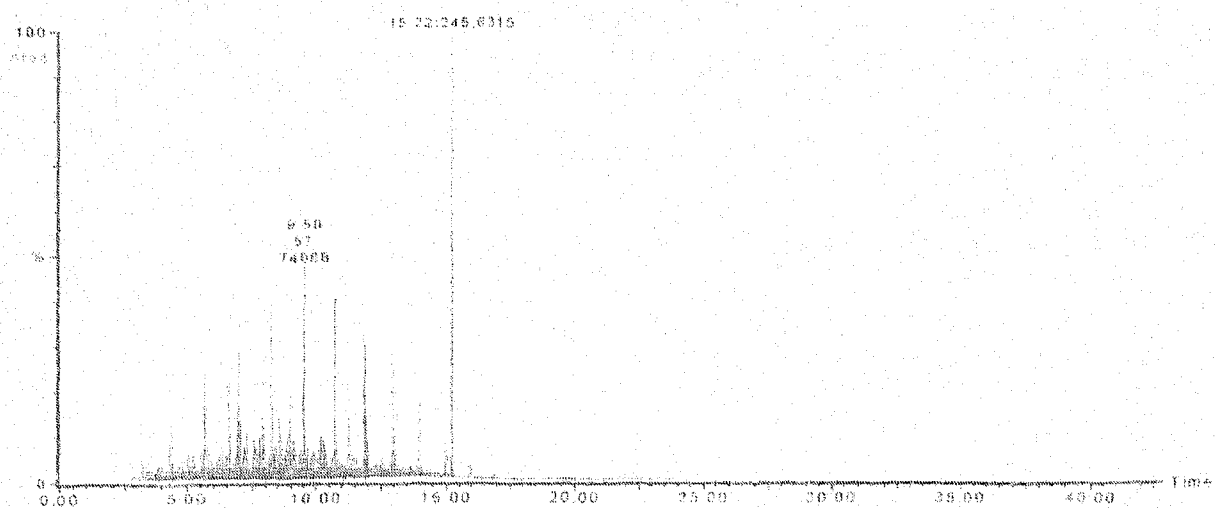
RAW DATA AND GAS CHROMATOGRAMS FOR PHASE IV: VALIDATION OF DIESEL BIODEGRADATION

PARAMETER	SET # 1	SET # 2	SET # 3	SET # 4
Diesel Concentration Feedwater (mg/L)	255.1	397.0	1038.0	1051.0
Dissolved Oxygen Feedwater (mg/L)	7.7	7.9	7.3	7.1
Dissolved Oxygen Effluent (mg/L)	8.1	8.2	7.8	7.8
Diesel Concentration Effluent (mg/L)	119.2	172.0	697.5	595.6

Diesel concentrations for validation of diesel volatilization in presence of diffusive air.



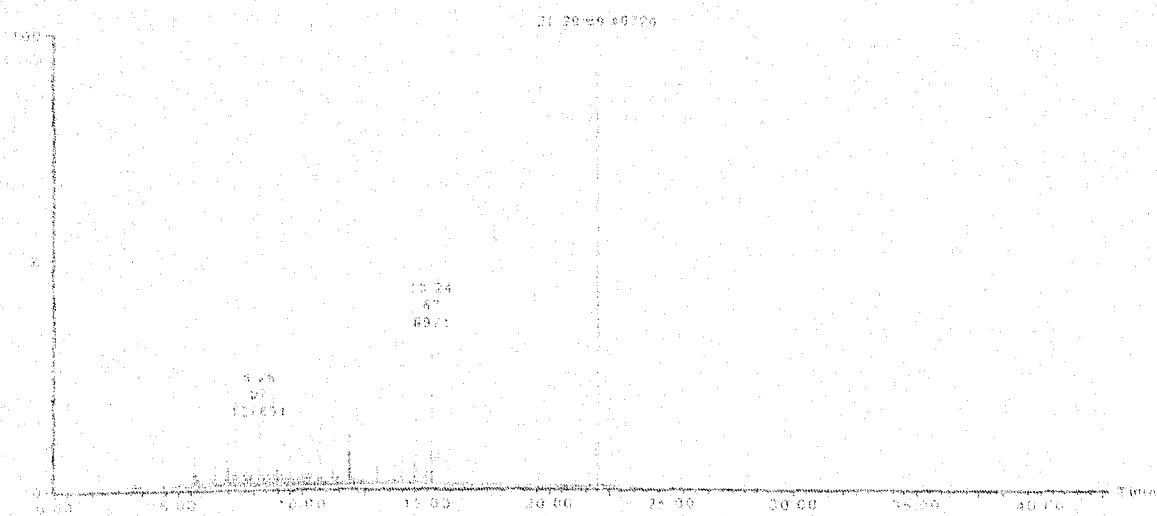
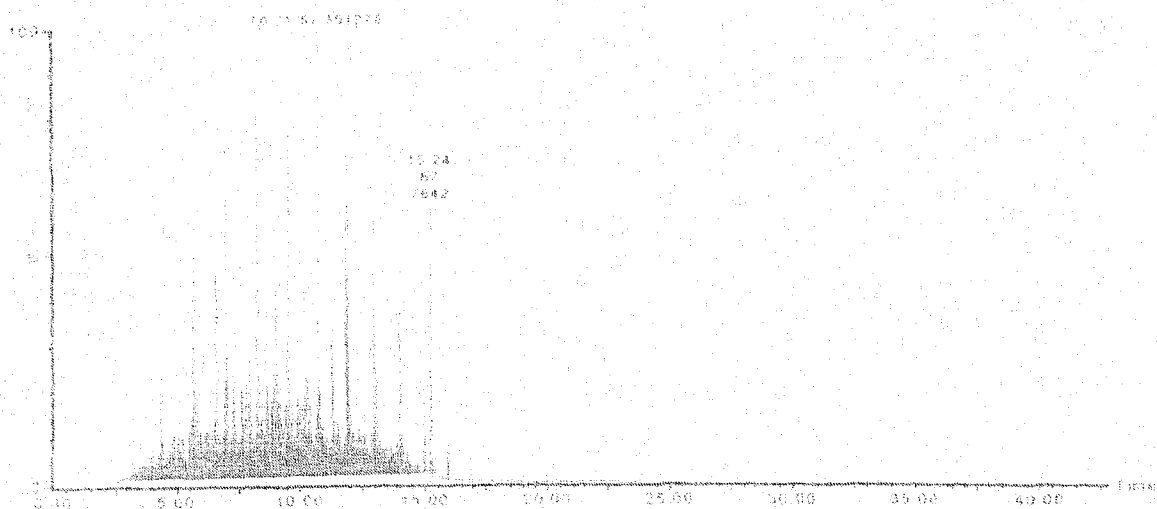
(A)



(B)

Gas chromatogram for validation of diesel biodegradation

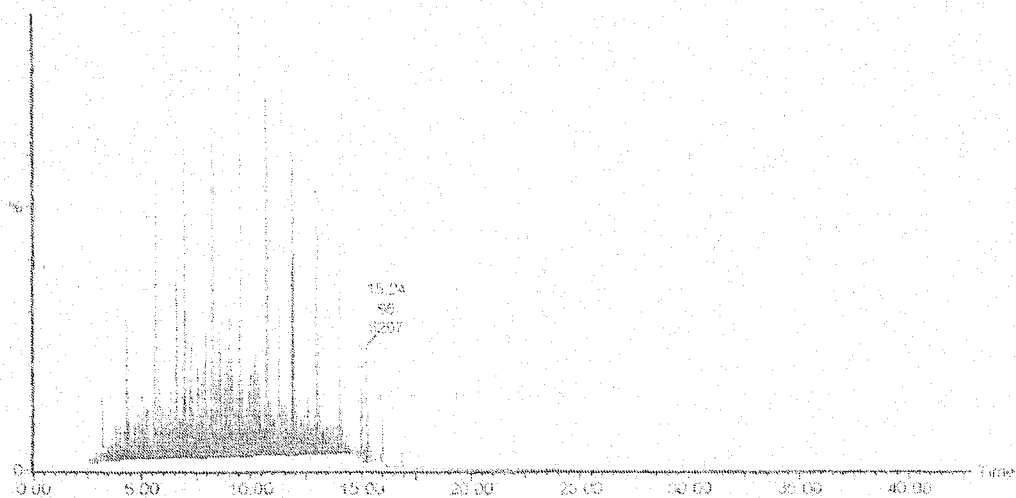
(A) Feedwater (255.1 mg/L) (B) Effluent



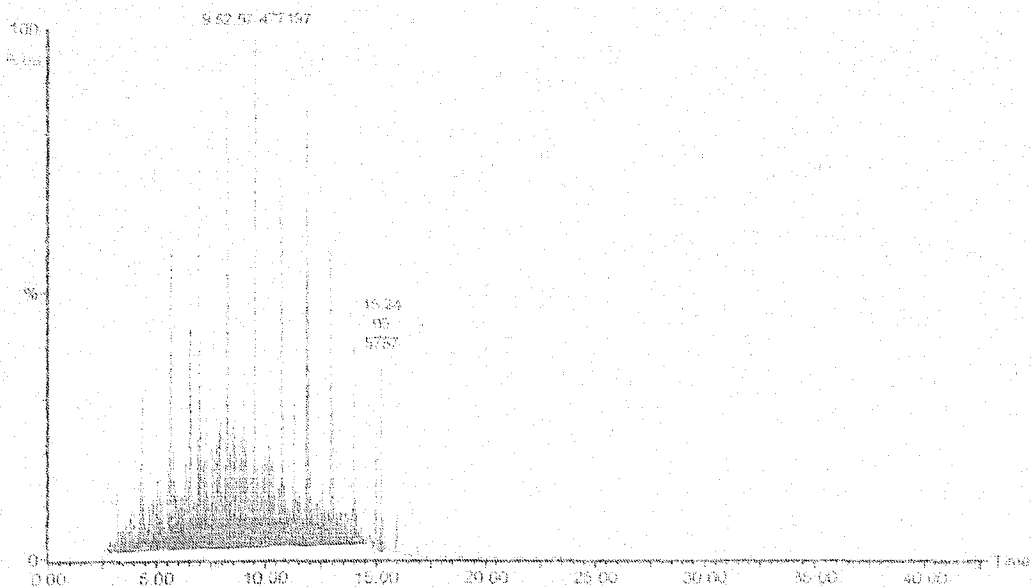
Gas chromatogram for validation of diesel biodegradation

(A) Feedwater (397.0 mg/L) (B) Effluent

9.51.67.770413



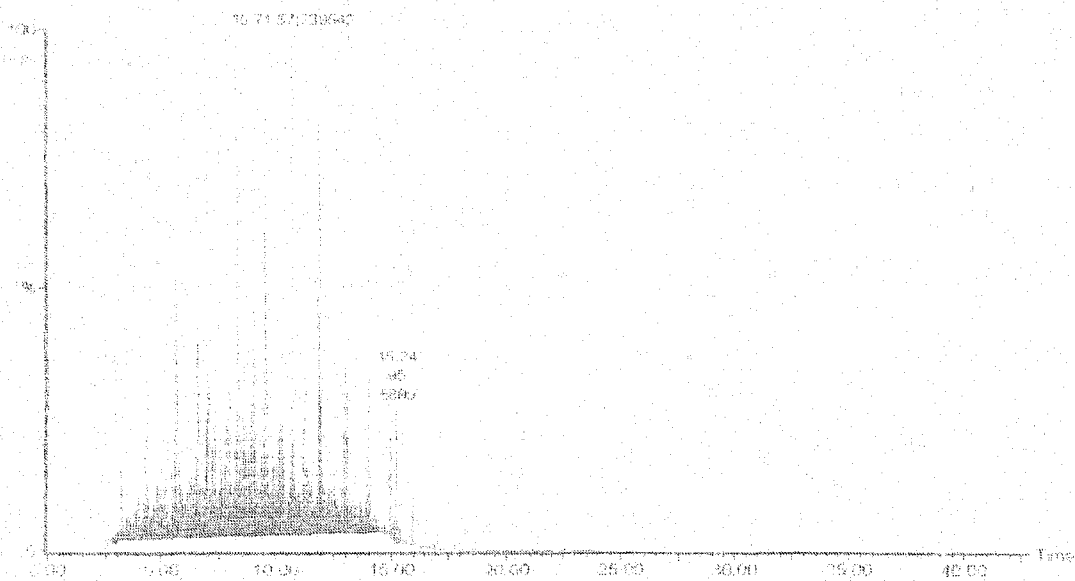
(A)



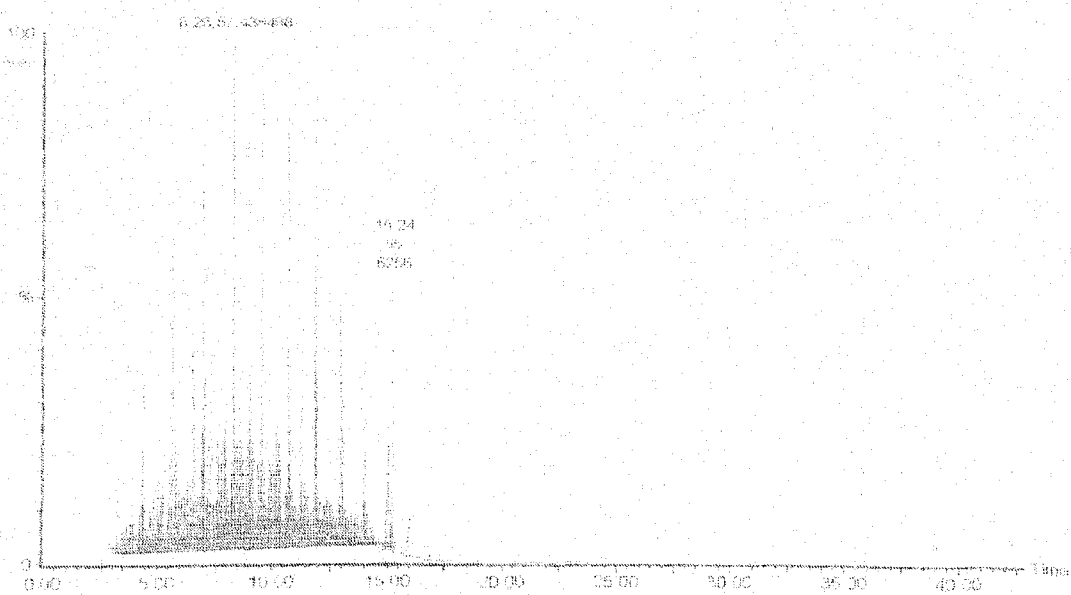
(B)

Gas chromatogram for validation of diesel biodegradation

(A) Feedwater (1038.0 mg/L) (B) Effluent



(B)



(A)

Gas chromatogram for validation of diesel biodegradation

(A) Feedwater (1051.0 mg/L) (B) Effluent

Simflui3p SOFTWARE: DESCRIPTION AND RESULTS

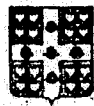
Simfui3p software has its basis in Larachi's Model. This model was based in multilayer perceptron artificial neural network, modeling techniques and dimensional analysis. Some of the upper and lower limits of operating conditions, fluid physical properties and packing properties are summarized in the following table.

FLUID PHYSICAL PROPERTIES	OPERATION CONDITIONS
$780 < \rho_l < 1623$ $8.9 \times 10^{-4} < \mu_l < 0.0719$ $0.025 < \sigma_l < 0.073$ $1.145 < \rho_g < 1.159$ $1.3 \times 10^{-5} < \mu_g < 1.8 \times 10^{-5}$ Gases: Air, N ₂	P=0.1 MPa $293 < T < 312$ Distributors: Tapered packed bed, perforated plate and nozzle-type distributor Solids: Alumina extrudate, glass bead, polypropylene bead, porous particles. Foaming System: Fermentation, Wastewater Treatment

More information about the limitation of this software can be found in Larachi et al.

Three-Phase Fluidization

Simulator



UNIVERSITÉ

LAVAL

Version: 28-06-2001

Data Entry $D_p = 2000 \mu\text{m}$

Liquid Properties:

superficial liquid velocity ul 2.000E-04
density (kg/m³), rol 1.00E+03
viscosity (kg/m.s), mul 1.00E-03
surface tension(kg/s²), sigl 7.20E-02

Gas Properties:

density (kg/m³), rog 1.20E+00
viscosity(kg/m.s), mug 1.25E-05
superficial velocity(m/s), ug 1.00E-02

Particles and Bed Properties:

grain equivalent diameter (m), dv 2.000E-03
sphericity factor (-), phi 1
density (kg/m³), ros 1.04E+03
column diameter (m), dc 0.17

Type of System:

coalescing 1 or foaming =2

Data Entry $D_p = 700 \mu\text{m}$

Liquid Properties:

superficial liquid velocity ul 2.000E-04
density (kg/m³), rol 1.00E+03
viscosity (kg/m.s), mul 1.00E-03
surface tension(kg/s²), sigl 7.20E-02

Gas Properties:

density (kg/m³), rog 1.20E+00
viscosity(kg/m.s), mug 1.25E-05
superficial velocity(m/s), ug 1.00E-02

Particles and Bed Properties:

grain equivalent diameter (m), dv 7.000E-04
sphericity factor (-), phi 1
density (kg/m³), ros 1.51E+03
column diameter (m), dc 0.17

Type of System:

2 coalescing 1 or foaming =2 2

RESULTS Data Entry $D_p = 2000 \mu\text{m}$

Liquid holdup = 0.579	
Gas holdup = 0.179	
Solid holdup = 0.242	
Bed Porosity = 0.758	
<i>Bubble wake model parameters</i>	
k =	0.80
x =	1.34

RESULTS Data Entry $D_p = 700 \mu\text{m}$

Liquid holdup = 0.501	
Gas holdup = 0.355	
Solid holdup = 0.144	
Bed Porosity = 0.856	
<i>Bubble wake model parameters</i>	
k =	0.80
x =	2.07